# A technical and economic feasibility study on repurposing copper mine tailings via microbial induced calcium carbonate precipitation

Department of Civil Engineering
University of Cape Town
February 2021

**Prepared by:**
Daniel de Oliveira

**Supervised by:**
Dr. Dyllon Randall

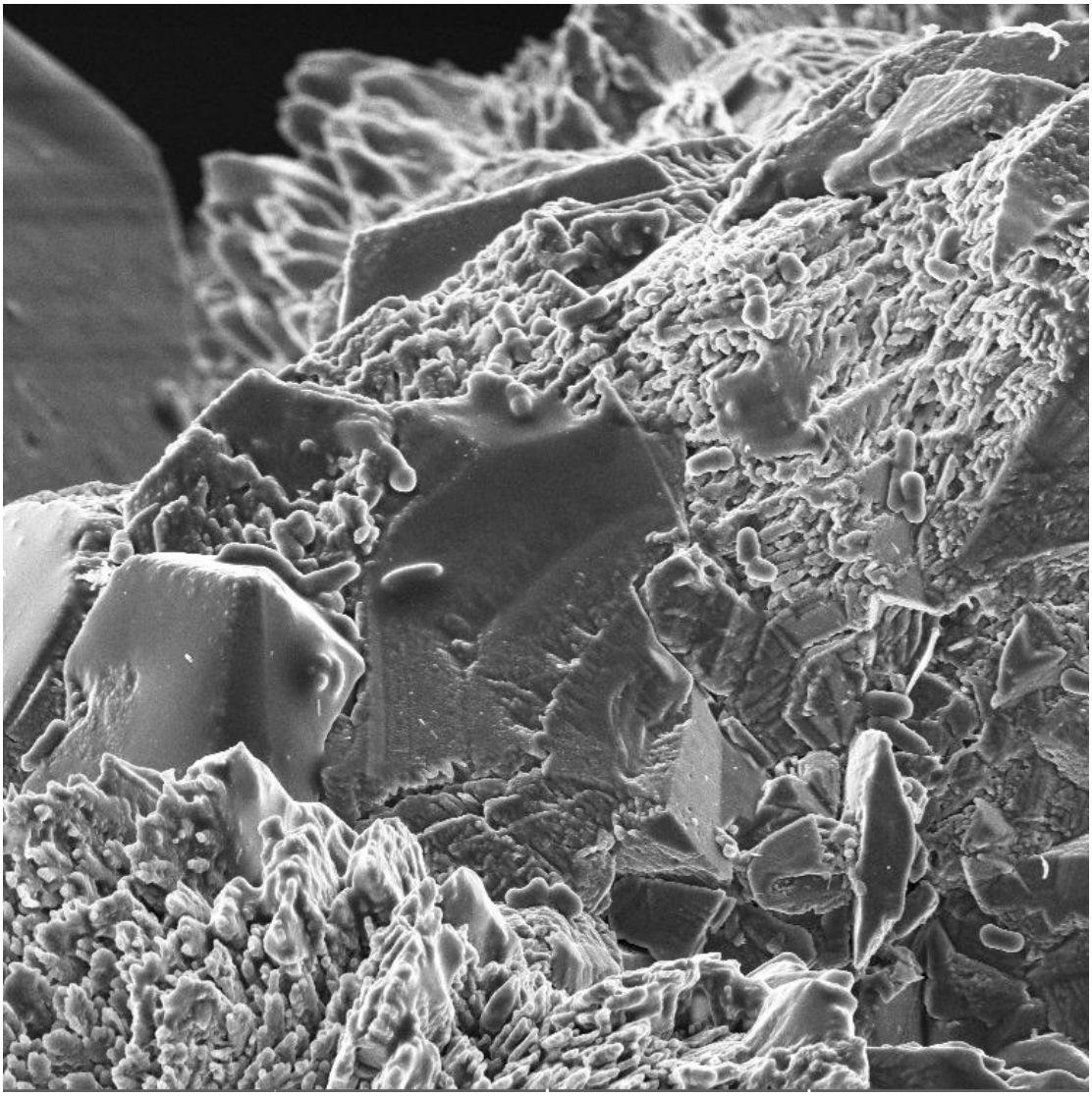

***“Nature is our biggest ally and our greatest inspiration. We just have to do what nature has always done. It worked out the secret of life long ago. In this world, a species can only thrive… when everything around it, thrives too”*** *– Sir David Attenborough*

# *Synopsis*

The current manufacturing of clay-fired and cement bricks has contributed greatly to anthropogenic global emissions and environmental damages. A possible solution that could be used to alleviate such environmental pressures is through the adoption of carbon neutral, microbial induced calcium carbonate precipitation (MICP) bio-bricks as a replacement for traditional bricks. MICP produced bio-bricks are formed by exploiting the ability of the microorganism, *Sporosarcina pasteurii*, to produce a bio-cement capable of binding sand particles (or any aggregate) together into a solid. Furthermore, such bio-bricks can be grown from otherwise 'waste' resources such as human urine. This significantly reduces energy inputs whilst creating value by 'upcycling' waste streams, resulting in a product which is sustainable whilst promoting the modern ethos of implementing environmentally friendly circular economies. However, the environmental benefits of MICP bio-bricks are hindered by the use of sand in their production. Sand, after water, is by volume the worlds most exploited and traded raw material and as such the supply of sand is being rapidly depleted globally. Added to this, sand extraction processes are known to cause extensive environmental damages. A possible solution to this issue is to replace the sand aggregate used to grow bio-bricks with mine tailings. The increasing global demand for metal products has resulted in the concurrent production of vast volumes of waste mine tailings which, if left untreated, pose a potential risk of leaching toxins into surrounding populations and biota. As such it was postulated that this risk to surrounding populations and the environment could be mitigated by repurposing mine tailings, as a replacement for sand, into MICP bio-bricks.

Both a technical and economic study was conducted to determine the feasibility of repurposing copper mine tailings into bio-bricks. As bio-bricks were resource intensive to produce (reagents, chemicals etc.), bio-columns were used as a proxy in studying the technical feasibility of such a process. The technical aspect of this study involved characterising copper mine tailings received from Columbia in terms of physiochemical make-up, particle size distribution and the development of a MICP submergent technique used in growing the bio-columns. This was necessitated by the fact that it was noted during the characterisation of the mine tailings that the cementation media could not be pumped through the columns filled with mine tailings aggregate, resulting in the traditional pumping method used to grow MICP bio-solids being impractical. The submergent technique was used to compare the MICP efficiency of growing bio-columns from either beach sand or copper mine tailings. In addition, the toxicity of copper to *S. pasteurii* was investigated and an attempt was made to acclimate a culture of *S. pasteurii* to the copper concentration found within copper mine tailings. Furthermore, the copper mine tailings were screened to determine if there were any indigenous, anaerobic and copper tolerant ureolytic extremophiles contained within, which had the potential to grow more robust bio-columns.

In terms of the economic feasibility of repurposing copper mine tailings into bio-bricks, the results of the technical study were used to construct a basic mass balance of an envisioned bio-brick production route. This in turn was used to delineate the potential margin which could be earned through the production and sale of a copper mine tailing bio-brick and associated by-product fertilisers. Additionally, a sensitivity analysis was conducted to determine areas of potential cost reduction as well as a comparison made between the sale of a bio-brick to a more valuable bio-tile.

Through the course of the technical investigation, it was determined that although the submergent technique developed in this dissertation offered a simpler means of producing bio-columns compared to the pumping technique, it came at the cost of a reduced calcium carbonate efficiency i.e. less calcium ions being precipitated as calcium carbonate. The bio-column grown from beach sand after being submerged in cementation media for five days exhibited a compressive strength of 1.85±0.39 MPa; this was despite only 44.1% of calcium ions added to the cementation media being depleted as well as only 57.6% of the theoretical maximum ammonium ions (had all the added urea hydrolysed) being produced – both factors indicating that further optimisation to the developed process can occur. The first known attempt to repurpose copper mine tailings into a MICP bio-column, resulted in the growth of a bio-column of 0.54 MPa compressive strength. This constituted no statistically significant compressive strength difference to untreated copper mine tailings (0.53±0.31 MPa). This indicated that insignificant levels of MICP occurred within the copper mine tailings; a point which was further illustrated by measurements of its cementation media which showed that only 14.3% of added calcium ions were precipitated and 26.0% of theoretical ammonium ions were produced.

Initially, the failure of *S. pasteurii* to induce MICP within the copper mine tailings was attributed to the presence of the excessive copper concentration (622 mg/L) inherent to the tailing. This was due to experimental results showing that the minimum inhibitory concentration (MIC) of copper on *S. pasteurii*, which resulted in less than 70% of optimal growth being achieved, was within range of 128-256 mg/L. A successful attempt was made to acclimate a culture of *S. pasteurii* to higher concentrations of copper in order to overcome this inhibition; cumulating in the successful growth of a culture capable of surviving in a copper concentration of 600 mg/L. An attempt to grow a copper mine tailing bio-column via the submergent technique using this acclimated culture resulted in the production of a bio-column of reduced compressive strength (0.11 MPa) compared to the untreated copper mine tailing columns. As such, this indicated that the copper inhibition of the ureolytic bacteria was not the sole factor resulting in the failure of copper mine tailings to be repurposed into bio-columns via MICP.

Rather, due to the observation that a ‘MICP shell’ formed around the outer edges of both the copper mine tailing bio-columns (standard and acclimated *S. pasteurii* cultures), it was postulated that the failure of adequate levels of MICP to occur was due to limited nutrient transfer throughout the bio-column as a direct result of the low particle size (d[0.5] = 5.17 µm) and hence porosity (0.29) of the copper mine tailings. This hypothesis was supported by literature which stated that fine aggregates (such as copper mine tailings) display a limited ability to transfer oxygen to, and waste away, from bacteria – which results in decreased bacterial growth and reduced bacterial movement and activity.

Further, scanning electron micrograph (SEM) imaging of the copper mine tailing bio-columns supported this conclusion by showing that the $CaCO_3$ crystal formation was concentrated in the outer extremities of the bio-columns. The $CaCO_3$ content measurements of bio-columns additionally confirmed that the spread of $CaCO_3$ precipitated throughout the columns was not homogenous but rather increased radially from the centre. It was believed that one of two alternative means of overcoming this nutrient inhibition would be through the use of an anaerobic bacteria (i.e. does not require oxygen) which was copper tolerant and capable of producing adequate volumes of urease. An attempt was made to isolate such a bacterium indigenous to the copper mine tailings. However, despite isolating numerous morphologically different colonies of bacteria, none tested positive for urease production and hence this hypothesis remains untested.

The second means of overcoming the nutrient transfer limitation experienced when using copper mine tailings, is to grow a thinner bio-solid, such as a tile, rather than target the manufacturing of thicker bio-bricks. Not only is such a transition supported by the observations of a shell formation during the technical analysis, but it is also strongly supported by the results determined in the economic analysis. Whereas it was determined that for a base case bio-brick (using the scaled-up chemical requirements to grow a copper mine tailing bio-column) a loss of US$2.35 would be incurred for every bio-brick produced. This is sharply contrasted by the US$7.50 income which could be earned through the production of a single bio-tile of equivalent volume to the bio-brick. It must be noted that the process designed in this work, was not optimised as the lowest calcium usage efficiency (14.3%) obtained by the copper mine tailing bio-column was used as a design basis. If a 100% MICP efficiency was assumed for each bio-solid, the cementation media required would be significantly reduced. However, due to the resultant loss in income from the reduced volumes of fertiliser by-product produced only a slightly improved margin of -US$2.02 and US$7.84 could be realised for the production of a bio-brick and bio-tile respectively. This analysis shows that calcium efficiency is not a key parameter in improving the cost of the process as, in the case of the bio-tile, a 100% calcium usage efficiency only improves the margin by 4.53%.

If significant cost reductions are to be achieved for such a process, an attempt must be made to reduce the cost of the bacterial nutrient media, which in both base cases were costed on the basis that laboratory grade ATCC®1376 media would be used. *S. pasteurii* is known to be capable of surviving and growing on a multitude of agriculture waste products such as mother lactose liquor. As such the possibility exists that the bacteria required to grow the bio-solids could be supplied from waste nutrient streams from nearby farms. If such an arrangement could be made, it was calculated that cost of bio-brick production would near breakeven at – US$0.16 and that the income earned from producing a bio-tile could increase by as much as third (US$9.68).

In conclusion, it was shown in this dissertation that with the current ureolytic bacteria (*S. pasteurii*) the repurposing of copper mine tailings into a bio-column via MICP is not technically possible. This is due to the inherently small particle size distribution, and hence porosity, of the tailing particles limiting the transfer of nutrients into the interior of the bio-column. It is speculated that this limitation could be overcome by utilising an anaerobic ureolytic bacteria indigenous to the copper mine tailings and thus is suggested that continued efforts be made to bioprospect for a suitable candidate. Additionally, the production of bio-bricks was also shown to be economically unfeasible. However, the production of bio-tiles, of equivalent volume of copper mine tailings aggregate to that of bio-bricks, shows economic promise. A transition in focus from bio-bricks to bio-tiles is also supported by the establishment that the depth at which MICP can be effective is limited by a nutrient transfer gradient. Hence, being thinner than a bio-brick, a bio-tile may form more optimally using the submergent procedure investigated in this dissertation. It is therefore suggested that an attempt be made to test the technical feasibility of repurposing copper mine tailings into bio-tiles instead.

# *Acknowledgements*

.

To **Dr. Dyllon Randall** thank you for giving me this opportunity to challenge myself, for your continued support even when the task at hand seemed impossible and for pushing me further than I ever thought I could go. Thank you for your constant feedback and advice, impeccable attention to detail and continued revision of my work (made all the more difficult by the global pandemic). The passion you exude for your work is self-evident and inspires those around you to reach for the stars.

To **AngloGold Ashanti**, I am greatly indebted for your funding support. It was an absolute pleasure working with you and I would like to express my profound appreciation for all the help, time and constructive feedback you provided in making this project a reality.

To **Dr. Robert Huddy** and the **CeBER laboratory** thank you for your initial assistance in the early stages of this project, it was much appreciated.

To the Water Quality Team - **Njabulo Thela, Hector Mafungwa, Amy Hislop, Caitlin Courtney, Rhonda Hyde, Vuhkheta Mukhari, Tarie Mufunde, Mwana Mwale and Hlumelo Marepula** - I am grateful for all the memories we created together in the lab as well as all the assistance and suggestions you have provided me along the way. To the **CoMSIRU** and the **Analytical** Laboratories, thank you for the training and lending of equipment you provided me in such a precarious and strange time, it is much appreciated.

To my family – **Mom, Dad and Dom** – everything I have achieved is because of you. Thank you for you continued support and love throughout years. You are, and remain, my constant source of inspiration.

## PLAGIARISM DECLARATION

I, Daniel de Oliveira, hereby declare that the work on which this dissertation/thesis is based is my original work (except where acknowledgements indicate otherwise) and that neither the whole work nor any part of it has been, is being, or is to be submitted for another degree in this or any other university. This thesis/dissertation has been submitted to the Turnitin module, and I confirm that my supervisor has seen my report and any concerns revealed by such have been resolved with my supervisor. I empower the university to reproduce, for the purpose of research, either the whole or any portion of the contents in any manner whatsoever.

Signature: …Signed by candidate…

Date: 12/02/2021

# *Contents*

# *List of Figures*

# *List of Tables*

# *Nomenclature*

## Abbreviations

| | |
|---|---|
| **ATCC:** | Ammonia-yeast nutrient broth |
| **BDL:** | Below detection limits |
| **$CaCl_2$:** | Calcium chloride |
| **$CaCO_3$:** | Calcium carbonate |
| **CFU:** | Colony forming unit |
| **CUA** | Christensen's urea agar |
| **EDS:** | Energy dispersive X-ray spectroscopy |
| **HCl:** | Hydrochloric acid |
| **$H_2SO_4$:** | Sulphuric acid |
| **ICP-MS:** | Inductively coupled plasma mass spectrometry |
| **kN:** | Kilo newton |
| **MICP:** | Microbially induced calcium carbonate precipitation |
| **MPA:** | Mega pascals |
| **NBA:** | Nutrient broth agar |
| **$NH_4^+$:** | Ammonium ion |
| **PSD:** | Particle size distribution |
| **R2A:** | Reasoner's 2A agar |
| ***S. pasteurii*:** | *Sporosarcina pasteurii* |
| **SEM:** | Scanning electron micrograph |
| **TEA:** | Tailings extract agar |
| **TMTC:** | Too many to count |
| **XRF:** | X-ray fluorescence |

## *Glossary*

| | |
|---|---|
| **Aerobic:** | require presence of oxygen |
| **Acclimatisation:** | process by which an organism adjusts to the selective pressures of its environment |
| **Acid mine drainage:** | outflow of acidic waters from metal mines |
| **Agar:** | a jelly-like substance attained from red algae used to grow bacteria on |
| **Anaerobic:** | existing in the absence of oxygen |
| **Anthropocene:** | current geological age where human activity has had a dominant influence on the environment and climate |
| **Aseptic:** | free from contamination of unwanted bacteria and/or other microorganisms |
| **Bacterial culture:** | method of multiplying microorganisms in a predetermined media culture under a controlled laboratory environment |
| **Bioimmobilisation:** | immobilisation of metals by microorganisms |
| **Bioleaching:** | extraction of metals from ores using microorganisms |
| **Biomass:** | measure of bacterial growth |
| **Biomineralisation:** | process by which microorganisms produce minerals |
| **Bioprospecting:** | screening for microorganisms from unique environments from which commercially valuable compounds can be extracted from |
| **Bioremediation:** | using microorganisms to remove pollutants, toxins and other contaminants from the surrounding environment |
| **Biota:** | plant and animal life of a region |
| **Comminute:** | reduction of a large particle into smaller, finer particles |
| **Cryogenic:** | very low temperatures |
| **Cupric:** | compound containing copper |
| **Deionised water:** | treated water containing no ions |
| **Enzyme:** | biological catalyst |
| **Halophile:** | microorganism capable in surviving in a hypersaline environment |
| **Hydrolysis:** | chemical reaction where water breaks down a compound |
| **In situ:** | a process which takes place on site |

| | |
|---|---|
| **Indigenous:** | originating/native to a particular environment |
| **Inoculate:** | to introduce a microorganism to a new environment |
| **Ionic strength:** | measure of the concentration of all ions in a solution |
| **Isolate:** | pure bacterial strain |
| **Metabolic activity:** | all biochemical reactions undertaken by a microorganism |
| **Mine tailings:** | waste material left over from the separation of the metal fraction from the uneconomic fraction of the ore |
| **Nacre:** | organic material forming the inner shell layer of some molluscs (mother of pearl) |
| **Nucleation site:** | site where the initial formation of a crystal begins |
| **Physiochemical:** | the physical and chemical properties of a substance |
| **Phytoremediation:** | using plants to remove pollutants, toxins and other contaminants from the surrounding environment |
| **Precipitation:** | formation of a solid substance from a solution |
| **Sequestration:** | process of capturing and storing $CO_2$ |
| **Sterile:** | an environment free of all microorganisms |
| **Subculture** | new microbiological culture made by transferring cells from a previous culture into fresh growth medium |
| **Ureolytic bacteria:** | bacteria capable of breaking down urea |

# Chapter 1

## 1. Introduction

For millennia, clay bricks have formed the literal building blocks upon which human civilisations have been built. The utility of bricks is immense, being used to construct such vital things as homes, transport infrastructure, hospitals, dams and powerplants but they also come at a cost.

The construction industry uses a significant amount of limited resources, consuming by weight more raw material (sand, gravel, clay, marble, cement and wood etc.) than all other industries combined (Koroneos and Dompros, 2007). This has led to an immense and unsustainable strain being placed on the environment. To counter this, pressure has been placed on the construction industry to develop sustainable infrastructure that utilises green materials instead. One of the largest transgressors responsible for the high environmental impacts created by the construction industry are bricks. Standard fired clay bricks (230 mm x 110 mm x 70 mm) each consume 4.25 MJ of thermal energy. This translates to approximately 0.20 kg of coal per brick being required while releasing 0.41 kg of carbon dioxide ($CO_2$) (Lippiatt, 2007; Venkatarama Reddy and Jagadish, 2003).

The global impact of cement is even more severe. It is estimated that the current average worldwide consumption of concrete, where cement is the major constituent, amounts to 1 ton per year per person. Due to this extensive use, cement has a significant environmental impact accounting for over 5% of all anthropogenic $CO_2$ emissions (Owens, 2013). As the global population continues to expand and developing countries, particularly in Sub-Saharan Africa and Southeast Asia, rapidly industrialise, a shift to a more sustainable method of brick manufacturing is required if the delicate natural equilibrium of our planet is to be maintained (Müller and Harnisch, 2008).

Fortunately, the ingenuity of nature has supplied a possible alternative to these challenges facing the construction industry. Microbial induced calcium carbonate precipitation (MICP) is a naturally occurring biological process that harnesses the metabolic activities of ureolytic bacteria to produce the bio-cement, calcium carbonate ($CaCO_3$), in the presence of a calcium source (Cheng et al., 2020). This bio-cement has the capability of ‘gluing’ loose solid particles, such as sand, together which can result in the formation of bio-solids such as bricks (Lambert and Randall, 2019). These nature-inspired bio-cemented bricks are known as “bio-bricks” and hold a distinct advantage over traditional masonry units as they require near negligible energy inputs and can use various waste streams during the manufacturing process. This implies that bio-bricks offer the construction industry an alternative brick production process which is intrinsically simple and has the potential to be more sustainable and cheaper than current brick manufacturing processes.

The need for such a process route is even more pressing if one considers that by 2050 over 3 billion people will dwell in informal settlements (Barbière, 2017), necessitating the need for construction materials which are quick to assemble, low cost, low risk and sustainable.

However, two major environmental concerns hinder the sustainability aspect of the process, and hence the upscaling and application of bio-bricks by the construction industry: (1) most bio-bricks are 'grown' using synthetic urea and (2) sand is the most commonly used aggregate for producing bio-bricks (Bu et al., 2018; Cheng et al., 2020; Henze, 2017).

The use of synthetic urea is problematic as it is produced using the Haber-Bosch process which is energy-intensive. Requiring high operating pressures and temperatures, this process is estimated to consume nearly 2% of the global energy supply (Pfromm, 2017). In addition, sand mining is considered to be unsustainable and is responsible for destabilising coastal areas and eroding riverbanks which has made these environments vulnerable to storms and flooding. Added to this, sand is (after water) by volume the largest raw material extracted and traded but has comparatively little regulation (UNEP 2019, 2019). This has resulted in sustainable reserves of sand being depleted rapidly and more and more sand being produced through environmentally damaging extractive practices in sensitive terrestrial, riverine and ocean ecosystems (UNEP 2019, 2019).

To create a sustainable bio-brick it is believed that underutilised 'waste' streams should be exploited to tackle these issues. The applicability of bio-bricks to successfully create value from seemingly waste products has already been demonstrated possible by researchers at the University of Cape Town who created viable bio-bricks using urea extracted from human urine (Lambert and Randall, 2019). By using human urine not only was the need for synthetic urea eliminated but the process also produced a phosphate-based fertiliser (Flanagan and Randall, 2018) by-product which adds additional value to the integrated urine treatment process (Lambert and Randall, 2019). However, the comparatively weaker compressive strength of these urine bio-bricks (2.7 MPa) to traditional fired-clay bricks (14.5 MPa) still needs to be addressed (Lambert and Randall, 2019).

The issue of replacing sand in the bio-brick matrix can be resolved by utilising a waste material such as mine tailings. The increasing global demand for products of the extractive industries has resulted in the concurrent production of vast amounts of mine tailings which are a mixture of gangue minerals and processing solutions that remain after the beneficiation of valuable metals and minerals from ore (Kossoff et al., 2014). The volume of these mine tailings greatly exceeds that of the liberated metals and these tailing often contain toxic contaminants within, such as heavy metals which pose severe risks to surrounding communities and local biota (Kossoff et al., 2014).

To ensure that these heavy metals do not leach out it is essential that mine waste undergoes a remediation process. However, such processes are often costly or cause more environmental damage (Kumari et al., 2016). Bioimmobilisation via MICP of heavy metals in mine tailings has been shown to offer a potential low cost and low-tech alternative to other remediation methods which does not harm the environment (Achal et al., 2011; Kumari et al., 2016; Yang et al., 2016). However, no known attempt has been made to harness this technology to create bio-bricks from mine tailings. Such a process will not only immobilize heavy metals, preventing them from leaching into the surrounding environment, but it would also eliminate any further extraction of sand for bio-brick production. This research therefore aims to establish the feasibility of creating bio-bricks from copper mine tailings by utilising the MICP process. Bio-columns were used as a proxy for bio-bricks to test the technical feasibility of the process because they require less resources (reagents, chemicals etc.) to manufacture. Nonetheless, the lessons learnt from growing these bio-columns can also be used for growing bio-bricks.

If the bio-columns grown in this study establish that bio-bricks can be both technically and economically viable, it is hoped that this work will form the basis for future bio-brick production from copper mine tailings. Such novel copper mine tailing bio-bricks would not only eliminate the strain on rapidly dwindling resources but also help remediate existing damages caused by anthropogenic activities, while creating value from what was once considered a ‘waste’ stream.

### *1.1. Project Aims*

The intersection of engineering and biology has resulted in a novel process to produce bio-bricks from human urine that have the potential to reduce the large carbon footprint of the construction industry. The sustainability of these bio-bricks can be further expanded by upcycling untapped sources of harmful waste material created by anthropogenic activities. Therefore, the aim of this project was to establish the technical and economic feasibility of repurposing copper mine tailings, based on the principles of MICP, into a bio-solid of higher value.

### *1.2. Scope*

The scope of this project involved determining the feasibility of repurposing copper mine tailings for use as the aggregate in the production of bio-bricks. Due to limited chemical and reagent resources, smaller bio-columns were grown and tested as a proxy for bio-brick production. Additionally, as part of the technical analysis, an investigation was conducted into the ability of the designated ureolytic bacteria (*S. pasteurii*) to grow in and/or acclimatise to an environment of high copper concentrations. Further, an attempt was made to isolate ureolytic bacteria indigenous to copper mine tailings. This research only considered MICP processes dictated by the enzymatic hydrolysis of urea catalysed by the enzyme urease and only copper mine tailings were investigated. Synthetic urea was used as a proxy for human urine due to the large volumes required and to allow for a greater consistency between experimental sets. For the economic feasibility analysis only operating costs were included and all capital expenses were excluded. The duration of experimental procedures as well as the periods at which experimental data was logged was restricted due to curfew restrictions (22:00 - 4:00) implemented during the COVID-19 pandemic.

# Chapter 2

# 2. Literature Review

## 2.1. Overview of microbial induced calcium carbonate precipitation

Microbial induced calcium carbonate precipitation (MICP) is a naturally occurring biomineralisation process which harnesses the metabolic capability of some microorganisms to induce calcium carbonate ($CaCO_3$) precipitation in the presence of urea and a calcium source (Cheng et al., 2020). The precipitation of calcium carbonate by MICP is facilitated through the hydrolysis of urea by the enzyme urease, with the enzymatic hydrolysis of urea being approximately $10^{14}$ times faster than the natural chemical decomposition of urea (Jabri et al., 1995).

MICP induced by ureolytic bacteria requires the presence of urea and a calcium-rich solution which permits the precipitation of calcium carbonate and involves a series of biochemical reactions (Kumari et al., 2016). Equation 1 shows the enzymatic hydrolysis of urea to form ammonia and carbamate which is then spontaneously hydrolysed into ammonia and carbonic acid (2). These products are then further hydrolysed according to reactions (3) and (4) to form bicarbonate, ammonium and hydroxyl ions. The resulting increase in pH favours the shifting of equilibrium reaction (5) forward into forming carbonate ions (Kumari et al., 2016).

$$CO(NH_2)_2 + H_2O \xrightarrow{\text{urease}} NH_2COOH + NH_3 \quad (1)$$

$$NH_2COOH + H_2O \rightarrow NH_3 + H_2CO_3 \quad (2)$$

$$H_2CO_3 \leftrightarrow HCO_3^- + H^+ \quad (3)$$

$$2NH_3 + 2H_2O \leftrightarrow 2NH_4^+ + 2OH^- \quad (4)$$

$$HCO_3^- + H^+ + 2NH_4^+ + 2OH^- \leftrightarrow CO_3^{2-} + 2NH_4^+ + 2H_2O \quad (5)$$

With the overall biochemical reaction mechanism being:

$$CO(NH_2)_2 + 2H_2O \rightarrow CO_3^{2-} + 2NH_4^+ \quad (6)$$

In a calcium-rich solution, the ureolytic bacteria will attract surrounding calcium ions to their surface (7) and thus, together with the now increased carbonate ion concentration, result in the precipitation of calcium carbonate around the surface of the bacterial cells (8) (Kumari et al., 2016):

$$Ca^{2+} + \text{Cell} \rightarrow \text{Cell-}Ca^{2+} \quad (7)$$

$$\text{Cell-}Ca^{2+} + CO_3^{2-} \leftrightarrow \text{Cell-}CaCO_3 \downarrow \quad (8)$$

Figure 2.1 illustrates and summarises the above biomineralisation process detailing how calcium carbonate is formed via MICP when a ureolytic bacteria encounters a urea-calcium solution.

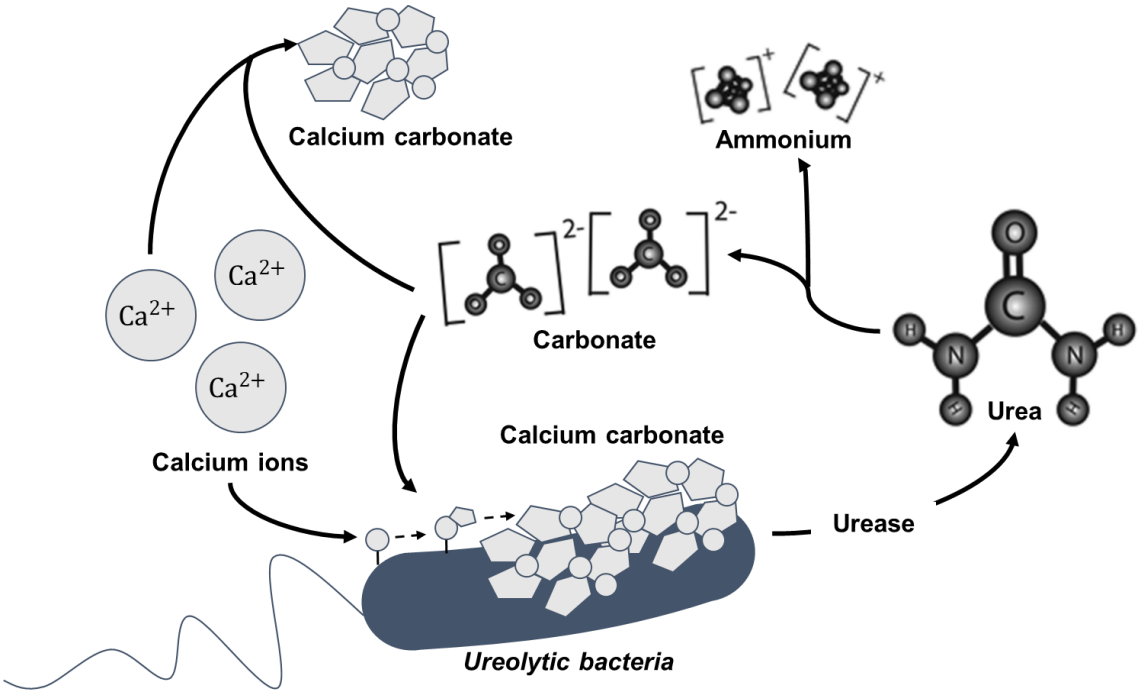


**Figure 2.1:** Diagram representing the mechanism of precipitation of calcium carbonate by a ureolytic bacteria via microbial induced calcium carbonate precipitation in a urea-calcium solution. Calcium ions migrate towards the ureolytic bacteria which acts as a natural nucleation site for MICP to occur. Urea is hydrolysed by the urease enzyme released from the bacterium which results in the eventual formation of carbonate ions. The increased concentration of carbonate ions allows for the formation of calcium carbonate when contacted with calcium ions. Adapted from (Li et al., 2014).

The calcium carbonate precipitate formed acts as a cementing agent which binds together loose material (such as sand) resulting in the formation of solid particles as shown in Figure 2.2, which further illustrates the three main arrangements in which calcium carbonate can deposit over loose solid material (Lin et al., 2016): (a) by precipitating around the sold grain contact points (contact cementing); (b) coating the solid particles or filling the void space between the solid particles but without coming into contact with a solid particle (grain coating) or (c) creating bridges which span the void gaps between the surfaces of the solid particles (matrix supporting).

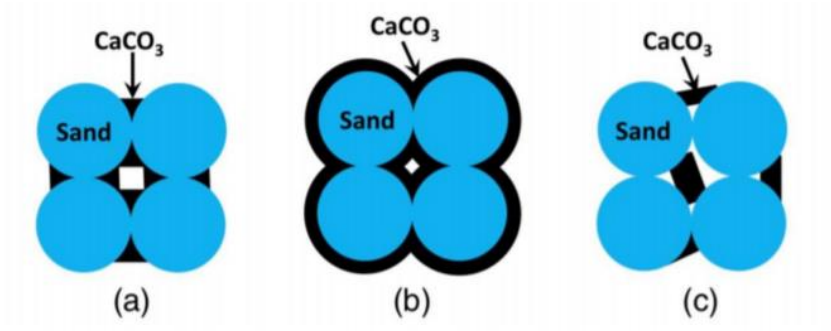


**Figure 2.2:** Possible arrangements of calcium carbonate precipitation around sand particles during MICP: (a) contact cementing, (b) grain coating and (c) matrix supporting (Lin et al., 2016).

Calcium carbonate can exist in six differing polymorphic forms: as three anhydrous polymorphs: calcite, aragonite and vaterite; as two hydrated crystalline species: monohydrocalcite and ikaite; and one amorphous form (Dickinson and McGrath, 2004). Of the three anhydrous crystalline forms, calcite is the most thermodynamically stable under ambient aqueous conditions (calcite > aragonite > vaterite) (Plummer and Busenberg, 1982). As such vaterite is rarely found in nature but both calcite and aragonite are frequently found in rocks or biominerals (Kamhi, 1963). Aragonite is of particular interest as it is a key component (approximately 95% (v/v)) of the biomineral nacre (also known as mother-of-pearl) , where the structure of aragonite crystals results in an extraordinary tensile strength of between 140-170 MPa (Jackson et al., 1988). Although showing huge potential, its application as a usable material is limited as synthetic crystallisation systems (such as MICP) have so far only been shown to generate a small fraction of aragonite compared to calcite at ambient conditions without the addition of additives (Ogino et al., 1987).

It has been determined that the shape of the calcium carbonate crystals is influenced by the rate of urea hydrolysis; with higher rates resulting in amorphous calcium carbonate and vaterite and lower hydrolysis rates resulting in predominantly calcite (Lin et al., 2016). Figure 2.3 details the characteristic shape of the three anhydrous isomorphs as well as the amorphous form of calcium carbonate: Vaterite (A) forms as large spherical crytsals, which are almost bulbous in nature. This is contrasted by aragonite (B) which forms as thin, needle-like crystatilne structures and calcite (C), which is commonly found in nature and forms as large rhombohedral crystals. Amorphous (D) calcuim carbonate lacks a clearly defined shape or structure. Being the least stable of the calcium carbonate polymoprhs, it generally exists as a precusor phase in biological systems which later transitions into a more stable crystalline form (calcite or aragonite) (Albéric et al., 2018).

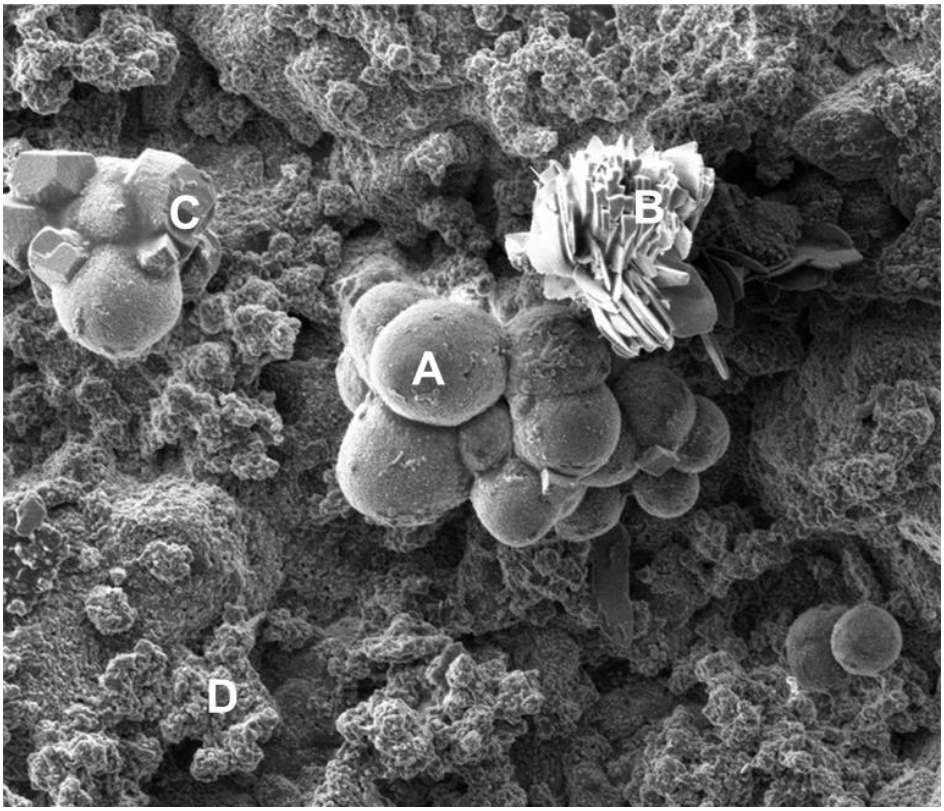


**Figure 2.3:** Scanning electron micrograph at 2 000 X magnification of a MICP produced bio-brick fragment detailing the differences in morphology of: (A) vaterite, (B) aragonite, (C) calcite and (D) amorphous (de Oliveira and Fahn, 2019).

There have been numerous investigations into different applications for MICP, including bioimmobilisation of heavy metals in mine tailings (Achal et al., 2011; Buikema, 2015; Kumari et al., 2016; Yang et al., 2016), $CO_2$ sequestration (Mitchell et al., 2010), bio-mediated soil improvement (DeJong et al., 2010; Soon et al., 2014), bio-cement to repair and remediation of cracks in concrete structures (Achal et al., 2013; Ramachandran et al., 2001) and an alternative construction material (Bernardi et al., 2014; Bu et al., 2018; Cheng et al., 2020). One possible alternative material which can be produced by the MICP process is a bio-brick, which has the potential to be a more sustainable and economical compared to conventional bricks used within the construction industry (Bernardi et al., 2014; Lambert and Randall, 2019)

The feasibility of creating such bio-bricks utilising synthetic urea (Henze, 2017) as well as using human urine (Lambert and Randall, 2019) as a source of urea have already been investigated. These feats were accomplished by using a system through which a cementation solution consisting of calcium ions and urea was sporadically pumped through a mould (see Figure 2.4 A). This mould contained within it a mixture of beach sand and Greywacke (a type of aggregate) which had previously been inoculated by the ureolytic bacteria, *Sporosarcina pasteurii*. Over a period of days the metabolic activities of the bacteria gradually resulted in calcium carbonate precipitation binding together, resulting in the creation of a solid bio-brick (Henze, 2017; Lambert and Randall, 2019).

Although this pumping method has been shown to be successful in producing viable bio-bricks, it is a labour-intensive process which limits the amount of bio-bricks that can be produced on an industrial scale. More recently, submergent methods (Bu et al., 2018; Cheng et al., 2020; Zhao et al., 2014) of growing bio-bricks have been developed (see Figure 2.4 B). This method involves the submerging of a loose sand matrix, inoculated with ureolytic bacteria, and moulded into the dimensions of a brick (or any desired shape) directly into the cementation solution. The cementation solution is kept homogenous through mixing. Over a period of days, as the solution diffused throughout the bio-brick material, bacterially controlled MICP processes resulted in the formation of a solid in the shape of bio-brick (Cheng et al., 2020). This submergent method is advantageous as it requires little labour input and near negligible energy requirements, as well as allowing for a large increase in the amount of bio-bricks produced as individual moulds are no longer needed.

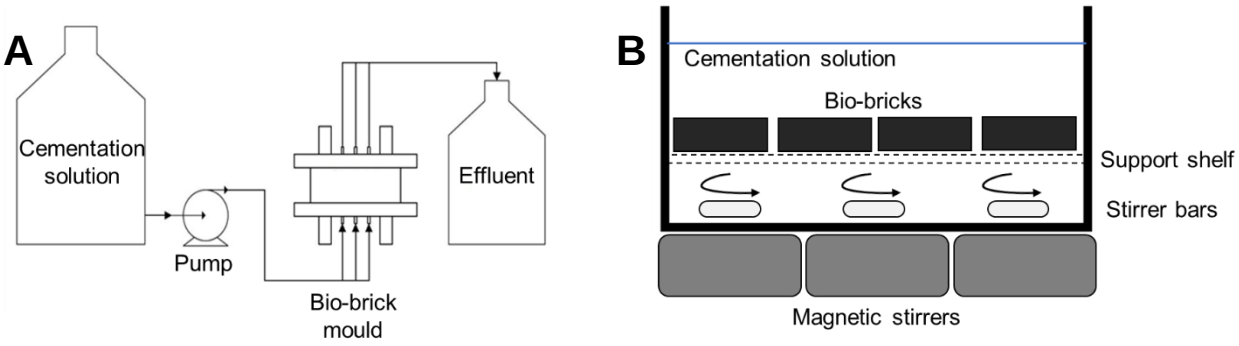


**Figure 2.4:** Schematics of possible systems which could be employed to manufacture bio-bricks via MICP: (A) details the pumping method employed by (Henze, 2017; Lambert and Randall, 2019) and (B) the submergent method applied by (Cheng et al., 2020). Figure B is adapted from (Cheng et al., 2020).

### *2.2. The role of bacteria in MICP processes*

Bacteria have an integral role in the formation of bio-solids as they provide the urease required for the biochemical reactions to proceed (Lambert and Randall, 2019). Although not entirely resolved, it is also thought that the bacteria used during the MICP process are responsible for: (1) increasing the alkalinity of the surrounding environment which favours the precipitation of calcium carbonate; (2) creating a localised concertation gradient which results in the improved efficiency of the MICP process and (3) serving as local crystal nucleation sites (See Figure 2.5B) (Krajewska, 2009).

Numerous and diverse varieties of ureolytic bacteria exist which have the capability to induce MICP (Kumari et al., 2016). It has been shown that the type of bacterial strain used during the MICP process affects the morphological characteristics (size, structure and appearance) of the calcium carbonate crystals precipitated as well as crystal type (calcite, aragonite, vaterite etc.) (Dhami, 2013; Hammes et al., 2003).

These impacts on morphology and crystal type, though not well understood, have been hypothesised to be attributed to either the extracellular polymeric substance (EPS) of the individual bacterium (Dhami, 2013) or due to the apparent presence of different urease genes in the bacterial isolates (Hammes et al., 2003).

The choice of ureolytic bacteria used in a MICP process is thus influenced by the type of product required as well as how adapted the microorganism is to the new environment. *Sporosarcina pasteurii* (*S. pasteurii*) is the model bacteria most commonly applied in MICP processes for bio-brick production (Cheng et al., 2020; Henze, 2017; Lambert and Randall, 2019). This is mainly as a result of *S. pasteurii* being non-pathogenic, having a strong tolerance for the highly alkaline conditions found during bio-brick production (Henze and Randall, 2018) and being capable of producing large volumes of urease (Lambert and Randall, 2019). These rod-shaped gram-positive microorganisms (Figure 2.5A), which are 2-3 µm in length, are also facultative anaerobes and halotolerant – making their application ideal for the inherently low oxygen and saline environment created during bio-brick production (Henze and Randall, 2018). Despite these advantages, the sterility requirements and high cost of the preferred cultivation media of *S. pasteurii* remains one of the largest production costs encountered during bio-brick production, preventing their widescale use in the construction industry.

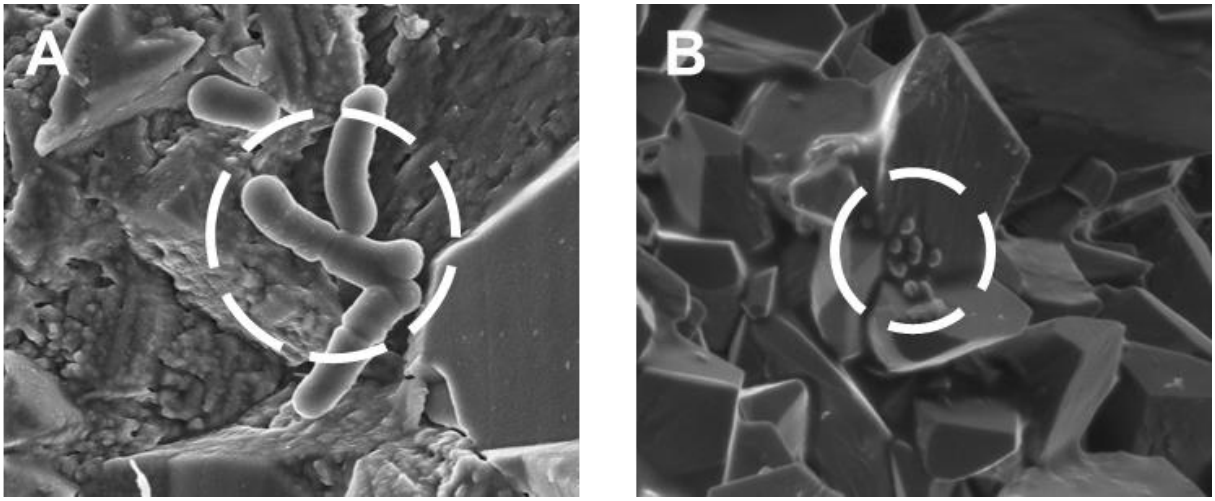


**Figure 2.5**: Scanning electron micrographs of (A) the morphology of S. pasteurii at 20 000 x magnification and (B) of what appears to be S. pasteurii, at 10 000 x magnification, entombed within a calcium carbonate crystal, hinting to the bacteria's importance as a nucleation site required for MICP to occur (de Oliveira and Fahn, 2019).

### 2.3. *Human urine - an environmentally friendly source of urea*

Bio-bricks grown utilising synthetic urea have been proposed to be a greener alternative to the manufacture of traditional masonry bricks. The US-based firm BioMason® is already in the process of commercializing synthetic urea based bio-bricks, and have shown that it is possible for such bio-bricks to have a comparative compressive strength to traditional bricks at 16.6 MPa with a large reduction in energy inputs (Dosier, 2017). However, any energy savings made through this biological process may be offset, when looking holistically at the bio-brick life cycle, by the use of synthetic urea as its production requires the use of the Haber-Bosch process which utilizes high pressures and temperatures (Razon, 2014). This large energy input can be overcome by sourcing an alternative, greener source of urea. One such possible candidate is the underutilised 'waste' stream, human urine, which contains a high urea concentration (approximately 9.3 – 23.3 g/L) and is widely available (Randall and Naidoo, 2018).

Containing a large number of other key resources - such as phosphorous and nitrogen - which can be utilised to create beneficial by-products, urine has been dubbed 'the liquid gold of wastewater' (Randall and Naidoo, 2018) and has the potential to create a more sustainable MICP bio-brick process. The benefit of utilising urine is not only in reducing energy costs, but in that it allows for additional value to be extracted from the process in the form of an inorganic fertiliser (calcium phosphate), which is a by-product formed during the urine treatment process (Flanagan and Randall, 2018). This is in addition to the ammonium sulphate fertiliser which could also be produced downstream of the bio-brick process (Lambert and Randall, 2019). As a result, if the production of bio-bricks via MICP utilises urine as a source of urea, it has the potential to significantly reduce energy inputs while producing valuable by-products such as calcium phosphate and ammonium sulphate (Lambert and Randall, 2019) as illustrated in Figure 2.6.

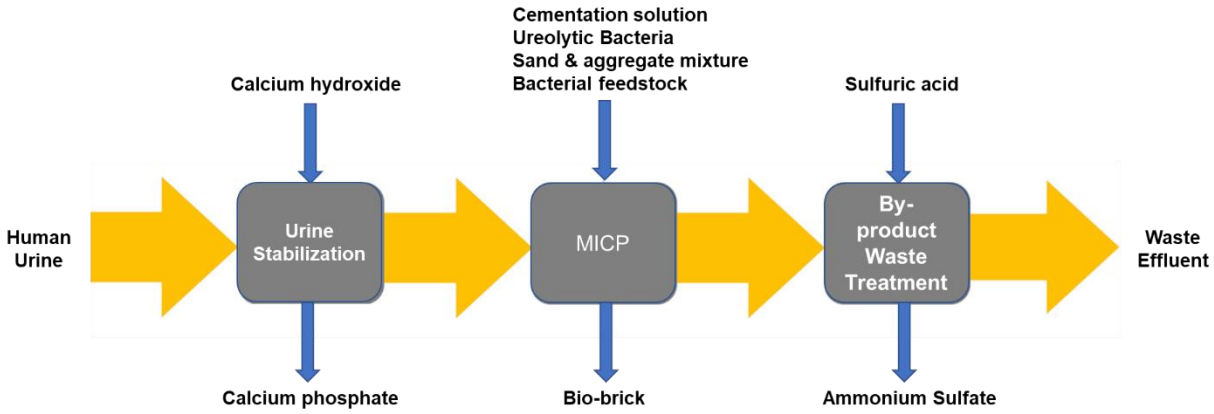


**Figure 2.6:** Theoretical process flow diagram for the production of bio-bricks utilising human urine, detailing required inputs as well as resultant outputs. By utilising human urine this MICP process does not only result in reduced energy inputs but also in the production of two valuable fertiliser by-products as well as the bio-bricks themselves. Adapted from (Lambert and Randall, 2019).

Furthermore, by extracting nutrients from urine upstream the mechanisms required to purify wastewater downstream will be alleviated which will further contribute to reducing the energy footprint of this process – for example it has been shown that the separation of urine upstream could result in the transformation of wastewater treatment plants into energy producing plants (Wilsenach and van Loosdrecht, 2003). However, the downside of manufacturing bio-bricks from urine is that they have, as of now, a low compressive strength (2.7 MPa) compared to conventional bricks (Lambert and Randall, 2019).

### *2.4. Treating and stabilising human urine*

Due to the large volumes of urine needed for bio-brick production the extended storage of collected urine is needed (Lambert and Randall, 2019). However, due to the inevitable presence of urease within urine, either from bacteria inherently within urine itself or from surrounding environmental bacteria, if left untreated the urine will begin to undergo enzymatic hydrolysis of urea as described previously in Equation 1:

$$CO(NH_2)_2 + H_2O \xrightarrow{\text{urease}} NH_2COOH + NH_3 \quad (1)$$

This reaction will result in the volatilisation of ammonia and the subsequent release of its characteristic unpleasant smell, resulting in environmental pollution as well as the loss of a corresponding amount of nitrogen which could be used as a fertiliser instead (Chipako and Randall, 2020) or for the production of bio-bricks. The extent of this loss of urea to ammonia in stored urine is detailed in Figure 2.7. The loss of urea (via Equation 1) will also limit the potential amount of calcium carbonate which can be precipitated during the MICP process.

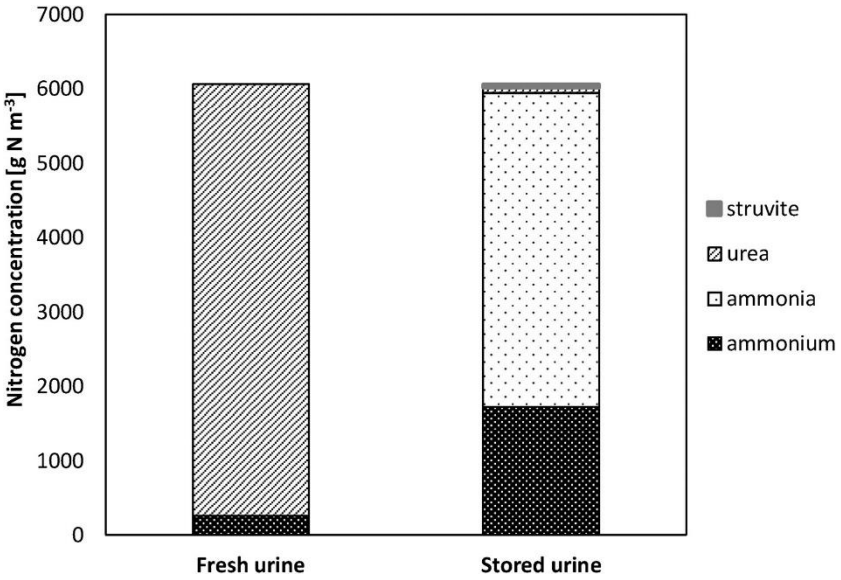


**Figure 2.7:** Figure detailing how nitrogen is distributed in fresh and stored urine (Henze and Randall, 2018).

Thus, if urine is to be stored for an extended period for later use, it requires a 'stabilisation' method which inhibits the activity of urease. Stabilisation for the context of this research simply refers to the maintaining the nitrogen in urine as urea by delaying urea hydrolysis.

Such stabilisation methods include: (1) the addition of acid (Hellström et al., 1999); (2) electrochemical treatment (Ikematsu et al., 2007); (3) the addition of heavy metal ions such as $Cu^{2+}$ (Zaborska et al., 2004) or (4) increasing the pH (>11) of urine using calcium hydroxide ($Ca(OH)_2$) (Randall et al., 2016) or magnesium oxide (Simha et al., 2021). Although the addition of acid to urine has been shown to successfully inhibit urease activity, allowing for long-term storage, its practical application is limited due to the dangers in handling high acid concentrations as well as due to requiring pumping and exact dosing equipment (Randall et al., 2016). Using electrochemical treatment is also complicated by the fact that this method only allows for short-term storage and does not prevent urine from coming into later contact with urease-producing microorganisms (Randall et al., 2016). Previous research has shown that urease is particularly sensitive to the addition of heavy metal ions and the inhibitory efficiency of metal ions towards urease has been reported in literature as: $Hg^{2+}>Cu^{2+}>Zn^{2+}>Cd^{2+}>Ni^{2+}>Pb^{2+}>Co^{2+}>Fe^{3+}>As^{3+}$ (Zaborska et al., 2004). For such an application to be feasible in stabilising urine, it would be essential that enzyme activity could be restored after exposure the metal ions. Restoration of the urease after heavy metal exposure ($Hg^{2+}$) has been shown to be possible by Zaborska and colleagues (2004) with the addition of dithiotreitol within the first two minutes of exposure. Thus, as of now, applicability of using heavy metal ions for the long-term storage remains elusive.

As such, inhibiting the enzymatic hydrolysis of urea by raising the pH level is seen as being the most suited solution to the solving the challenge of storing large volumes of urine for the MICP process. Calcium hydroxide is an effective base to increase the pH of a solution because it is cheap and widely available (Randall et al., 2016). In addition, the high pH considerably limits the amount of pathogens within urine (Eriksen et al., 1996; Pancorbo and Overman, 1988) and that it results in calcium phosphate being precipitated out of the human urine which can be sold on as a fertiliser (Flanagan and Randall, 2018) rather than precipitating within a bio-solid such as a bio-brick. Importantly, the use of this stabilisation method as demonstrated by the urine bio-brick process developed by Lambert and Randall (2019) merely delays the onset of Equation 1, allowing it to be reinitiated when required within a bio-brick mould. Figure 2.8 describes the conditions at which urea is degraded, be it by the chemical or enzymatic hydrolysis of urea (Randall et al., 2016). The lightly shaded rectangular area represents the conditions where enzymatic urea hydrolysis occurs and line 2 to 3 illustrates the ideal operating line.

The ideal operating line shows that to have minimal urea losses, urine must be stored between a temperature of approximately 15°C - 40°C and at a pH greater than 11 but less than 13. Thus, according Figure 2.8, the stabilisation of urine can easily be achieved at 25°C and a pH of 12.5, which is the saturation pH of the solution.

On a practical level, the stabilisation of urine can thus be achieved by a passive dosing system where excess amounts of calcium hydroxide are added to urine collection devises and the calcium hydroxide dissolves as required to maintain the desired high pH at saturation with respect to the calcium hydroxide. It has been recommended, that 10 g $Ca(OH)_2$ per litre of urine is adequate to maintain the required pH of 12.5 assuming ambient temperature is 25°C (Randall et al., 2016) and ensures this pH for a wide range for urine compositions. Through this method, Randall and colleagues demonstrated that urea hydrolysis could be successfully inhibited in stored urine for a minimum of 27 days. Such a stabilisation process would therefore ensure that there is a steady supply of stored urine by controlling the pH of the urine (Chipako and Randall, 2020) with minimal losses of urea, for later use in MICP processes while also producing a valuable source of calcium phosphate.

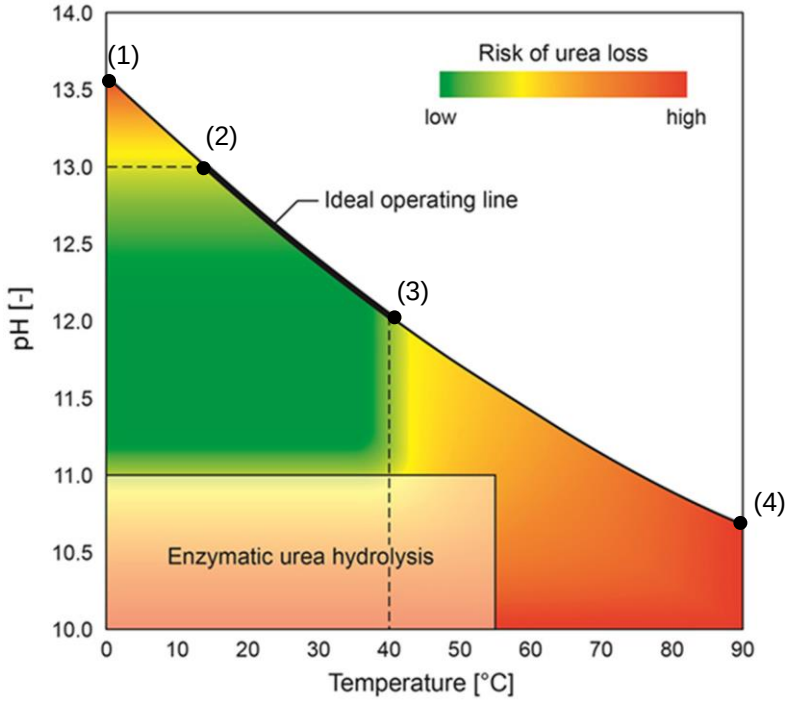


**Figure 2.8:** Design chart describing the conditions for urea stabilisation (where negligible urea loss occurs) in green, the conditions at which enzymatic urea hydrolysis occurs ($0 < T < 55$°C and $10 < pH < 11$) in the bottom left rectangle as well as the conditions where the chemical decomposition of urea is more likely to occur in yellow-orange-red. Dark red describes the conditions at which the greatest loss of urea is most likely to occur. The $Ca(OH)_2$ saturation pH curve is described by lines (1) through to (4) and the ideal operating lines is described by line (2) to (3) (Randall et al., 2016).

### 2.5. Impact of initial pH on MICP processes

As discussed previously, for urine to be successfully stored at room temperature it must be stabilised to a pH above 11 using calcium hydroxide. Such a high pH creates a hostile environment which is too extreme for most bacteria to survive including *S. pasteurii*. For this reason, the pH of stored urine must be decreased to a suitable level before any MICP process can occur to allow the bacterium to undergo all necessary metabolic activities. As such, it has been determined previously that *S. pasteurii* can successfully survive a maximum initial pH of 11.2 (Henze and Randall, 2018).

As a pH of 11.2 falls within range of both urease inhibition and bacterial activity, it makes it the ideal pH for the initial cementation solution. It has also been determined that MICP is in fact improved by increasing the pH of the cementation solution (Henze and Randall, 2018). This is illustrated by the speciation curve in Figure 2.9 which shows that at higher pH levels the formation of carbonate ions is favoured. A greater availability of carbonate ions results in a greater chance of calcium carbonate being precipitated as detailed previously in Equation 8.

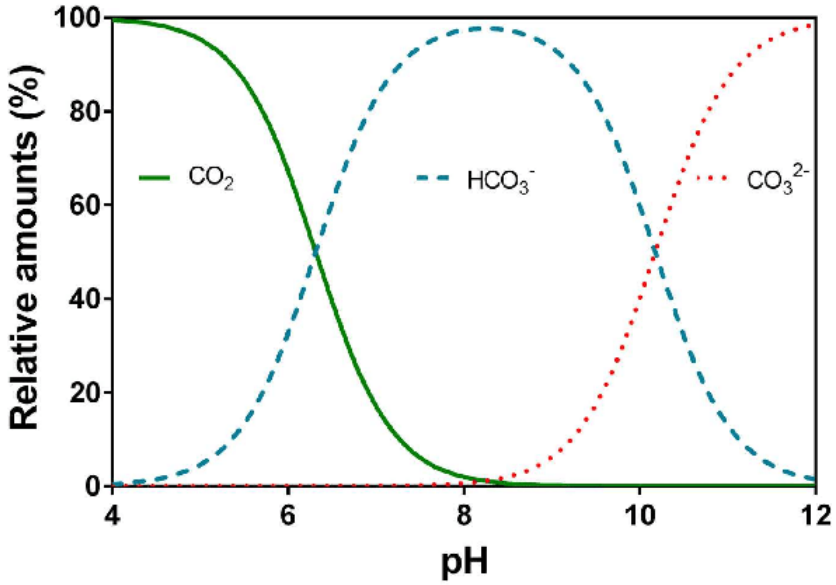


**Figure 2.9:** Speciation curve detailing the relative distribution of dissolved carbon dioxide (green), bicarbonate (blue) and carbonate ions (red) as a function of pH in water at 20°C (Pedersen et al., 2013). At elevated pH levels the bicarbonate ions are further dissociated into carbonate ions. The greater volumes of carbonate ions available will contribute to greater levels of calcium carbonate precipitation during MICP processes, thus improving the overall efficiency of the process.

### 2.6. Impact of influent calcium concentration on MICP processes

For the MICP process to precipitate calcium carbonate a source of calcium ions, typically calcium chloride ($CaCl_2$), is needed as seen in Equation 8. $CaCl_2$ is chosen as it is cheap and readily available. However, the addition of extra calcium and chloride ions also increases the ionic strength of the solution (Henze and Randall, 2018). If a low calcium concentration in the cementation solution is applied, then by analysis of Equations 6 and 8, the calcium ions become the limiting reactant within the process.

Therefore, in theory, a ratio of one mole of calcium to one mole of urea should result in maximum precipitation of calcium carbonate. This however does not seem to be the case. When bio-brick experiments were carried out utilising synthetic urea, it was noted that an initial calcium concentration that is approximately a third higher than the concentration of urea resulted in an overall decrease in urease activity (Henze, 2017). This has been attributed as a potential stress reaction by the ureolytic bacteria in response to the increased ionic strength of the cementation solution caused by the addition of calcium chloride (Lambert and Randall, 2019).

### 2.7. Impact of ionic strength on MICP processes

As detailed above it has been theorized that a high ionic strength (which is a function of the concentration of all ions present in a solution) reduces the efficiency of the MICP process as result of creating a hostile environment which the urease-producing bacteria cannot tolerate. Human urine too has an inherently high ionic strength (~0.429), detailed in Table 2.1, which is believed to be one of the causes of the lowered compressive strength of urine bio-bricks when compared to conventional cement bricks (Lambert and Randall, 2019).

**Table 2.1:** Details the resultant overall ionic strength of fresh human urine as a result of constituent components, adapted from (Lambert and Randall, 2019).

| **Human Urine** | |
|---|---|
| **Species** | Ionic Strength (mol/L) |
| **Acetate** | 0.106 |
| **$NH_3$** | 0.030 |
| **P** | 0 |
| **Ca** | 0.029 |
| **Mg** | 0 |
| **Na** | 0.104 |
| **K** | 0.009 |
| **S (6)** | 0.025 |
| **Cl** | 0.125 |
| **N** | 0.001 |
| **Overall** | 0.429 |

The ureolytic activity of urease, the enzyme released by *S. pasteurii* during the MICP process, has been shown by previous research to be adversely impacted by high ionic strengths (Kistiakowsky and Shaw, 1953). This adverse relationship is illustrated in Figure 2.10, which shows that the rate of enzymatic urea hydrolysis is severely hindered by the high ionic strengths found during the bio-brick production via the MICP process. As the high ionic strength of stabilised urine negatively impacts the ability of urease to hydrolyse urea; it has been theorised that less carbonate ions are available for calcium carbonate precipitation which in turn is responsible for the weaker compressive strength of human urine bio-bricks as seen in Table 2.2 (Lambert and Randall, 2019).

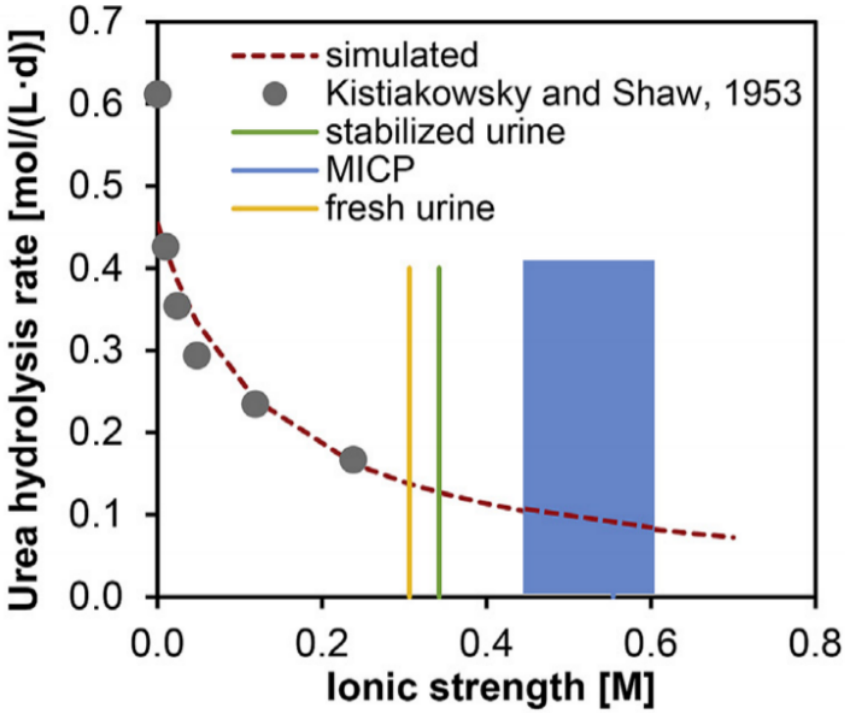


**Figure 2.10:** Graph illustrating the adverse impact of increasing ionic strength on the rate of enzymatic urea hydrolysis together with the typical ionic strength of fresh urine (yellow) and stabilised urine (green) as well as detailing the range of ionic strength found during MICP driven bio-brick production (blue) (Lambert and Randall, 2019).

As it has been shown by previous research that it is possible for *S. pasteurii* to grow in saline conditions equivalent to that of a marine environment (Mortensen et al., 2011) i.e. that of a high ionic environment. As such it seems that high ionic strengths only adversely impacts the activity of urease and not the growth potential of the bacterium. For this reason, methods devised to overcome the high ionic strength of urine should concentrate on physical means rather than on biological methods in which the ureolytic bacteria are acclimatised to environments of higher ionic strengths.

Physical means of reducing the ionic strength of urine could be achieved by either using evaporation or reverse osmosis technologies (Chipako and Randall, 2020). By removing the spectator ions in respect to the MICP process, these methods result in the extraction of either pure urea crystals (evaporation) or a concentrated urea solution (from reverse-osmosis) – both would result in negligible levels of ionic strength. Now containing a significantly lowered ionic strength, calcium chloride could then be added into the cementation solution in an equimolar amount to the urea.

This method would theoretically result in the growth of a stronger bio-brick as the reduced impact of ionic strength on urease will result in more carbonate ions being produced which, together with an increase of surrounding calcium ions, should increase the potential for calcium carbonate precipitation. Possible bio-brick process schemes, as seen in Figure 2.11, which extract urea from urine for the production of bio-bricks were envisioned by (de Oliveira and Fahn, 2019).

de Oliveira and Fahn (2019) also investigated the impact of ionic strength on bio-brick compressive strength and found that using a synthetic source of urea, together with an equimolar ratio of urea to calcium chloride, resulted in a bio-brick with a compressive strength of 16.1 MPa. This is nearly a six-fold increase to the urine bio-bricks produced by Lambert and Randall (2019) (see Table 2.2). However, only one bio-brick was produced by de Oliveira and Fahn and process optimisation was not investigated, hence further research is required.

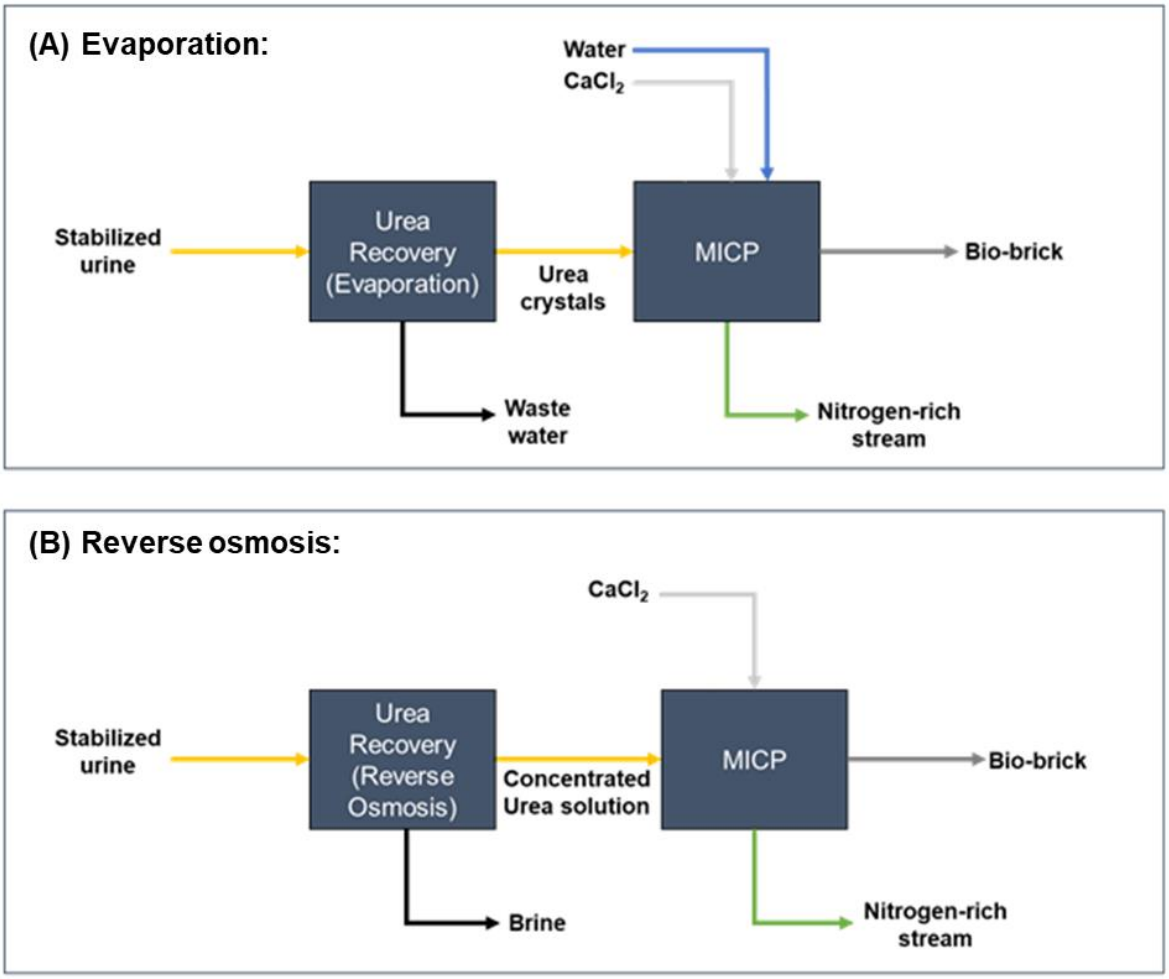


**Figure 2.11:** Possible process streams for the production of bio-bricks via MICP utilising human urine which has been deionised through either (A) evaporation or (B) reverse osmosis as envisioned by (de Oliveira and Fahn, 2019).

Alternatively, although it has been shown that a high ionic strength does have an impact on the growth of *S. pasteurii*, it is known that there are differences between the types of urease produced by different ureolytic species (Hammes et al., 2003). Thus, bioprospecting for halophilic bacteria, known as halophiles, in hypersaline environments may result in the discovery of a strain of bacteria capable of producing a type of urease which is more tolerant towards the high ionic environment of stabilised urine. It has also been shown by (de Oliveira and Fahn, 2019) that a large diversity of ureolytic bacteria exist within easily accessible environments such as marine harbours; some of which seem to produce greater volumes of urease than *S. pasteurii*.

### *2.8. Compressive strength of bio-bricks*

Compressive strength is the ratio of the uniaxial applied load at failure divided by the cross-sectional area of the object being tested (Broughton, 2012). As it allows for the determination of a materials load bearing capacity, compressive strength is therefore a key parameter in providing guidance for assessing the applicability of a material to certain tasks and environments, for this reason, it is desirable that any bio-bricks grown have a compressive strength on par with or greater than traditional masonry units such as fired-clay bricks or cement bricks. Currently, as can be seen in Table 2.2, urine bio-bricks (2.7 MPa) are significantly weaker than traditional masonry units (14.5 MPa) but progress in recent years has led to higher compressive strengths when using synthetic urea to grow bio-bricks (16.6 MPa and 16.1 MPa).

**Table 2.2:** Comparison of differing masonry units and their respective compressive strengths

| | Compressive Strength (MPa) | References |
|---|---|---|
| **BioMason® bio-brick** | 16.6 | (Dosier, 2017) |
| **Synthetic urea bio-brick** | 16.1 | (de Oliveira and Fahn, 2019) |
| **Fired-clay brick** | 14.5 | (Lambert and Randall, 2019) |
| **Cement brick** | 10.43 | (Reddy et al., 2007) |
| **Submergent bio-brick** | 9.70 | (Cheng et al., 2020) |
| **Human urine bio-brick** | 2.70 | (Lambert and Randall, 2019) |

### *2.9. The issue of sand*

To create a truly environmentally friendly bio-brick, it is not enough to only replace synthetic urea. Currently, most bio-bricks are produced by cementing a mixture of fine sand and coarse aggregate particles together using calcium carbonate (Bernardi et al., 2014; Henze, 2017; Lambert and Randall, 2019). Though effective in forming a solid bio-brick matrix, the extensive use of sand is problematic.

Sand has seen extensive and significant use within the construction industry for thousands of years – it has been used for construction of buildings and urban infrastructure, to make glass and concrete, to fill roads and for land reclamation (Sonak et al., 2006). The demand for sand continues to grow exponentially, particularly in industrializing countries, where rapid economic development is driving the strong growth of construction industries (de Leeuw et al., 2010). This too is the case in South Africa where the primary mandate of the government is based on service delivery which necessitates the large-scale construction of schools, housing, dams and healthcare facilities (Asabonga et al., 2017).The use of sand as a natural resource is in fact so important that the United Nations Environment Programme (UNEP) has stated that “sand and gravels are the unrecognized foundational materials of our economies” (UNEP 2019, 2019).

This is further emphasised by the fact that after fresh water, sand and gravels represent the highest volume of raw material used on earth (Chilamkurthy et al., 2016). But the overreliance on this versatile, but precious material comes at a significant environmental cost.

Anthropogenic activities involved with and including sand mining have been shown to adversely impact surrounding ecology and societies physically, biologically and chemically (Sonak et al., 2006). Sand miners clear off vegetation prior to sand extraction to make way for roads and other equipment, which significantly adds to the amount of vegetation already cleared for the open mine pits needed to extract quality sand and gravels (Asabonga et al., 2017). This large-scale clearance of vegetation and subsequent land exposure, results in the formation of gullies and a heightened risk of landslides which can pose a serious risk to local communities (Asabonga et al., 2017). As well as this, sand mining has been identified as being directly responsible for the erosion of coastal areas and instability of riverbanks which significantly increases the vulnerability of surrounding areas to flooding and storms. This has been shown to impair groundwater systems which negatively affects the supply of fresh water to local communities (Sonak et al., 2006). These threats all are due to sand mining causing changes in river flow, channel changes and floodplain alterations (Sonak et al., 2006; Sreebha and Padmalal, 2011). The dredging for sand in marine environments also results in severe habitat destruction, resulting in a major decline in both the biomass and species richness of this environment (Desprez, 2000; Kondolf, 1997; Le Bot et al., 2010).

These negative impacts are bound to worsen with an ever-expanding global population, along with sand becoming a more scarce resource as emphasised by UNEP which recently stated that sand cannot be produced from our terrestrial, riverine and marine environments in quantities needed to meet demand from a world of 10 billion people without effective policy, planning, regulation and management (UNEP 2019, 2019). Thus, as the environmental impacts of sand mining are significant and as sand increasingly becomes a scares commodity, an alternative solid particle material is needed if the industrial-scale production of eco-friendly bio-bricks is to come to fruition. One possible material which could replace sand in the bio-brick matrix is mine tailings.

### *2.10. Mine tailings – repurposing a toxic waste*

Rapid global urbanization and an ever-increasing population has resulted in uncontained industrial development. To continually drive this on-going industrial development, an ever-increasing necessity for metals such as iron and copper is required (Kossoff et al., 2014). These metals are most often extracted through mining deep into the earth's crust. Mine tailings are major waste heaps produced as a by-product from metal extraction. Mine tailing heaps are typically uniform in structure with rectilinear slopes and flat tops and composed of mainly pre-processed, comminuted rock which contains significant amounts of clay but virtually no organic content (Esterhuysen et al., 2018). The major danger posed by mine tailings is in the fact that they are a source of heavy metal contamination, harbouring large concentrations of toxic metal(loid)s such as copper, cadmium, mercury and lead etc (Kumari et al., 2016). Left to settle, these metals have the capability to form metal sulphides which have the potential to leach into the surrounding environment. This can result in damage which can linger on for decades even after the mine tailing site has been abandoned (Esterhuysen et al., 2018; Nordstrom et al., 2015). Such damage includes direct and indirect impacts on human health (Zinjarde et al., 2014); high economic losses and the accumulation of heavy metals by surrounding biota (Gadd, 2010). The behaviour of metals in soils, such as in the case of mine tailings, makes it difficult to remove the threat of heavy metals leaching into the environment as they often form complexes with other naturally occurring substances, bind to the soil components or precipitate into other insoluble mineral forms (Kumari et al., 2016).

Although many types of heavy metals exist within mine tailings, the focus of this study will be on copper mine tailings extracted by Minera de Cobre Quebradona, a subsidiary of AngloGold Ashanti, in Columbia. Copper is a soluble and exchangeable heavy metal and considered to be toxic at high levels (Hu et al., 2014). With the accumulation of heavy metals in humans having been shown to be responsible for several severe and often irreversible consequences such as developmental abnormalities, bone growth defects and carcinogenesis (Duruibe et al., 2007).

Additionally, if the mine tailings contain a high content of sulphide minerals, then the potential exists for the sulphides to become easily oxidised if exposed to water containing molecular oxygen (Yang et al., 2016). As a result of such oxidation, the water becomes highly acidic and the heavy metals, such as copper, associated with the sulphides can leach out (Yang et al., 2016). This phenomenon is known as acid mine drainage and it is often considered to be the single worst environmental danger posed by mining activities (Yang et al., 2016). To prevent toxic copper leaching into the environment and the occurrence of acid mine drainage it is thus important to determine means to immobilize the heavy metals within mine tailings.

Several methods exist which have been developed to immobilize and remediate metal mine tailings such as excavation, land fill, and soil capping but all of these methods are costly and result in additional destruction to the environment (Yang et al., 2016). Physiochemical methods to treat heavy metals are also popular but they suffer from high energy and chemical consumption costs and result in the further emission of secondary pollutants (Krishna and Philip, 2005). Additionally, phytoremediation methods have proven popular for the in-situ remediation of heavy metals but this method is limited by the dependence on plant growth conditions such as climate, altitude, geology and temperature as well as the low amount of metals which can be accumulated by the biota (Achal et al., 2012).

Alternative biological remediation methods exist which have shown considerable potential for the remediation of heavy metals, namely: bioleaching and bioimmobilisation. In general, bioimmobilisation is widely considered to hold more potential than bioleaching, which is costly and time consuming (Achal et al., 2011). However, the application of bioimmobilisation techniques are hindered by the fact that heavy metals immobilized through this technique can be released again (Achal et al., 2011). MICP processes, which have been shown to be highly effective in immobilizing toxic metals, such as copper, by forming insoluble metal carbonates, may provide a possible solution to this problem (Achal et al., 2011; Fujita et al., 2000; Yang et al., 2016).

This is due to the fact that the products of MICP, such as calcite, have the capability to absorb heavy metals to their surfaces and/or incorporate heavy metals with ion radius close to $Ca^{2+}$, such as $Cu^{2+}$, $Pb^{2+}$ and $Cd^{2+}$, into their crystal structure (Achal et al., 2011). Thus, due to its ability to trap heavy metals, MICP, may provide a new in-situ method for remediating mine tailings, with an added benefit being the fact that MICP is not sensitive to redox potential (Achal et al., 2011). This implies that the products formed from the heavy metals are most likely to remain immobilised. However, not all bacteria are conducive to surviving in environments with high heavy metal concentrations and the ability of *S. pasteurii* to survive these conditions will need to be investigated.

The success of such a process is not however limited to the applicability of *S. pasteurii* as multiple indigenous bacteria have been bio-prospected from mine tailings which have shown strong urease-producing potential (Achal et al., 2011; Yang et al., 2016). One such bacterium, *Kocuria flava* CR1, which was isolated from a copper mine in China has shown exceptional potential for the bioimmobilisation of copper containing tailings via MICP. Being capable of producing large volumes of urease (472 U/ml) and immobilising 95% of copper in a solution containing 500 mg/L of copper sulphate (Achal et al., 2011).

Thus, due to the high cost and/or the furthered destruction current remediation methods pose to the environment it is proposed that MICP-manufactured bio-bricks may prove to be a viable, low-cost and low-tech method of immobilizing heavy metals found in mine tailings. Mine tailings, although by no means green or environmentally friendly, are already present globally in vast quantities and require immediate and safe disposal. By 'disposing' of them in the form of a brick, not only is one safely immobilising the heavy metals contained within, but the process would also eliminate the need for sand and the costly environmental concerns attributed to sand mining itself. As well as this, utilising mine tailings in the bio-brick matrix will contribute to eliminating another otherwise valueless waste stream and ensure that the mining industry is further integrated within a circular economy which benefits both the business, society and the environment.

### *2.11. Detailed project objectives*

Throughout this dissertation, bio-columns were used as a proxy for the manufacturing of bio-bricks due to them requiring less resources (reagents, chemicals etc.). Based on the above literature review, the following objectives for this study were drawn, which in turn were used to inform the development of the materials and methodology section.:

1. Characterise the copper mine tailing samples received from Quebradona, Columbia in terms of physiochemical makeup;
2. Test whether it is possible to produce bio-columns from repurposed copper mine tailings using the commonly applied pumping method;
3. If not possible, further develop (and compare) a submergent technique as an alternative method to the pumping method;.
4. Test the feasibility of growing a bio-columns from copper mine tailings, using said submergent method;
5. Observe the growth response of *S. pasteurii* to an environment of high copper concentration;
6. Investigate whether incremental increases in copper concentration during the growth of *S. pasteurii* would, over several generations, result in a strain of *S. pasteurii* acclimatising to the high copper concentration found within copper mine tailings;
7. Screen for, isolate and identify alternative urease-producing bacteria, indigenous to copper mine tailings, capable of enduring the high copper concentration encountered when producing bio-columns from repurposed copper mine tailings;
8. Investigate the economic feasibility of repurposing 'waste' copper mine tailings to create an industrial process, revolving around a mining community, capable of mass-producing MICP bio-solids and related fertilisers.

### *2.12. Hypothesis*

From the above literature review and informed by the defined objectives it is hypothesised that:

The leaching of heavy metals, such as copper, from mine tailings into the environment poses significant risks to both society and the surrounding biota. This threat can be overcome by repurposing said mine tailings into bio-bricks, using a naturally occurring biological method known as microbial induced calcium carbonate precipitation.

# Chapter 3

# 3. Materials & Methodology

The following sections contained within this chapter describe the means and methods undertaken in determining the technical feasibility of repurposing copper mine tailings into bio-columns via MICP as a proxy for bio-brick production. Section 3.1 describes the methods necessary for growth and maintenance of the microbial culture used throughout this dissertation. Section 3.2 details how the copper mine tailings where characterised in terms of both physical and chemical make-up. Section 3.3 – 3.5 describes the methodology undertaken to develop, analyse and test the technical feasibility of utilising copper mine tailings to from bio-columns. Due to finite resources, bio-columns were used in section 3.3 - 3.5 as a proxy for bio-bricks. Lastly, section 3.6 describes the biologically inspired techniques used to overcome the inhibition of the MICP process within the copper mine tailing bio-bricks.

## 3.1. Microorganism

The non-pathogenic ureolytic soil bacteria *Sporosarcina pasteurii*, formerly *Bacillus pasteurii*, was used throughout this study. Previous research has shown that *S. pasteurii* can be successfully grown under aerobic conditions at pH 9 and 30°C (Henze and Randall, 2018).

### 3.1.1. *Culture media and agar plate preparation*

*S. pasteurii* was propagated in the ammonia-yeast medium (ATCC®1376) which consisted of 20 g/L yeast extract, 10 g/L ammonium sulphate and 0.13 M (15.75 g/L) Tris buffer adjusted to pH 9 using a 32% HCl solution. Each ingredient was prepared individually in deionised water and autoclaved separately. Once autoclaved, the ingredients were mixed aseptically at room temperature. ATCC®1376 agar plates were prepared following the same recipe as described above but with the addition of 20 g/L of agar added to the ammonium sulphate solution. Once autoclaved, and aseptically mixed, the solution was poured immediately into individual petri dishes. The poured agar plates were left to solidify overnight and then stored at 4°C in sealed plastic bags until needed.

### 3.1.2. *Reviving bacterial glycerol stocks*

To ensure the continued stability of the *S. pasteurii* strain in use it was revived weekly from previously prepared glycerol stocks. Under aseptic conditions in a laminar flow hood, a heated wire loop was used to remove the *S. pasteurii* biomass from a previously prepared bacterial glycerol stock. Ensuring the biomass did not thaw, the wire loop was then used to streak said sample onto an ATCC®1376 agar plate which was previously prepared using the method described above. After 48 hours of incubation at 30°C the agar plate was examined for the presence of bacterial colonies.

### *3.1.3. Starter culture growth*

Once colony growth was visible on the ATCC®1376 agar plate, a starter culture was grown. This was achieved by inoculating 10 mL of sterile ATCC®1376 liquid media, contained within a sterile McCartney bottle, with a single bacterial colony grown on the previously prepared ATCC®1376 agar plate. The bacterial colony was transferred from the agar plate to the McCartney bottle using a sterile loop. The liquid culture was then cultivated for approximately 24 hours, in an inclined position, under aerobic conditions at 30°C and 120 rpm.

### *3.1.4. Direct cell counting*

Direct cell counts were performed to track bacterial growth at any given moment by following standard practices as defined by the Centre of Bioprocess Engineering Research (CeBER) located within UCT. Briefly, to perform each cell counts, a Helber Cell Counting Chamber placed under a Leica DM500 (Leica Microsystems, Heerbrugg, Switzerland) compound microscope was used. The microscope was set to use a 100x objective. For each cell count, 1 mL of bacterial sample was aseptically drawn from its container and diluted with Tris buffer. After being vortexed, 25 µL of this diluted sample was transferred into the counting chamber and the cell count was recorded. To ensure statistically significance, 30 - 300 cells, were counted and the dilution factor was continually increased as the experiment progressed. To convert the physical count into cell density (Cells/mL), equation 9 was applied:

$$\text{Cell density} = (3\ 125\ 000)\ (D)(\text{Cell count}) \tag{9}$$

Where:

3 125 000 = conversion factor which adjusts for the volume of sample counted
D = dilution factor
Cell Count = number of individual bacteria cells counted

### *3.1.5. Standard growth curve preparation*

To delineate the growth stages of *S. pasteurii* under standard conditions (described above) the growth curve of the culture had to be determined. The growth curve of *S. pasteurii* under standard conditions (ATCC®1376 culture media, T=30°C & 120 rpm) was prepared by aseptically subculturing a 10 mL starter culture of *S. pasteurii* into 90 mL of ATCC®1376 contained within in a 1 L flask. The flask was incubated under aerobic conditions at 30°C and 120 rpm for 16 hours. Starting at t = 0 hours, the growth of the culture was tracked via a standard direct cell count as described above. Cell counts were performed every two hours for the first eight hours, followed by every four hours until the 16-hour mark was reached. Two further recordings were taken at the 24- and 28-hour mark. The reason for the discrepancy in the time taken between measurements is due to the curfew restriction (22:00 – 04:00) applied by the South African government as well as the laboratory restriction times applied by UCT during the COVID-19 pandemic. The above experiment was performed in triplicate.

### ***3.1.6.*** *Bacterial glycerol stock preparation*

To ensure the viability and stability of the bacterial strain for future use, glycerol stocks were prepared which allowed for safe long-term storage of the bacterial culture. To prepare the glycerol stocks, a starter culture was cultivated using the method described above. Once cultivated the starter culture was used to inoculate 90 mL of freshly prepared sterile ATTC®1376 liquid media contained within a sterile Erlenmeyer flask which was then incubated overnight (~ 16 hours) at 30°C and 120 rpm. The liquid culture was grown overnight as previous research has shown this is when the bacteria reached the stationary growth phase (Lambert and Randall, 2019). Once stationary phase was reached, 500 µL of the overnight culture was extracted and aseptically mixed with 500 µL of autoclaved 50% (v/v) glycerol solution into a sterile 2 mL cryovial. The cryovials were then frozen and stored in a -50°C freezer.

## *3.2. Characterisation of copper mine tailings*

The purpose of these experiments was to analyse the key physiochemical characteristics of the copper mine tailings used in this study. Such experiments were necessary to guide the design and development of the experiments to follow. For the chemical analysis of the tailings, attention was focused on determining the quantity and type of heavy metals concentrated withing the tailings as a high concentration of heavy metals would likely result in the inhibition of *S. pasteurii's* capability of initiating MICP (Mugwar and Harbottle, 2016). In terms of the physical characterisation, a basic geotechnical analysis was performed to determine particle size and porosity of the copper tailings.

### *3.2.1. Site description*

The copper mine tailing samples used in this study were received from a Greenfields copper mine project in Columbia. The mine site was located in Quebradona which is situated in the Middle Cauca region, in the Department of Antioquia, 60 km south-west of Medellín. The copper mine tailings collected came directly from a final stage flotation process but otherwise would have been stored in a tailings dam. Table 3.1 summaries the physicochemical properties of copper mine tailings samples, conducted through in-house research by the mining company.

**Table 3.1:** Physicochemical properties of copper mine tailing samples collected from Quebradona, Department of Antioquia, Columbia.

| Parameter | Unit | Quantity |
|---|---|---|
| **pH** | - | 8.00 |
| **Quartz [$SiO_2$]** | wt.% | < 80 |
| **Pyrite [$FeS_2$]** | wt.% | < 10 |
| **Chalcopyrite [$Cu_2FeS_2$]** | wt.% | < 10 |
| **Asbestos [$Mg_3Si_2O_5(OH)_4$]** | wt.% | < 0.01 |

### *3.2.2. ICP and XRF analysis of copper mine tailings*

X-ray fluorescence (XRF) was applied to determine the type and mass fraction of compounds making up the received copper mine tailings. The elemental concentration of heavy metals contained within the provided copper mine tailings was conducted using inductively coupled plasma-mass (ICP-MS) spectroscopy. Triplicate, representative samples of approximately 10 g of copper mine tailings were prepared by oven-drying at 90°C overnight before being transported for analysis. Both analyses were performed externally by the ICP-MS Laboratory located within the Central Analytical Facility at University of Stellenbosch, South Africa.

### *3.2.3. Particle size distribution of copper mine tailings*

To determine the particle size distribution (PSD) of the provided copper mine tailings, laser diffraction analysis was applied using the Mastersizer2000 (Malvern Instruments Ltd., Worcestershire, United Kingdom). The Mastersizer 2000 was set to use the Standard Operating Procedure (SOP) 'Copper Ore' which had manually been pre-defined by the Analytics Department located within the Chemical Engineering Building in the UCT. Deionised water was used as the dispersant for all samples. To perform the PSD analysis, discrete and representative samples of the provided copper mine tailings were collected in triplicate and oven-dried overnight at 90°C. A solution of 5% NaOH was then added to the dried copper mine tailings samples to ensure the separation of clumped particles. The copper mine tailing samples were then gently added to the dispersing deionised water within the Mastersizer2000 until an obscuration value of approximately 10% was achieved. Once, the desired obscuration was reached the Mastersizer2000 was started and the PSD analysis conducted.

### *3.2.4. Void ratio of copper mine tailings*

Following the convention established by Henze and Randall (2018), the void ratio of the bio-column matrix was to be used to determine the volume of cementation media needed to form a bio-column. To calculate the void ratio of a given soil, it was necessary to first determine the specific gravity of the copper mine tailings. The specific gravity ($G_s$) of the copper tailings was determined using the Density Bottle Method detailed in the British Standards (BS 1377:1975) and calculated using equation 10:

$$G_s = \frac{G_l(m_2 - m_1)}{(m_4 - m_1) - (m_3 - m_2)} \qquad (10)$$

Where:

$G_l$ = specific gravity of the liquid $\left[\frac{g}{mL}\right]$

$m_1$ = mass of empty bottle [g]

$m_2$ = mass of the bottle and dry substrate material [g]

$m_3$ = mass of the bottle, substrate and liquid [g]

$m_4$ = mass of the bottle and liquid [g]

Once the specific gravity of the copper mine tailings was calculated, it could then be used to calculate the total volume of solids ($V_s$) using equation 11:

$$V_s = \frac{G_s}{M} \quad (11)$$

Where:

M = weight of copper mine tailings [kg]

Subsequently, porosity ($\phi$) and void ratio (e) and could be calculated using equations 12 and 13 respectively:

$$\phi = \frac{e}{1 + e} \quad (12)$$

$$e = \frac{V_t - V_s}{V_s} \quad (13)$$

### ***3.2.5.*** *Pumping cementation media through tailings*

Initially, the bio-column experiments (detailed in section 3.5) were to be carried out using the 'pumping' method as carried out by Henze and Randall (2018) and Lambert and Randall (2019). Using the pumping method, as illustrated in Figure 3.1A, cementation media was to be pumped directly through moulds (d = 52 mm; h = 100 mm) containing copper mine tailings inoculated with *S. pasteurii*. However, based on the results of the PSD analysis it was noted that the tailings were likely too fine for any fluid to be pumped through them and any attempt to do this would likely result in a pressure build up and hence a failure of the pump. It was hypothesised that the addition of a small volume of particles with a larger PSD ratio (such as sand), would have the resultant effect of increasing the porosity of the overall bio-column matrix. This in theory would then allow for a greater volume of fluid to be pumped through the tailings without causing a pump failure.

To confirm this, a novel pumpability experiment (as illustrated in Figure 3.1B) was conducted where deionised water would be pumped through various ratios of copper mine tailings to beach sand. Beach sand was used as it was known from experiments conducted by Henze and Randall (2018) that fluid could effortlessly be pumped through it using a setup similar to that seen in Figure 3.1A. The beach sand was obtained from the Civil Engineering Laboratory within the New Engineering Building at UCT and sieved using a 0.15 mm pore size sieve. Copper tailing to beach sand ratios were set at: 100, 80, 60, 40, 20 and 0 vol.%. Each ratio of copper tailings to beach sand was fully saturated with deionised water (based on the void ratio of the copper tailings calculated in section 3.2.4) and packed into a bio-column mould (shown in Figure 3.2).

The top inlet of each mould was then connected to an outlet of an auto-dosing pump which was calibrated to dose each mould with 100 mL of deionised water over a period of 210 seconds. A 150 mL beaker was placed at the outlet of each mould to capture and then weigh any deionised water pumped through. In this manner, the captured deionised water was used as an indirect proxy to compare the 'pumpability' of each ratio of copper tailings to sand. The experiment was performed in triplicate for each ratio of copper tailings to beach sand.

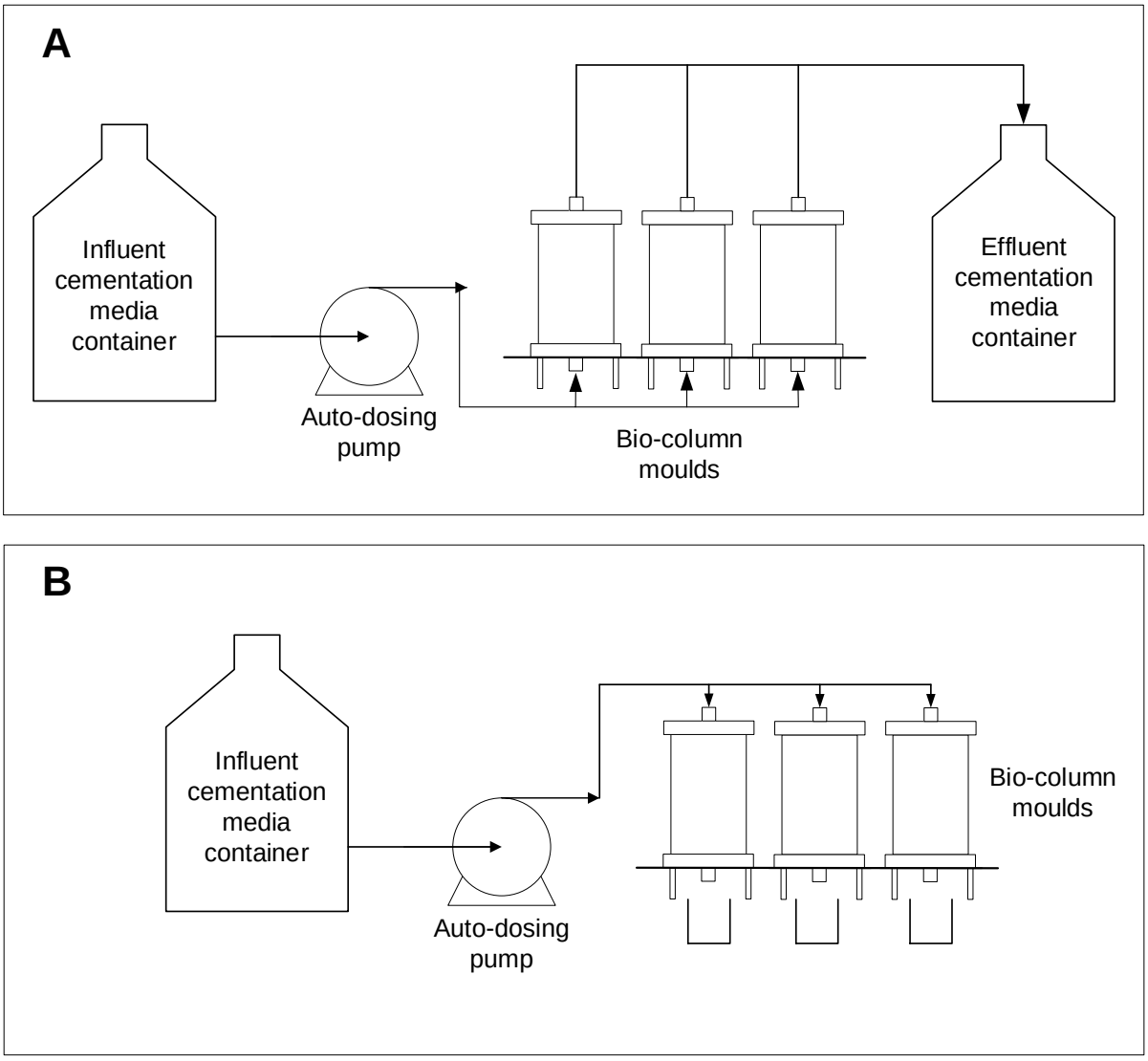


**Figure 3.1:** Schematic of (A) the initially planned experimental setup to be used to produce MICP bio-columns. Cementation media was to be pumped through the bottom of specially designed bio-columns containing mine tailings inoculated with *S. pasteurii*. However, it was noted, due to the small particle size (0.03 - 150 µm), that the tailings were too fine to have fluid pumped through them. It was hypothesised that this lack of 'pumpability' could be overcome through the addition of larger beach sand particles (which had a greater porosity). To test this hypothesis, a novel pumpability experiment was set up (B) where a 100 mL of deionised water would be pumped through pre-defined ratios of copper tailings to beach sand over a two- minute period. The weight of fluid collected from each column after said pumping period was used as a proxy to determine how 'pumpable' each ratio was.

The moulds designed for the above experiments, as seen in Figure 3.2, were fabricated from 5 mm thick polyvinyl chloride (PVC) piping and had a height of 100 mm and diameter of 52 mm. The inlet and outlet nozzle each had a diameter of 10 mm. Shown in Figure 3.2, the inside of both lids was modified so that the any incoming or outgoing fluid was forced through four small holes. This was done so that fluid would be dispersed more homogenously throughout the mould. Additionally, a 1 cm thick layer of sponge was placed between the lid and the packed material to disperse incoming fluid and prevent any soil particles being pushed through the mould.

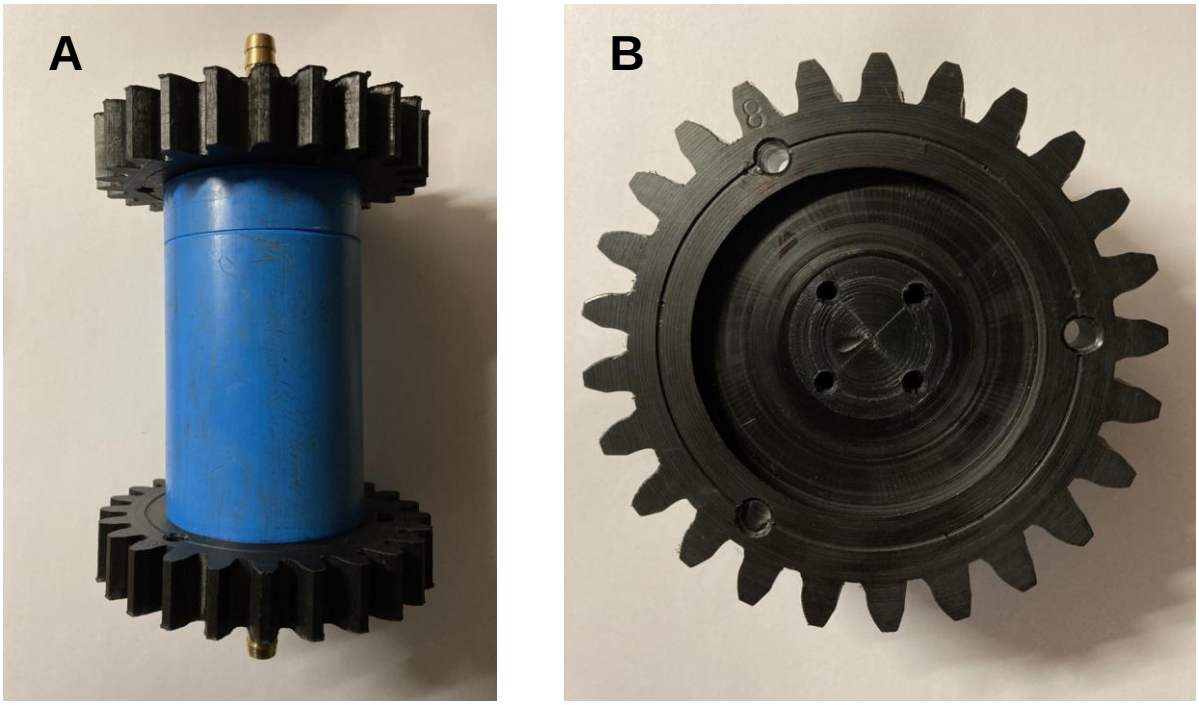


**Figure 3.2:** Images of (A) the bio-column mould in its entirety as well as (B) the inside of the lid of said bio-column. Of note is the four inlet/outlet holes fabricated into the inside of each lid. This was done to ensure the homogenous dispersion of any incoming liquid throughout the bio-column mould.

### *3.3. Development of a low cost submergent bio-solid technique*

The following experimental design was setup to determine whether the copper mine tailings provided by Minera de Cobre Quebradona could be used to form viable bio-columns using the principles of MICP. To date most MICP bio-solids have been grown using a pumping setup like that shown in Figure 3.1A. However, based on the results of the pumping experiment detailed in section 3.2.5 (See Figure 4.3 in Chapter 4), such a method for copper tailings was deemed unfeasible; unless the tailings were mixed with a large volume of alternative aggregate such as beach sand (which is both economically and environmentally undesirable).

As such, an alternative method was needed if bio-columns were to be created entirely from waste copper mine tailings. It was decided that a possible viable alternative to the pumping method would be to employ a submergent method such as that used by (Cheng et al., 2020). The use of such a submergent technique would circumnavigate the need to pump cementation media as when using the submergent technique, a chemical concentration gradient is formed. Discussed below is the general design, setup and preparation of all equipment and consumables used in developing a submergent technique to create bio-columns from copper mine tailings.

Note: Due to the large volume of chemicals and aggregate needed, bio-columns were used as proxy for determining the feasibility of creating bio-bricks from the copper mine tailings so as to reduce chemical costs.

#### ***3.3.1.*** *Submergent setup*

Figure 3.3 illustrates the schematic of the experimental setup used to grow bio-columns utilising the submergent technique favoured by Cheng and colleagues (2020). Material moulds containing loose copper mine tailings inoculated with *S. pasteurii* were directly submerged into a defined volume of cementation media. The cementation media was held in a 30 L container and kept homogenous using a magnetic stirrer. The bio-columns were rested on a stainless-steel rack which allowed for the cementation media to enter the columns at all angles. To prevent the volatilisation of ammonia, formed as a by-product of the overall MICP reaction, a lid was placed on the container.

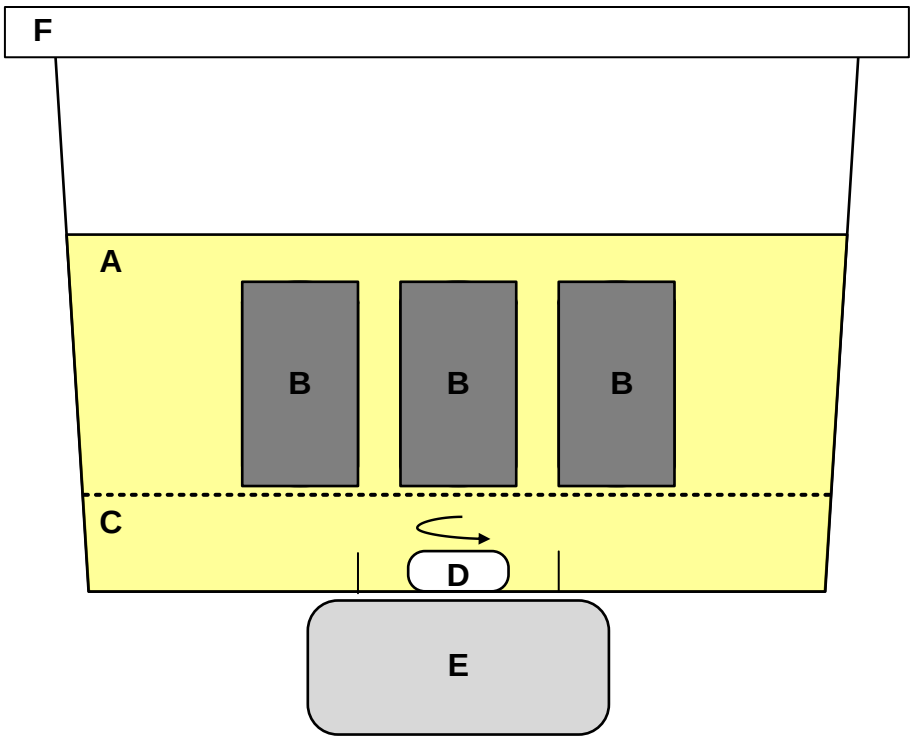


**Figure 3.3:** A schematic drawing of the experimental setup used for growing bio-columns based on a method described by Cheng and colleagues (2020). A large container is used to contain the cementation media (A) into which the bio-columns (B) are submerged into. The bio-columns are rested on a raised stainless-steel rack (C) which ensures that cementation media can enter the bio-columns from all angles. The cementation media is kept homogenous throughout the time needed to grow the bio-columns using a stirrer bar (D) powered by a magnetic stirrer (E). The container was kept sealed (F) to prevent ammonia, formed as a by-product of bio-column growth, from being released into the environment.

### ***3.3.2.*** *Fabric mould design*

When bio-columns were produced using the submergent setup, a stiff fabric bio-column mould was utilised. The fabric moulds, pictured in Figure 3.4, were fabricated from non-woven needle punched geotextile. The geotextile fabric was tightly sewn together to form a stable cylindrical framework with a height of 100 mm and diameter of 45 mm. Due to the tight stitching of the geotextile fabric, as well as the fabrics inherent relative stiffness, the material moulds were shown to retain structural integrity even when packed with loose solids and submerged in liquid. The material moulds fabricated consisted of an annular part and a sewn-on bottom.

**Figure 3.4:** Image of geotextile fabric mould used to form bio-columns via the submergent technique. The fabric mould consisted of a 100 mm annular part to which a bottom part of diameter 48 mm was tightly sewn onto.

Additionally, a cover made of 1 cm thick foam was fabricated for each bio-column. The cover was not sewn to the mould and was used to prevent solid material from dissipating away when the bio-columns were submerged.

### ***3.3.3.*** *Bio-column packing protocol*

To ensure that both structural and dimensional stability was maintained as the fabric moulds were packed with loose aggregate material prior to submergent, a novel packing process was developed. The first step of the process was to place the fabricated moulds into the annular part of the PVC moulds discussed in section 3.2.5. This was done to ensure that the dimensional integrity of the packed aggregate was maintained throughout the entirety of the packing process. The PVC moulds were tapered gradually lengthwise by 2 mm as shown in Figure 3.5. This helped to ensure that the filled fabric moulds could be effortlessly removed from PVC moulds into the submergent setup once packing was complete. Once the fabric mould was fitted inside the PVC mould, it was packed with aggregate (mine tailings) inoculated with the ureolytic bacterial culture. The packing procedure followed was adapted from the same standard procedure used in the COMSIRU Laboratory located in UCT to perform a proctor compaction test.

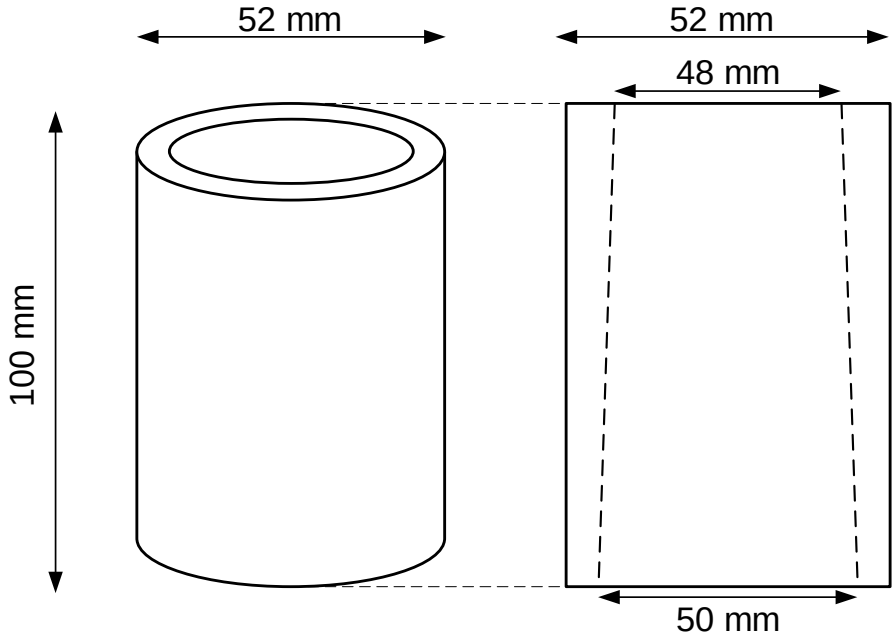


**Figure 3.5:** Cross section schematic of PVC mould used to maintain the dimensional integrity of the fabric moulds during the aggregate packing process. The PVC mould was tapered by 2 mm in total to ensure ease of removal of the fabric mould once packing was completed.

Figure 3.6 illustrates the method used to pack the aggregate. As seen in Figure 3.6A, the aggregate is packed in three successive layers, each accounting for approximately one third of the height of the column. As one layer is deposited, it is tightly compressed using a wooden press to strike it 27 times in a circular pattern as shown in Figure 3.6B.

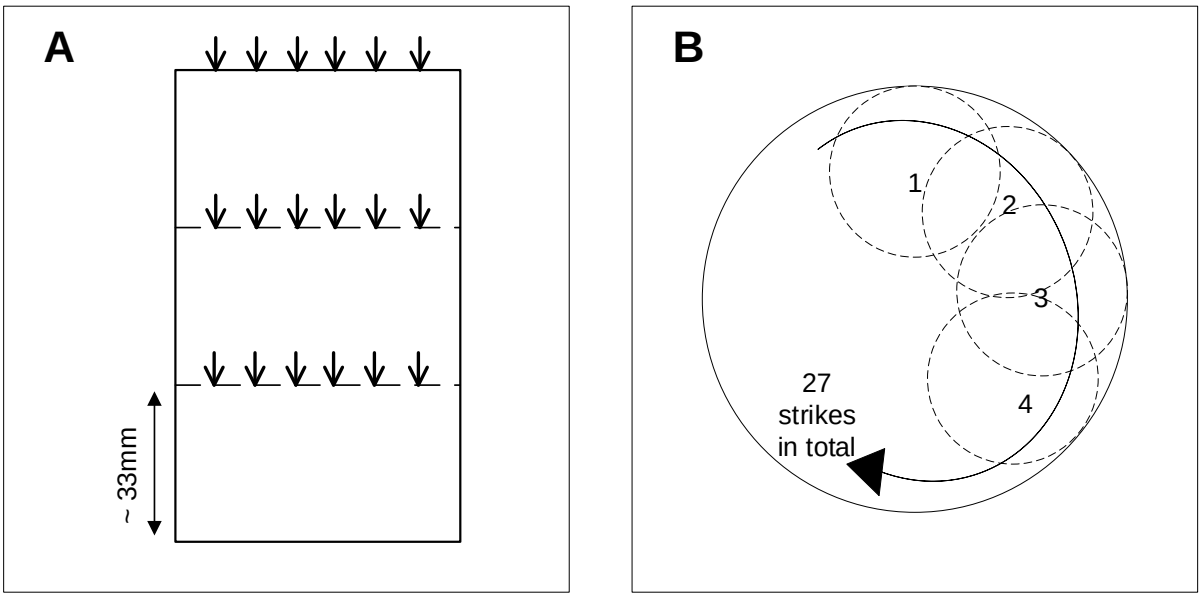


**Figure 3.6:** Cross sectional (A) and aerial (B) views of PVC column mould which detail how aggregate was packed into the moulds. Inoculated aggregated was packed into each mould in three successive layers. Before depositing a successive layer, the previous layer was compacted by 27 strikes in a circular pattern using a wooden press.

Once the aggregate was tightly packed into the fabric mould following the above procedure, it was capped with a foam lid as seen in Figure 3.7, ready to be submerged into the cementation media.

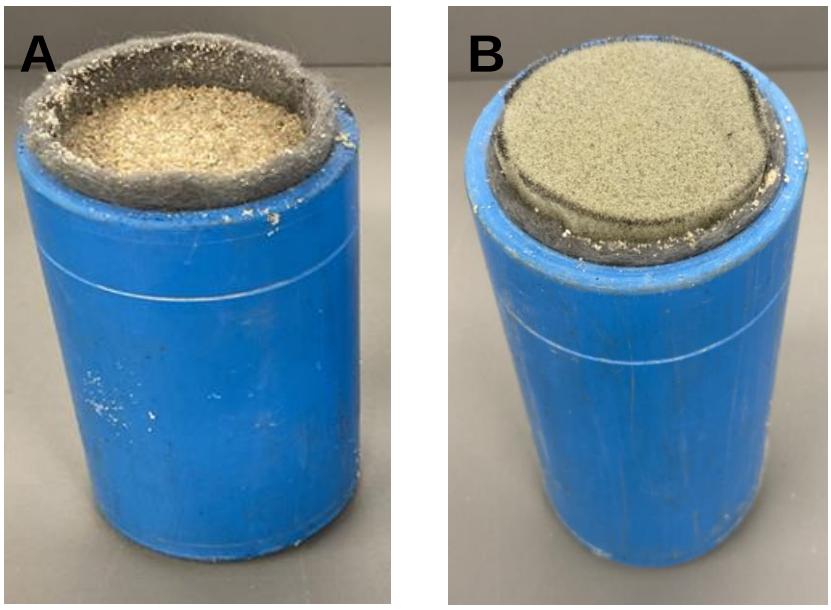


**Figure 3.7:** Image of a fabric bio-column mould (A) packed tightly with inoculated aggregate and contained within a PVC mould to ensure dimensional stability. Once packed, a foam lid was added to each fabric mould (B).

### ***3.3.4.*** *Cementation media preparation*

A predetermined volume of cementation media, containing the urea and calcium ions required for MICP to occur, was added to a 30 L container. The volume of cementation media required was calculated based on the porosity of the copper mine tailings and the volume of the bio-columns being grown. Due to the large volumes of human urine required for this research and the fact that the restrictions imposed by the COVID-19 pandemic made collection of urine difficult; synthetic urea was used as a substitute for human urine. The concentration of urea in human urine was reported to be in the range of 0.15 M to 0.39 M (Putnam, 1971). Thus, it was decided that the cementation media would consist of 0.3 M synthetic urea (purity > 99.5%) to mimic the approximate concentration of urea found in human urine as done by Henze and Randall (2018). It must however be noted that this synthetic urine recipe had a negligible ionic strength. As ionic strength is known to retard the activity of urease or the bacteria (Lambert and Randall, 2019), it was noted that the compressive strength of any of the bio-columns grown in the following experiments may not be reflective of the compressive strength of said bio-columns had human urine been used. However, as the focus of the study was to test the feasibility of applying MICP to copper mine tailings and to keep consistency between experimental sets, it was deemed that a synthetic source of urea would serve as an adequate replacement.

## 3.4. Bio-column analytical methods

The following sections details the analytical means and methods used to describe and test the feasibility of repurposing copper mine tailings into bio-columns.

### 3.4.1. *Dissolved calcium and ammonium determination*

Indirect measurements of enzymatic urea hydrolysis and calcium carbonate precipitate formation occurring during the bio-column experimental runs were performed using a Thermoscientific Gallery (ThermoFisher Scientific, Massachusetts, United Sates). The Thermoscientific Gallery could not directly measure the rate of calcium carbonate formation nor the rate of degradation of urea into ammonium ions. Rather it could only measure concentrations of calcium ions and ammonium ions at a set point in time. As such, the calcium concentration depletion in solution over the course of an experimental run was used as a proxy to represent the rate of calcium carbonate precipitation (see Equation 8). In the same manner, the concentration of ammonium ions over the course of an experimental run was used as a proxy for measuring the rate of urea hydrolysis (see Equation 6). As the Thermoscientific Gallery has an upper measurement limit of 5 mg/L for nitrogen and 200 mg/L for calcium, all samples taken were diluted by a factor of 100 using deionised water. For all experiments, 1 mL of sample was diluted to 100 mL using deionised water. This solution was then vortexed and filtered through a 0.22 µm pore syringe filter and immediately analysed using the Thermoscientific Gallery.

### 3.4.2. *Compressive strength test*

Compressive strength is calculated as the ratio of the maximum uniaxial load carried by the bio-columns to the cross-sectional area of its surface (Owens, 2013). The compressive strength of each bio-column unit was tested using the Proline Z100 (Zwick Roell, Ulm, Germany) in accordance with general column testing standards. Before testing, the flatwise surface of each bio-column was smoothed down using sandpaper to remove any jutting irregularities to ensure fair testing between columns. Each bio-column unit was then placed flatwise on the lower bearing of the Proline Z100 and centred underneath the spherical upper bearing as pictured in Figure 3.8. A loading force of 100 kN was them progressed on the bio-column unit at a rate of 1 mm/min until the specimen failed. Failure was defined as the maximum stress the bio-column unit withstood even without the presence of visible external fractures. The overall compressive strength of the bio-column was calculated according to equation 14. Where possible, the compressive strength of each bio-column was then determined by averaging the calculated compressive strength of the triplicate set. On the occasion that any bio-column cracked before compressive strength testing, a salvageable piece of it was cut to have a height equivalent to its diameter. This salvaged piece was then tested for compressive strength.

$$C = \frac{F}{A} \quad (14)$$

Where:

C = compressive strength [MPa]
F = maximum uniaxial load [N]
A = cross-sectional area of the bio-column unit [$mm^2$]


**Figure 3.8:** Proline Z100 setup used to test the compressive strength each individual bio-column unit. Each unit was placed on the lower bearing and centred beneath the upper bearing which applied a loading force of 100 kN at a rate of 1 mm/min until the unit failed.

### ***3.4.3.*** *Calcium carbonate content measurement of MICP formed bio-solids*

After compressive strength testing, discrete shards of each grown bio-column were harvested and assessed to determine the mass fraction of calcium carbonate formed by the MICP process. From each bio-column, shards were collected from two distinct locations: the surface (shell) and the innermost centre (inner). This was done to determine if the growth of calcium carbonate was homogenous throughout each column. To measure the calcium carbonate content of each sample harvested from the respective bio-columns, a procedure adapted from Rebata-Landa (2007) was followed. Briefly, each bio-column sample was crushed and then oven-dried at 90°C to remove any residual water content. The dried bio-column shards were then weighed ($W_i$) before being washed in a dilute solution of HCl (0.1 M) so as to dissolve any precipitated $CaCO_3$ formed during the MICP process. The remaining loose particles were then vacuum filtered and rinsed using deionised water before being oven-dried at 90°C.

The remaining solid particles were then once again weighed ($W_f$) and the difference between the two weights was considered to be the weight of calcium carbonate present in the original sample. The mass percentage of calcium carbonate within each bio-column shard was calculated using equation 15.

$$CaCO_3\ (wt.\%) = \frac{W_i - W_f}{W_i} \times 100 \qquad (15)$$

Where:

$W_i$ = total weight of solid [g]
$W_f$ = weight of solid after acid addition

### ***3.4.4.*** *Microstructure analysis of MICP formed bio-columns*

Discrete samples harvested from the bio-column units (taken from the shell and inner sections) were prepared and examined using scanning electron microscopy (SEM) and energy-dispersive X-ray spectroscopy (EDS). A small amount of each sample was placed onto 10 mm aluminium stubs which had previously been coated with carbon glue, and any excess/loose particles were removed via dust-off. The prepared stub was then sputter-coated with gold palladium alloy, allowing the samples to be visualised using scanning electron microscopy (FEI NovaSEM 230 equipped with an Oxford X-Max EDS detector). To characterise the chemical make-up of the mounted samples EDS was used to perform an elemental analysis, with the analysis being carried out on Oxford INCA software.

### ***3.4.5.*** *Statistical analysis*

Where possible, all experiments outlined within this report were conducted in triplicate and an average value for each experimental condition was taken. The standard deviation of the triplicate set was calculated and used to give a quantitative representation of the average error of the experimental results. Error bars on the graph show standard deviation.

## 3.5. Bio-column experiments

The purpose of the following experiments was firstly to determine whether it was possible to grow bio-columns from a synthetic urea solution (which mimicked the urea content of human urine) using the submergent technique described above. Secondly, if shown to be feasible, the aim of the remaining experiments was to determine if copper mine tailings could be used as an apt aggregate replacement for beach sand in growing bio-solids. As mentioned previously, bio-columns were used as a proxy for bio-bricks.

### 3.5.1. *Experimental conditions*

All bio-column experiments were to be conducted in accordance with the setup described in section 3.3 and all analytical measurements were carried out following the procedures detailed in section 3.4. A summary of all the bio-column experiments conducted and the conditions at which they were run at are detailed in Table 3.2.

Experiment A was used to determine the feasibility of using a 0.3 M urea cementation media to grow bio-columns using the submergent technique. Beach sand was used for experiment A due to the fact that it is an inert material and has been used successfully in the past to grow bio-columns when utilising a submergent technique (Bu et al., 2018). As such, experiment A formed the reference experiment against which all other bio-columns were compared. Experiment B followed the exact same setup as experiment A with the sole exception that 3 g/L of nutrient broth was added to the cementation media of experiment B. This was done to determine if the addition of nutrient broth to support the growth of *S. pasteurii* during the experimental run would result in a bio-column of increased compressive strength.

Experiment B was of particular interest as it was implied from work conducted by Lambert and Randall (2019) that the addition of nutrient broth was the most expensive costs accrued when manufacturing bio-bricks. Hence, for the economical production of bio-bricks to occur in the future it was essential to determine the significance of adding nutrient broth to the cementation media.

Experiment C followed the same setup as experiment A but replaced the beach sand aggregate with the copper mine tailings. Experiment C was performed to provide insight into one of the central tenets of this thesis, that being if it is technically possible to repurpose copper mine tailings into environmentally friendly and economically viable bio-columns and hence bio-bricks.

Additionally, to determine if the MICP process directly resulted in the solidification of the copper mine tailings into a bio-column, a subsidiary experiment (experiment D) was conducted where triplicate bio-columns were formed by simply mixing deionised water with the copper mine tailings. The resulting mixture was packed into columns and allowed to dry naturally over the same time period as the growth time of the bio-columns and was used to act as a blank against experiment C.

**Table 3.2:** The experimental conditions and aims for the bio-column experiments conducted as a proxy for determining the feasibility of producing urea bio-bricks from copper mine tailings.

| Exp. | Aggregate | Cell density ($x10^{-9}$ Cells/mL) | Aim |
|---|---|---|---|
| **A** | Beach Sand | 32.5 | Develop model submergent technique for bio-solids grown using a synthetic urea solution |
| **B** | Beach Sand | 31.3 | Determine the impact (if any) of the addition of nutrient broth to cementation media. |
| **C** | Copper mine tailings | 33.8 | To determine if copper mine tailings can be repurposed into bio-columns. |
| **D** | Copper mine tailings | N/A | To act as a blank to Experiment C. |

### ***3.5.2.*** *Experimental setup*

As shown in Figure 3.9, triplicate sets of each of the above defined experiments (except experiment D) were performed using the submergent setup described in section 3.3.1. Beach sand aggregate collected from the COMSIRU Laboratory in the New Engineering Building at the University of Cape Town was utilised for experiments A and B. For experiments C and D, beach sand aggregate was replaced by copper mine tailings provided by the Columbian Mine. Before the copper mine tailings were used, they were oven-dried overnight at 90°C to remove any residual water content. The relative aggregates for each experiment (see Table 3.2) were then inoculated with bacteria and packed within the fabric moulds according to the method detailed in section 3.3.3. The bio-columns made in experiment D were not inoculated with bacteria but rather mixed with 86.4 mL of deionised water. Unlike the remainder of the experiments, experiment D was also not submerged in cementation media but rather allowed to air dry for four days. experiments A-C were then submerged into cementation media and allowed to form over a period of four days. Analytical measurements were taken once daily.

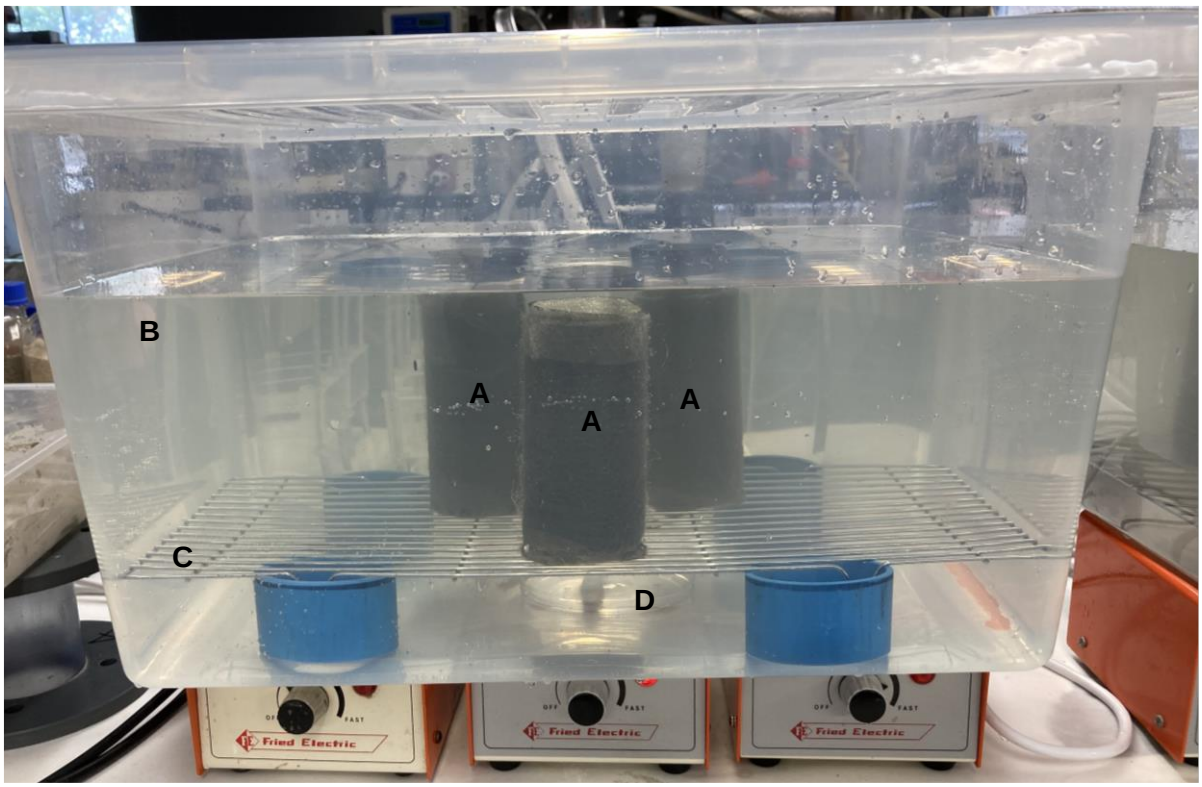


**Figure 3.9:** Image of experimental setup used to perform all bio-column experiments, showing the inoculated aggregate encased within the geo-textile moulds (A) which were submerged within cementation media (B) over a four-day period. The bio-column moulds were supported on a stainless-steel grid (C) so as to allow for a magnetic stirrer (D) to ensure that the cementation media was kept homogenous throughout the experimental run.

### ***3.5.3.*** *Cementation media*

As mentioned previously, the volume of cementation media needed to form triplicate bio-column units for each experiment was calculated as a function of the porosity of the aggregate in use. For fair comparison and to ensure an equal volume of cementation media was used in each experiment, the porosity of the copper mine tailings was used in all experiments. Porosity of the mine tailings was calculated to be 29% (see Table 4.2 in Chapter 4). As the moulds could each accommodate a volume of approximately 188 mL, the pore volume of each mould was 54.7 mL and 164 mL for each experimental set. The volume of cementation media needed was calculated based on the volume of $CaCO_3$ needed to fill the pore volume of each column. Assuming all the $CaCO_3$ formed is calcite, which has a density of 2.7 g/mL, then the mass of $CaCO_3$ needed to fill a single column could be calculated as approximately 148 g (54.7 g x 2.7 g/mL). Knowing that a 0.3 M solution of $Ca^{2+}$ was being used and assuming complete conversion of $Ca^{2+}$ into $CaCO_3$ during the MICP process ($Ca^{2+} + CO_3^{2-} \rightarrow CaCO_3$), it could be calculated that 30 g/L of calcite (MW = 100 g/mol) would be formed. Thus, to achieve this concentration of $CaCO_3$ formation, 4.93 L (148 g ÷ 30 g/L) of cementation media would be required per bio-column. Therefore, to complete a triplicate set, approximately 15 L of cementation media would be required.

### *3.5.4. Bacterial inoculation*

For each bio-column a single starter culture was cultivated as outlined in section 3.1.3. Each starter culture was then subcultured into a sterile 1 L Erlenmeyer flask which contained 90 mL of freshly prepared sterile ATCC®1376 liquid media. The cultures were grown overnight at 30°C and 120 rpm. After approximately 16 hours a direct cell count performed as detailed in 3.1.4. The cell density achieved for each experiment is detailed in Table 3.2. For each experimental condition described in Table 3.2, approximately 55 mL of the inoculum was mixed into each respective aggregate. Once the aggregate of each respective condition was completely saturated it was left to stand for four hours, allowing the bacteria to colonise and adjust to the environment inside the bio-column mould. Once the four hours elapsed, the fabric bio-columns were removed from the PVC moulds and submerged into the cementation media.

### *3.5.5. MICP sampling and analysis*

The sampling procedure described in section 3.4.1 was followed to track the chemical make-up of cementation media over the course of the experimental run. The concentration of calcium ions and ammonium ions in each sample were measured using a Thermoscientific Gallery at the start of every experimental run, followed by another sample being taken daily over a period of four days. During every sample measurement the pH of the cementation media was also measured using a calibrated pH probe. The calcium depleted efficiency and ammonia production efficiency were then calculated using equations 16 and 17 respectively:

$$\text{Calcium depleted } (\%) = \frac{[Ca^{2+}]_f}{[Ca^{2+}]_0} \times 100 \quad (16)$$

$$\text{Ammonium produced } (\%) = \frac{[NH_4^+]_{measured}}{[NH_4^+]_{theoretical}} \times 100 \quad (17)$$

Where:

$[Ca^{2+}]_0$ = initial calcium concentration [mg/L]

$[Ca^{2+}]_f$ = final calcium concentration [mg/L]

$[NH_4^+]_{measured}$ = measured ammonium concentration [mg/L]

$[NH_4^+]_{theoretical}$ = theoretical ammonium concentration based off initial urea concentration [mg/L]

After four days of growth, the bio-columns were removed from the cementation media and dried in a controlled environment at 30°C for 48 hours (this step included experiment D). Each bio-column then underwent compressive strength testing following the method described in 3.4.2. Once the compressive strength of each bio-column unit had been tested, a microstructure analysis was carried out on one bio-column from each experimental condition (A, B, C and D) following the method described in section 3.4.4 using shards collected from the outermost and inner most regions of each bio-column unit. As well as this, the $CaCO_3$ content of each bio-column grown was measured using the method described in section 3.4.3.

### ***3.5.6.*** *Economic analysis*

The results of the above experiments were used to inform both the calculations and discussion of a basic economic analysis revolving around repurposing copper mine tailings into bio-bricks. The economic analysis (including the methodology used to develop it) is given in Chapter 5. As this dissertation used bio-columns as a proxy for bio-bricks, all cementation media as well as bacterial media required was scaled up to that of a standard size South African brick (220 mm x 110 mm x 70 mm).

## 3.6. *Overcoming heavy metal (copper) inhibition*

MICP failed to occur to a great extent when copper mine tailings were used as a replacement for beach sand and hence bio-columns could not be formed (See Figure 4.4 in Chapter 4). It was hypothesized that this was due to the high copper concentration of the copper mine tailings, which inhibited the growth of *S. pasteurii* as well as the ability to produce urease; and observation which is also supported by literature (Mugwar and Harbottle, 2016). The first experiment thus conducted in this section was aimed at determining the magnitude of the impact of copper inhibition on the growth of *S. pasteurii*. This was followed by the application of two biologically inspired methods (acclimatisation and bioprospecting for indigenous bacteria) used in an attempt to overcome the perceived retardation of the MICP process by the copper mine tailings.

### ***3.6.1.*** *Minimum inhibitory concentration of copper on* S. pasteurii

To investigate how the toxicity of copper affects the growth of the urease-producing bacterium *S. pasteurii*, a minim inhibitory concentration (MIC) test was performed. MIC typically is defined as the minimum concentration of heavy metal which prevents the growth of the microorganism in question. For the MIC experiment, it was decided that the concentration of copper ions to be tested would range from 1 mg/L to 1024 mg/L – which was nearly double (622 mg/L) the maximum concentration of the copper contained within the copper mine tailings being tested (See Figure 4.1 in Chapter 4).

To perform the MIC experiment, 2 mL of ATCC®1376 (see section 3.1.1 for preparation) was aseptically added to each well of a 12-well microplate. A stock solution containing 2048 mg/L $Cu^{2+}$ was prepared by mixing copper sulphate pentahydrate crystals into deionised water. Once prepared the stock solution was filter sterilised using a 0.22 µm sterile syringe filter. Using a sterile pipette tip, 2 mL of the stock solution of copper ions was transferred into the top left well of the microplate. The solution was mixed well by drawing the fluid up and down in the pipette tip and resulted in the top left well having a copper concentration of 1024 mg/L. From the top left well 2 mL of solution were drawn using a fresh sterile pipette tip and transferred to the adjacent well, now resulting in a copper concentration of 512 mg/L. As shown in Figure 3.10, this process was repeated until the stock copper solution was diluted down to 1 mg/L. The bottom right well was left untouched to act as a blank in the experiment.

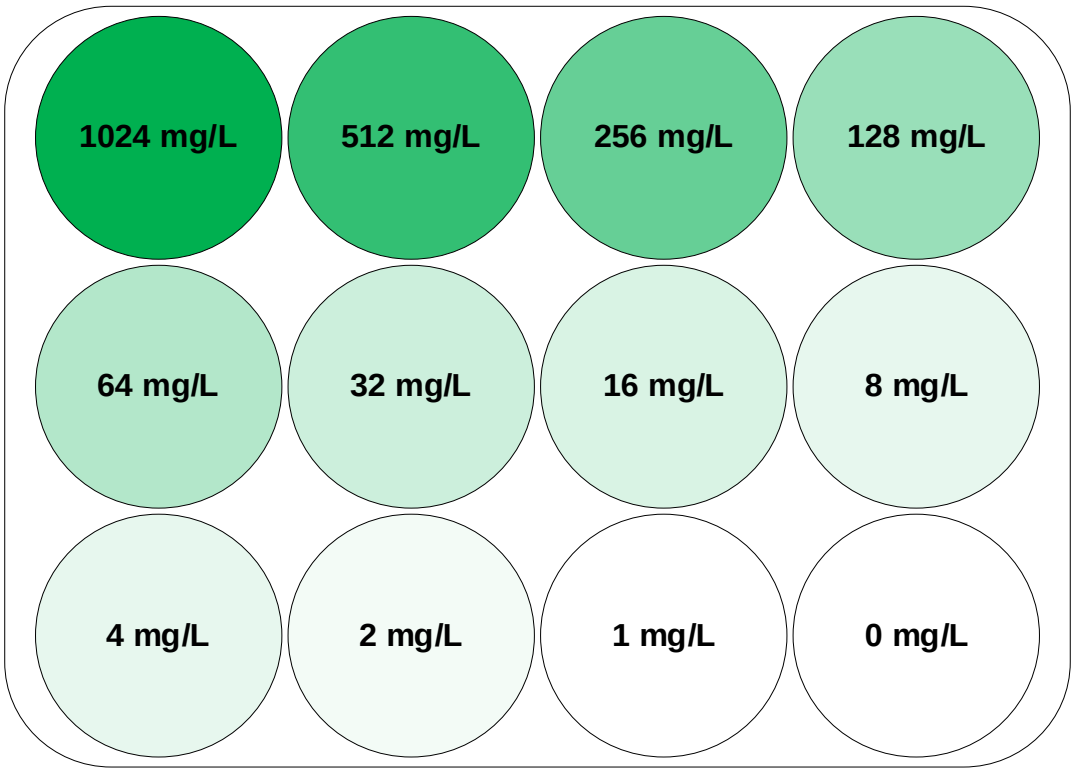


**Figure 3.10:** Schematic of 12-well microplate used in determining the toxicity effect of copper on the growth of *S. pasteurii*. The copper concentration of each well was doubled from that of the previous well starting at the second well from bottom right (1 mg/L) until reaching the top-left well (1024 mg/L). The bottommost right well (0 mg/L) acted as a control. Each of these wells were inoculated with *S. pasteurii* and then incubated over 24 hours; by observing the well where no growth occurred after 24-hours, the MIC of copper could be determined.

A sterile loop was then used to transfer a single colony of *S. pasteurii* from a previously streaked agar plate (see section 3.1.1) into each well of the microplate. The microplate was then incubated under aerobic, shaking conditions (120 rpm) at 30°C for 24 hours. To determine the MIC of copper on *S. pasteurii*, both a qualitative and quantitative approach was taken. Qualitatively it was defined as being the concentration at which visible growth of the culture could no longer be viewed after 24 hours of incubation. Quantitatively, it was defined as a 70% reduction in growth measured by direct cell counting (Ruggiero et al., 2004). The above experiment was performed in triplicate.

### *3.6.2. Acclimatisation of* S. pasteurii *to an increased copper concentration*

The purpose of this experiment was to determine whether *S. pasteurii* could be acclimatised, through incremental increases in copper ion concentration, to survive in an environment subject to high heavy metal concentrations such as copper mine tailings. To acclimatise the bacteria to increased copper concentrations, an experimental method was setup which employed the subculturing of a pure strain of *S. pasteurii* into liquid nutrient medias of ever-increasing copper concentrations. By applying this environmental pressure (copper ions) on an initially small magnitude in a controlled environment and then gradually increasing it over time; it was hoped that each successive generation of bacteria grown would show an increased tolerance towards copper inhibition.

To begin this experiment, a *S. pasteurii* starter culture (described in section 3.1.3) was inoculated into 90 mL of ATCC®1376 supplemented with 50 mg/L of filter sterilised copper ions (which was provided in the form of copper sulphate). The copper ions were added after the ATCC®1376 media had been autoclaved using a 0.22 µm sterile syringe filter so as to prevent the copper ions from precipitating out of solution. This solution was incubated under aerobic, shaking conditions (120 rpm) at 30°C for 24 hours. The growth curve of this culture was recorded against the standard growth curve plotted in Appendix A: Standard Growth Curve Preparation. with a direct cell count (following the method described in 3.1.4) being performed at 16, 20 and 24 hours. It was believed that after 24 hours, any lag growth as a results of an increased copper concentration would have been overcome. As such it was deemed unnecessary to record the cell growth at any previous point in time as for the needs of the experiment, only the stationary phase of growth was required. The task of methodically recording the entirety of the growth curve of the various bacterial strains was also made impossible due to curfew restrictions put in place during the COVID-19 pandemic. The bacteria were considered to have been successfully ‘acclimatised’ if after 16 hours the cell density recorded was within error of the stationary growth seen in the standard growth of *S. pasteurii* (see Figure A.0.1 in Appendix A: Standard Growth Curve Preparation). The above approach was repeated with 10 mL of the previously acclimatised culture being subcultured after 24 hours into 90 mL of fresh ATCC®1376 media supplemented with 50 mg/L copper ions. This was done to ensure the cells had enough time to adapt to the environmental pressure caused by the addition of copper by allowing for the ‘fitter’ copper tolerant cells to outcompete the other cells via genetic selections.

Once it was deemed that the recorded growth curves of the acclimatised bacteria showed robust culture growth on par with the growth of *S. pasteurii* in an environment of containing no copper ions, the concentration of copper ions within the fresh ATCC®1376 media was increased to 100 mg/L and the acclimatisation process was repeated.

From this point onwards, after every 24 hours, 10 mL of previously acclimatised culture was subcultured into 90 mL of fresh ATCC®1376 media supplemented with an additional 100 mg/L copper ions. This process was repeated with the goal to reach a copper concentration of 600 ppm which was in range of the copper concentration contained within the received copper mine tailings. Once again, for each subculture, direct cell counts were taken every four after the 16-hour mark. Figure 3.11 summarises the entirety of the experimental procedure used to acclimatise *S. pasteurii* to an environment of increased copper concentration. If an acclimatised strain of *S. pasteurii* were to reach the desired copper concentration it was to be cryogenically stored following the procedure laid out in section 3.1.6 to await further testing.

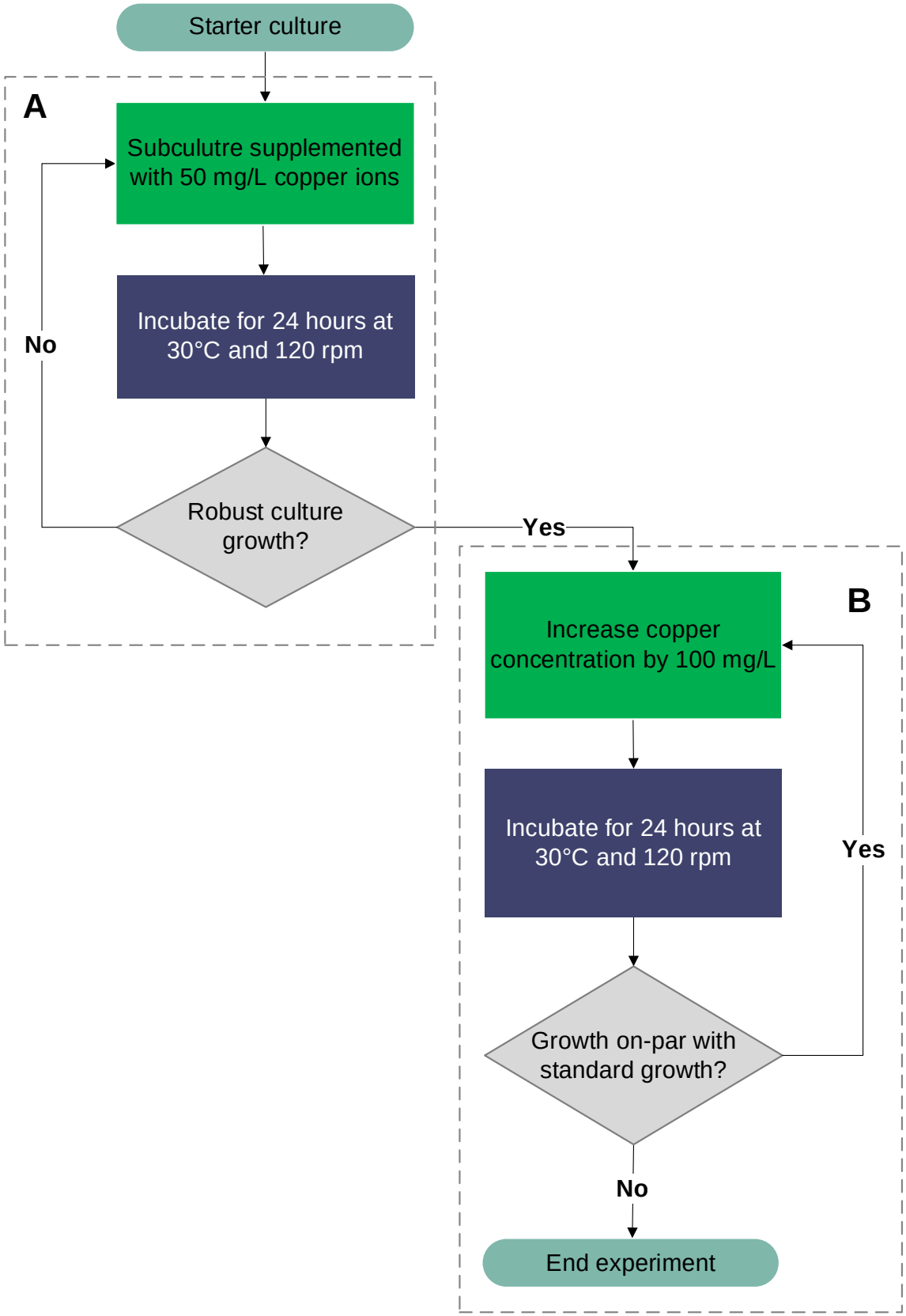


**Figure 3.11:** Decision diagram describing (A) the initial acclimatisation of a starter culture of *S. pasteurii* to 50 mg/L of copper ions. Once a robust culture of *S. pasteurii* was achieved, the second phase of acclimatisation (B) occurred where the concentration of copper ions was ramped up by 100 mg/L every day until failure.

### *3.6.3. Bioprospecting for ureolytic bacteria indigenous to copper mine tailings*

This experiment was conducted to determine whether alternative indigenous ureolytic bacteria could be isolated from the copper mine tailings. It was hypothesised that that the use of a Cu-resistant bacteria, indigenous to copper mine tailings, would provide a more viable alternative to the bacteria strain (*S. pasteurii*) currently applied to the MICP process. It was hoped that these indigenous bacteria would be capable of enduring the high heavy metal concentrations found within mine tailings and hence be exploited to produce viable bio-bricks.

To isolate the indigenous bacteria contained within the copper mine tailings by Minera de Cobre Quebradona, an adapted bacterial isolation method as laid out by Yang and colleagues (2016) was followed. One gram of the collected tailings was inoculated into 50 mL of nutrient broth containing 2 wt.% urea and 25 mM $CaCl_2$. It was hoped that the enrichment of the sample with urea and $CaCl_2$ would promote the prevalence of urease-producing bacteria being isolated. The pH of the enrichment solution was adjusted to 8 to match the conditions found within the copper mine tailings. The enrichment solution was then incubated at 30°C under aerobic, shaking conditions (120 rpm) for 96 hours. To isolate the bacteria present within the nutrient enrichments onto nutrient agar plates, the serial dilution technique was applied. To capture a greater variety of bacterial diversity, the above enrichment was grown onto three differing nutrient compositions:

1. **A copper tailing extract agar (TEA)** which was a nutrient agar made directly from the collected copper mine tailings and hence most closely mimicked the environment of the bacteria under study.
2. **A R2A agar** which is nutrient poor and hence allows for slow-growing bacteria, whose growth would otherwise be supressed by faster-growing bacteria, to be isolated.
3. **A nutrient broth agar (NBA)** which is nutrient rich, and a general-purpose agar used for the cultivation of a wide-variety of bacteria.

Each of the above nutrient agars, except for the TEA agar, was supplemented with 100 mg/L of $Cu^{2+}$ ions to ensure a selective pressure for copper resistant microorganisms was present. Once the agar plates were prepared (see Appendix M: Agar Plate Recipes) the serial dilutions were performed to isolate a manageable number of pure bacterial colonies onto each type of agar plate from the above-described enrichment culture. Serial solutions were performed by transferring 100 µL of enrichment culture into 900 µL sterile saline solutions, resulting in a 1:10 dilution. Once vortexed, this process was repeated until a 1:100 000 000 dilution was achieved. Starting at a dilution of 1:10 000 (due to the enrichment culture resulting in large amounts of bacterial growth), 100 µL of said dilutions were transferred and spread onto each of the three differing plates. The entirety of this serial dilution technique is illustrated in Figure 3.12.

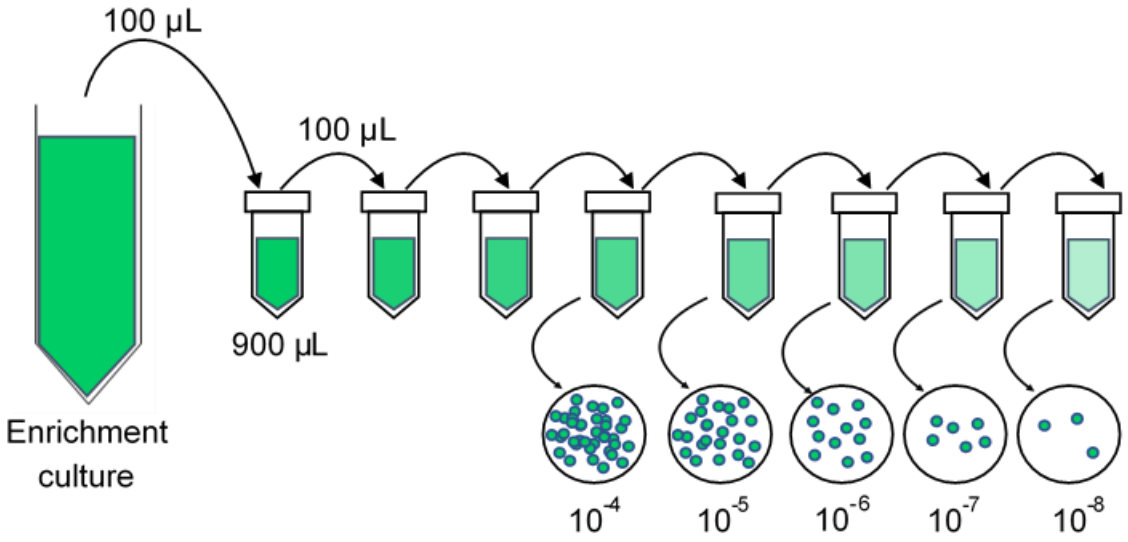


**Figure 3.12:** Schematic of the serial dilution process used to isolate the microorganisms collected from the copper mine tailing sample.

Once spread, the plates were incubated at 30°C. Colony growth was observed and recorded over a period of two days. Following the incubation period morphologically distinct bacteria species were identified and re-streaked onto agar plates of the same nutrient composition, which were then incubated at 30°C for 48 hours.

To determine the urease-producing potential of the of the isolated microorganisms, Christensen's Urea agar (CUA) plates were prepared (see Appendix M: Agar Plate Recipes), which are commonly applied to detect rapid ureolytic activity caused by the metabolic activities of bacteria. Urease activity (the hydrolysis of urea into ammonia ions by urease) is detected by CUA as it contains the pH indicator phenol red which changes colour from yellow to bright pink as the ammonia ions raises the pH of the agar above 8.01. To assess the potential of the bacterial isolates to produce urease, each of the individual bacterial strains isolated above was streaked onto the prepared CUA plates and compared against a negative control plate which contained no bacteria as well as to a CUA plate streaked with *S. pasteurii*. Each plate was then assessed for the formation of a pink imprint on the otherwise yellow-orange CUA agar. If the formation of a pink imprint was noted after 20 minutes, the isolate was considered positive for urease activity. If any bacterial isolates were to test positive for urease activity, it was to be stored cryogenically (as described in section 3.1.6) to await genome sequencing.

### ***3.6.4.*** *Bio-column experiments*

Additionally, if a promising bacterial candidate from either method (acclimatisation or bioprospecting) was to be procured, it would be used to grow a bio-column from copper mine tailings following the method described in section 3.5. Once grown, the bio-column was to be subjected to a compressive strength test, measured for calcium carbonate content and have its microstructure analysed following the methodologies laid out in sections 3.4.2, 3.4.3 and 3.4.4 respectively

# Chapter 4

# 4. Results & Discussion

## 4.1. Characterisation of copper mine tailings

### 4.1.1. *ICP and XRF analysis of copper mine tailings*

To determine the chemical makeup of the copper mine tailings, collected samples were subjected to an ICP-MS and XRF analysis according to the experimental procedure established in section 3.2.2. This was done as literature had stated that high heavy metal concentrations have been shown to have a detrimental impact on the growth and function of some microorganisms, including *S. pasteurii* (Mugwar and Harbottle, 2016). The experimental data for the ICP-MS experiment as well as the XRF experiment are recorded in Appendix B: ICP Data and Appendix C: XRF Data, respectively.

Figure 4.1 details the results of the ICP-MS analysis performed on the copper mine tailings used throughout this dissertation. The five most common heavy metals contained within the bulk of the copper mine tailings are copper (Cu), manganese (Mn), barium (Ba), chromium (Cr) and vanadium (V). Each of these five elements are present in a concentration of greater than 100 mg/kg, but of these (and as expected) the copper concentration within the tailings is by far the greatest being within the range of 622±156 mg/L. As can be seen in Figure 4.1, the error of the copper concentration is large, most likely because the fact copper is distributed unevenly throughout the tailings.

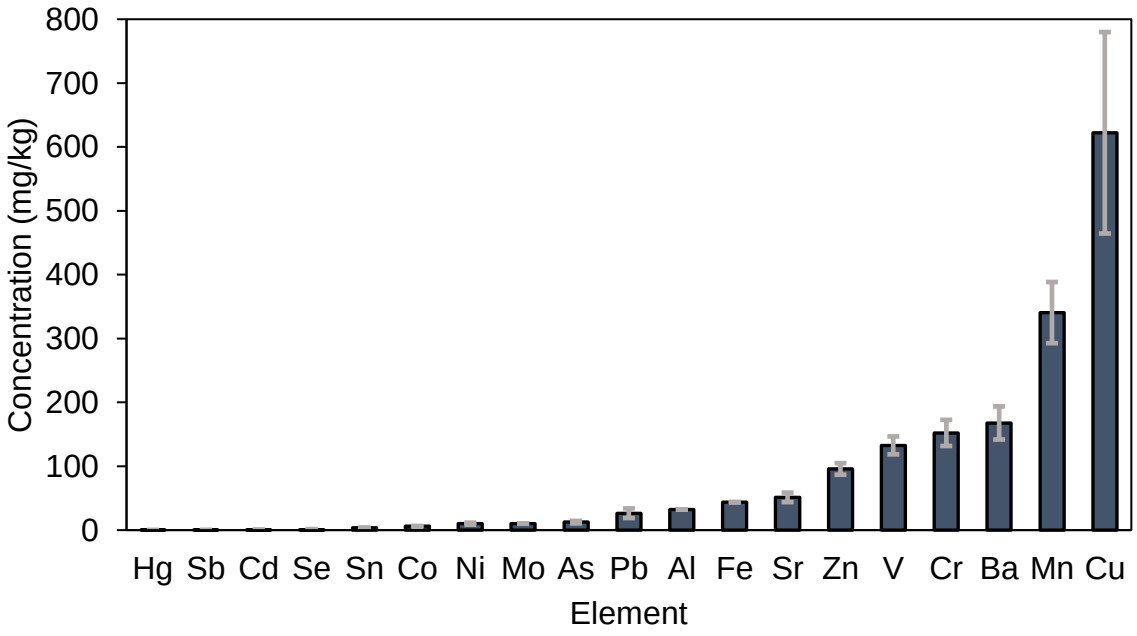


**Figure 4.1:** Results of the ICP-MS analysis performed on the samples of collected copper mine tailings detailing the concentrations of the heavy metal elements contained within.

Few studies before this one have attempted to grow bio-bricks from repurposed copper mine tailings and as such, little literature exists describing the impact these heavy metal concentrations will have on *S. pasteurii* and hence the MICP process. However, from recent available literature, it has been stated of heavy metals tested for (Cd, Cu, Pb and Zn), cadmium exhibits the greatest toxicity (MIC = 3.36 – 6.72 mg/L) to *S. pasteurii* followed by copper and zinc, which exhibit similar toxicity levels (MIC = 16.3 – 32.5 mg/L) (Mugwar and Harbottle, 2016). The resistance of *S. pasteurii* to lead was shown to be the greatest with growth being uninhibited at concentrations under 207 mg/L (Mugwar and Harbottle, 2016). Thus, as can be seen of all the heavy metals elements previously examined, as well as from the results illustrated in Figure 4.1, the high copper concentration of the copper mine tailings used throughout the experiments of this study would most likely be partly responsible for the poor performance of the MICP process when using copper mine tailings as an aggregate source for MICP. As such, the acclimatisation and bio-prospecting experiments performed in section 3.6 would focus on overcoming the impacts that copper has on the growth of *S. pasteurii*.

Table 4.1 displays the results of the XRF analysis which was performed to determine the molecular compounds constituting the make-up of the copper mine tailings used throughout this study. As can be seen in Table 4.1, the major constituents of the copper mine tailings were the mineral oxides $SiO_2$, $Al_2O_3$ and $Fe_2O_3$; which together accounted for nearly 90% of the overall composition. The concentrations of these oxides within the copper mine tailings is not unexpected considering that the host rock from which these tailings are extracted from in Middle Cauca region, Columbia are typically rich in these oxides (Bartos et al., 2017). Based on the oxide contents of the tailings, it can be seen that the mineral assemblage of copper tailings is dominated by quartz as the $SiO_2$ content was approximately 70% of the total. As $SiO_2$ is also the main constituent of beach sand, which has been successfully used to produce bio-bricks previously (Lambert and Randall, 2019), and is generally an inert material, the copper mine tailings may thus hold the potential to be successfully repurposed into bio-bricks. However, this is on the basis that the MICP process is not inhibited by the high copper concentration determined by the ICP-MS analysis. Other compounds detected in the copper mine tailings at significant levels were $K_2O$ (3.87%), CaO (2.56%) and $Na_2O$ (1.69%). The presence of CaO within the copper mine tailings may also prove to be beneficial to the MICP process when producing bio-bricks, as it could supplement the need for external calcium ions thus reducing the overall operating cost of bio-brick production.

**Table 4.1:** Results of XRF analysis on the copper mine tailings used in this study.

| Compound | Quantity (wt.%) | Std dev. (± wt.%) |
|---|---|---|
| **$SiO_2$** | 67.8 | 1.66 |
| **$Al_2O_3$** | 13.7 | 0.87 |
| **$Fe_2O_3$** | 6.18 | 0.22 |
| **$K_2O$** | 3.87 | 0.22 |
| **CaO** | 2.56 | 0.08 |
| **$Na_2O$** | 1.69 | 0.03 |
| **$TiO_2$** | 0.56 | 0.04 |
| **$P_2O_5$** | 0.23 | 0.00 |
| **S** | 0.17 | 0.02 |
| **P** | 0.10 | 0.01 |
| **$Cr_2O_3$** | 0.01 | 0.01 |
| **MgO** | BDL* | - |
| **MnO** | BDL | - |

* BDL = Below detection limits

### *4.1.2. Physical characteristics of copper mine tailings*

The physical characteristic of the copper mine tailings are described in Figure 4.2 and Table 4.2 and were determined following the experimental procedures laid out in sections 3.2.3 and 3.2.4. The data used to construct the Particle size distribution (PSD) of the copper tailings (Figure 4.2) can be found in Appendix D: PSD Data and the porosity and void ratio calculations can be found in Appendix E: Void Ratio Calculation.

Figure 4.2 illustrates the PDS analysis performed on a triplicate set of the collected copper mine tailings. As can be seen in Figure 4.2, the PSD of the copper mine tailings is relatively consistent between the triplicate set tested and the overall the particles making up the copper tailings are small, being no greater than 100 µm. Conventionally, soils have been classified, based on differing particle size distribution, as gravel (>2000 µm), sand (50-2000 µm), mud (2-50 µm) and clay (<2 µm) (Diaz-Zorita and Grosso, 2000). Hence, the copper tailings used throughout this dissertation were clay-like to muddy in texture.

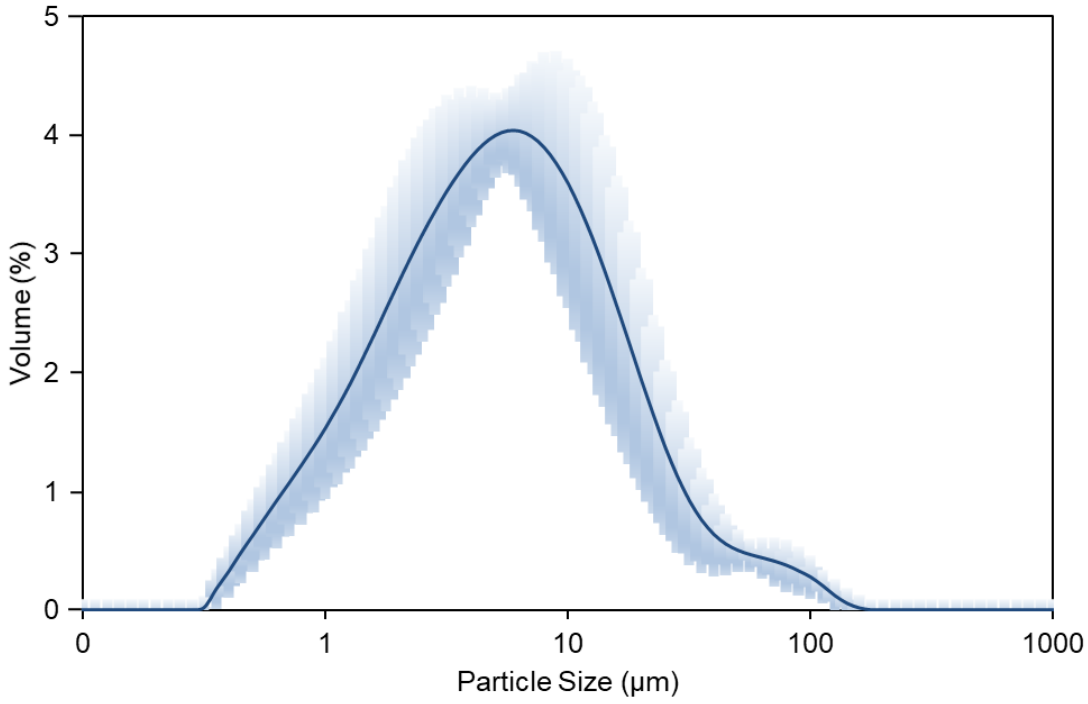


**Figure 4.2:** Particle size distribution (PSD) of copper mine tailing samples used throughout all experiments. The blue shaded area represents the standard deviation between the triplicate sample set.

Other important physical characteristics of the copper mine tailings are detailed in Table 4.2. The d(0.1), d(0.5) and d(0.9) of the measured copper mine tailings were 1.16±0.22 µm, 5.17±1.55 µm and 19.7±3.9µm respectively. These values represent the portion of analysed tailing particles (10, 50 and 90%) which are smaller than the described values. The volume weighted mean (size of the particles which constituted the bulk volume of the copper mine tailings) was recorded as 9.41±1.51 µm.

The determinisation of the porosity and hence the void ratio of the copper mine tailings was essential as it was used to determine the volume of cementation media needed to grow a single bio-column as well as the volume of bacteria needed to inoculate a bio-column. The porosity, and reciprocally the void ratio of the copper mine tailings, was calculated as being 29.0% and 0.41 respectively.

**Table 4.2:** Physical characteristics of the copper mine tailings used throughout all experiments

| Parameter | Unit | Quantity | Std dev. |
|---|---|---|---|
| **d(0.1)** | µm | 1.16 | 0.22 |
| **d(0.5)** | µm | 5.17 | 1.55 |
| **d(0.9)** | µm | 19.7 | 3.90 |
| **Surface weighted mean D[3,2]** | µm | 2.81 | 0.57 |
| **Volume weighted mean D[4,2]** | µm | 9.41 | 1.51 |
| **Specific surface area** | $m^2/g$ | 0.69 | 0.15 |
| **Specific gravity** | - | 2.65 | 0.01 |
| **Void ratio** | - | 0.41 | 0.01 |
| **Porosity** | % | 29.0 | 0.01 |

The porosity of the copper mine tailings was significantly lower than the porosity of the beach sand (38%) used by Henze and Randall (2019) to form a bio-column. The low porosity of the copper mine tailings is due its smaller PSD and implies a lower bacterial volume will be needed to fully saturate the tailings. It also implies that less cementation media may be needed to form a bio-column. However, a perceived consequence of the lowered PSD and porosity of the copper mine tailings is that these factors may act together to retard the transfer of oxygen throughout the bio-column matrix. This is problematic as the ureolytic bacteria, *S. pasteurii*, used to inoculate the bio-columns, and which drives the MICP process, is aerobic. Thus, if anaerobic conditions were to arise in the bio-column due to the poor transfer of oxygen, it is likely the bacteria will cease to function and the bio-column will fail.

### *4.1.3. Pumping cementation media through tailings*

Another perceived issue with the low PSD of copper mine tailings was that they would resist the flow of cementation media through them, preventing the use of the pumping method to form bio-columns (or bio-bricks) from said copper mine tailings. To determine if this would be the case, the experimental procedure detailed in section 3.2.5 was performed and the experimental data for said experiment can be found in Appendix F: Pumping Experiment Data.

Figure 4.3 details the mass of fluid which could be pumped through each of the various mixtures of copper mine tailings and beach sand over a 210 s period. As can be seen, as the volume of copper mine tailings to beach sand decreased there was an exponential increase in the amount of fluid which could be pumped through. At a 100% and 80% volume of copper mine tailings to beach sand, no fluid could be pumped as the force created by the tight compaction of the mine tailings caused the motor of the pump to cease functioning.

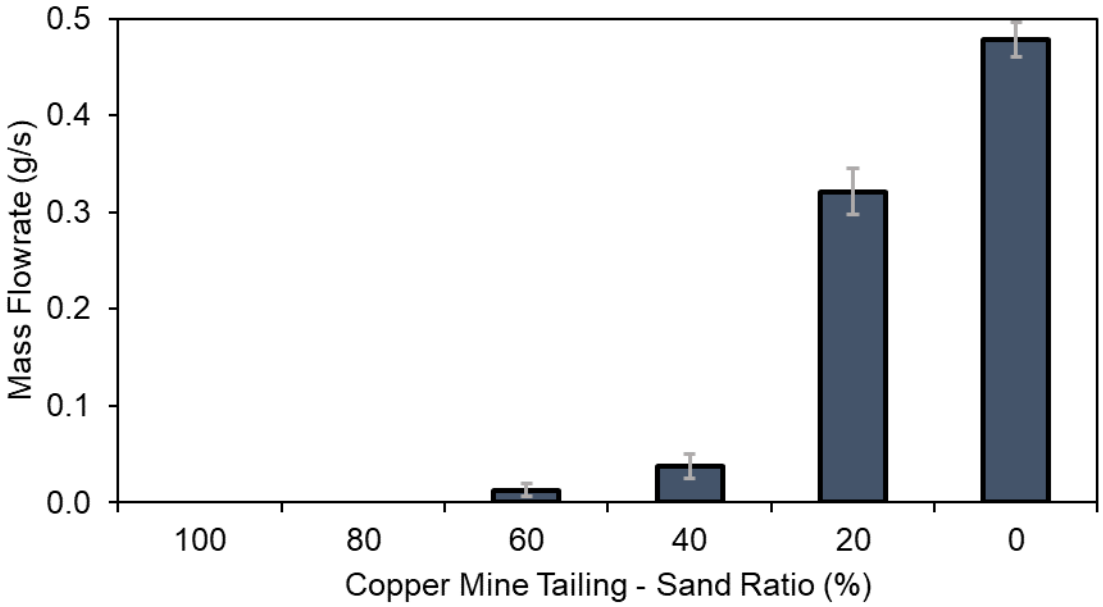


**Figure 4.3:** The mass flowrate of deionised water through various ratios of copper mine tailings to beach sand. The extent of the mass flow rate of the fluid through the aggregate mixtures was used as a measure of pumpability.

Thus, based on the results of Figure 4.3, it is evident that for the pumpability technique to be performed, it requires a ratio of copper mine tailings to sand which is lower than 20% copper mine tailings. As this would negate any environmental benefits gained by repurposing the copper mine tailings into a bio-columns as well as add to the operating costs of bio-column production, it was decided to not consider the pumping technique for growing of bio-columns when using copper mine tailings as an aggregate. Instead, a submergent technique was investigated.

### *4.2. Bio-column experiments*

The experimental method described in section 3.5 was followed to perform a series of bio-column experiments ranging from firstly developing a submergent technique (Experiment A) to repurposing copper mine tailings into MICP bio-columns (Experiment C). Analytical methods used to determine the results of the bio-column experiments are described in section 3.4 and the data for these experiments are recorded in Appendix G: Gallery Measurements and Appendix H: Compressive Strength Tests.

Experiment A focused on establishing whether the submergent technique (described in section 3.3) was capable of producing viable bio-columns. Beach sand was used as an aggregate for experiment A as it has a well-established history of being used in experiments involving MICP (Henze and Randall, 2018; Lambert and Randall, 2019). Experiment B was identical to that of experiment A with the exception that the cementation media was supplemented with 3 g/L of nutrient broth. This was done to determine whether the addition of nutrient broth would improve the compressive strength of the developed bio-columns (but with the expense of increasing operating costs). The focus of experiment C was to determine whether copper mine tailings could be repurposed into bio-columns (and hence bio-bricks) via MICP using the submergent technique. Experiment D acted as a control experiment for experiment C; where copper mine tailings were simply shaped into a bio-column by the addition of deionised water and allowed to dry and solidify at ambient conditions. A summary of the above-mentioned experimental conditions and aims can be found in Table 3.2.

Figure 4.4 shows a sample of each of the bio-columns formed after 5-days for each experimental condition (A-D). Only experiment A and D formed in triplicate. For experiment's B and C, only one bio-column of each experimental set was salvageable for compressive strength testing, as the others broke along the packing lines (see Figure 3.6). Of particular interest is what happened to the bio-column formed from copper mine tailings (Experiment C; Figure 4.4C). From direct observation, it seemed that a thin (~2 mm) 'MICP veneer' formed at the outer extremity of the bio-column; which held in place otherwise loosely held together copper mine tailings (see Figure 4.6B). Each salvageable bio-column formed had a height of 10 cm and a flat surface area of approximately 45 $mm^2$.

Of the bio-columns formed, experiment A (which employed beach sand) displayed the greatest compressive strength (1.85±0.39 MPa) as can be seen in Figure 4.5; which was significantly higher than that of Experiment B (0.31 MPa). Experiment B was supplemented with 3 g/L of nutrient broth in the cementation media. The compressive strength of the bio-column formed from copper mine tailings (experiment C) was 0.54 MPa, which was surprising as the compressive strength of the untreated copper mine tailing column (experiment D) was recorded as 0.53±0.31 MPa.

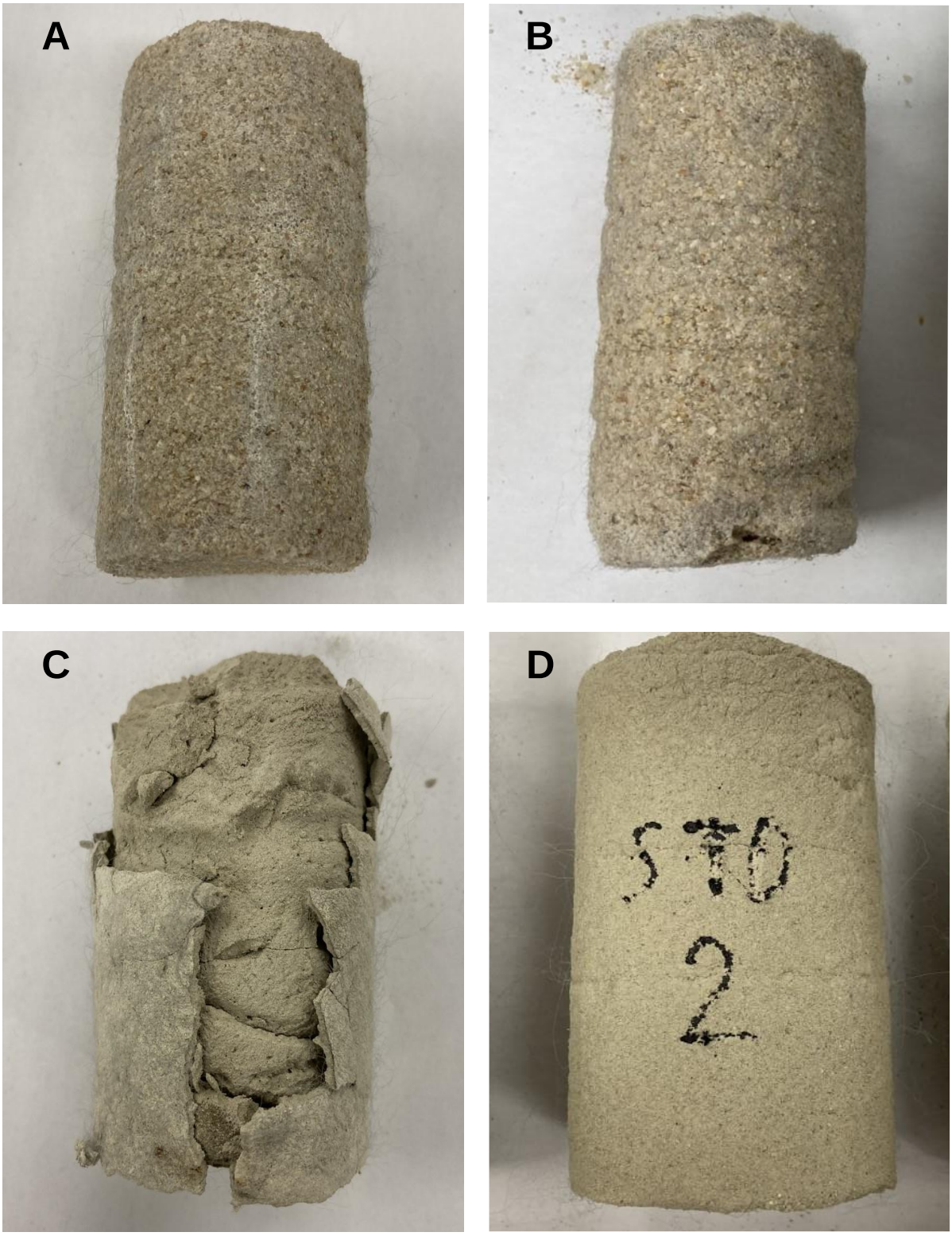


**Figure 4.4:** Images of the bio-columns formed in experiment A (beach sand), experiment B (beach sand supplemented with nutrient broth), experiment C (copper mine tailings) and experiment D (copper mine tailings but no bacteria).

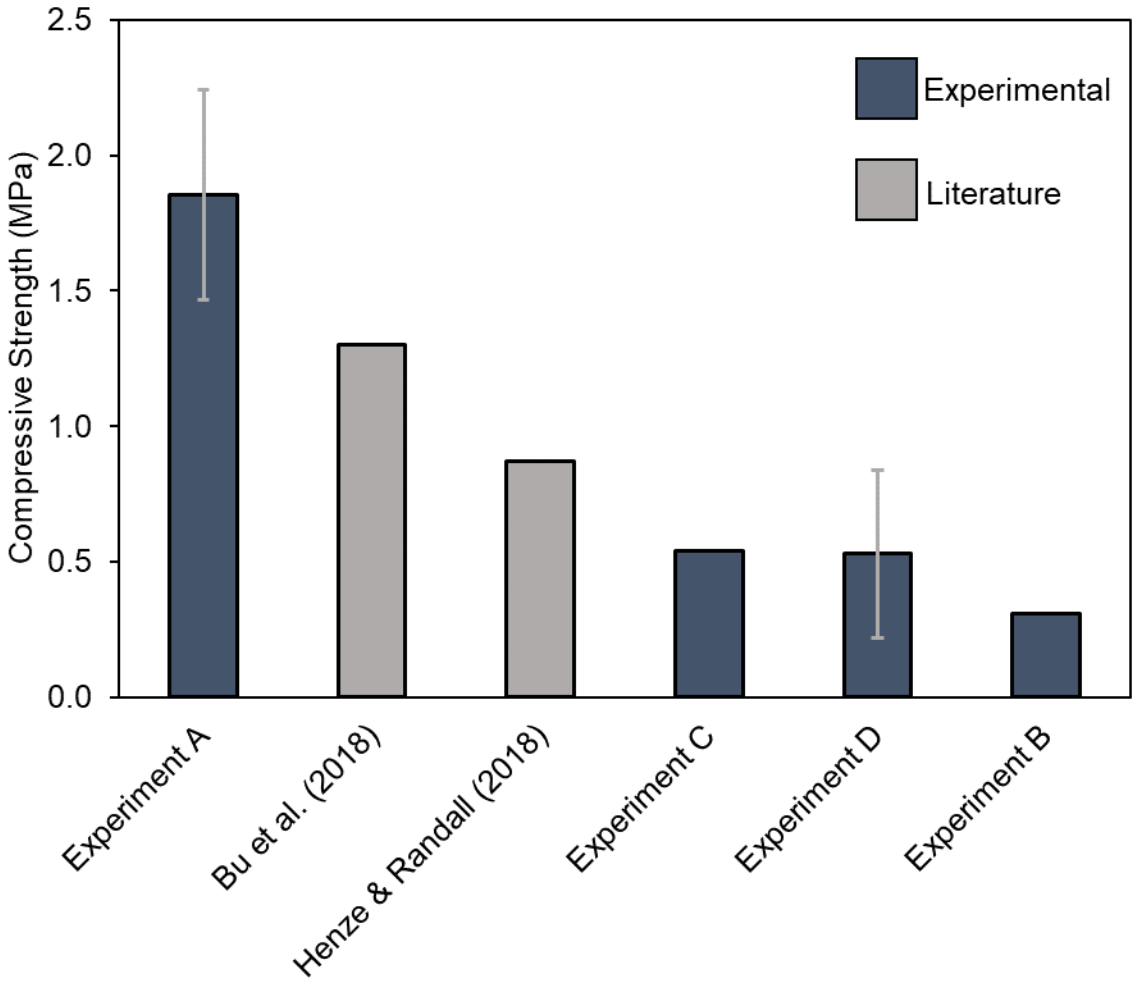


**Figure 4.5:** Comparison of the compressive strength of bio-columns found in literature to that of the bio-columns formed in experiemnt A-D. Experiment A involved growing bio-columns from beach sand. Experiment B was identical to experiment A but its cementation media was supplemeted with 3 g/L of nutrient broth. Experiment C was the first known attempt to grow bio-columns from copper mine tailings via MICP. Experiment D acted as a blank to experiment C, being copper mine tailings which were not treated with *S. pasteurii* and hence did not undergo MICP. Bu et al. (2018) grew their bio-columns from Ottawa silica sand using a similar submergent technique to this study whereas Henze and Randall (2019) grew their bio-columns from beach sand using a pumping technique.

Based on the results of experiment A, it can be concluded that the submergent technique developed for this dissertation could be used to form bio-columns, and hence possible bio-bricks as well. This is based on the fact that the bio-columns formed in experiment A displayed a compressive strength 1.4x and 2.1x greater than comparable bio-columns found in literature which employed a similar submergent technique (Bu et al., 2018) and pumping technique (Henze and Randall, 2018) respectively. It was noted, however, that the addition of nutrient broth to cementation media (experiment B) severely retarded the compressive strength of the formed bio-columns.

This was believed to be due to the fact that the bio-column formed in experiment B did not solidify homogenously. Rather, a solid 'shell' was formed which was about 1 cm thick and encased a loose centre of beach sand which was easily hollowed out by a light touch as seen in Figure 4.6A. It was postulated that this shell was formed due to the concertation gradient employed by the submergent technique to form the bio-columns. This concentration gradient would, in theory, drive the ions ($Ca^{2+}$ and $CO_3^{2-}$) from the cementation media (high concentration) into the interior of the loose beach sand particles (low concentration), allowing for MICP to occur.

However, in the case of experiment B, it was hypothesised that the presence of extra nutrients within the cementation media drastically improved the efficiency of the MICP process and hence resulted in all the $Ca^{2+}$ ions precipitating out as $CaCO_3$ before reaching the centre of the bio-column. This would thus result in a bio-column with a solid outside but no internal support, explaining the poor performance of experiment B displayed in Figure 4.5.

From what could be assessed from literature, this dissertation was the first known attempt to create MICP bio-columns using repurposed copper mine tailings. However, as can be seen from Figure 4.5, further studies are needed in this field as the bio-column formed from the copper mine tailings performed only slightly better than the untreated copper mine tailing columns (experiment D). However, of interest is the shell which formed in experiment C. Similar to that seen in experiment B, but being much thinner (~2 mm), this shell entirely enclosed otherwise loosely held together copper mine tailings (see Figure 4.6B). The reason for this occurrence once again is believed to be due to the reliance of a concentration gradient to transport the chemicals needed to perform MICP throughout the bio-column. However, unlike what was discussed for experiment B, it was believed that formation of the shell in experiment C was not due to rapid ureolytic activity but rather inhibition created directly by the copper mine tailings.

As has been stated previously by literature (Mugwar and Harbottle, 2016), it is known that copper is toxic to *S. pasteurii* and it was believed that the high copper concentration within the tailings may have prevented the bacteria from performing MICP. As such only the bacteria at the outer extremity of the bio-column, which were in direct contact with the cementation media, would have been able to undergo MICP. Alternatively, it was also hypothesised that the low PSD of the copper mine tailings may have prevented the transfer of vital chemicals into the interior of the column. It is speculated that the low PSD (and hence low porosity of the tailings) not only prevents essential MICP chemicals ($Ca^{2+}$ and $CO_3^{2-}$) from entering the interior of the bio-columns but also starves the aerobic ureolytic bacteria of chemicals essential to life such as oxygen.

Such a claim is substantiated in literature where it has been recognized that a low porosity in soil can limit the transport of nutrients and waste (Wellsbury et al., 2002), slow the rate of bacterial growth (Boivin-Jahns et al., 1996) and restrict bacterial activity and movement (Fredrickson et al., 1991).

However, regardless of the poor compressive strength of the bio-columns grown from copper mine tailings, the formation of a MICP-induced shell is believed to be a promising find. This is due to the fact that it could be applied to another major environmental issue created by mining activities which is tailings dust emissions. Experiment B has shown that by using MICP a protective veneer could be formed in situ over copper mine tailing dumps which would act to prevent the dispersion of fine tailings particles in the atmosphere. The means and mechanisms as to how such a process should be performed was beyond the scope of this discussion but it is suggested that this finding informs the basis of a future work. Further, it believed thinner materials such as wall or floor tiles would be more viable to produce using the submergent technique developed in this study; as the thin nature of tiles could potentially overcome many of the nutrient transfer challenges explained above.

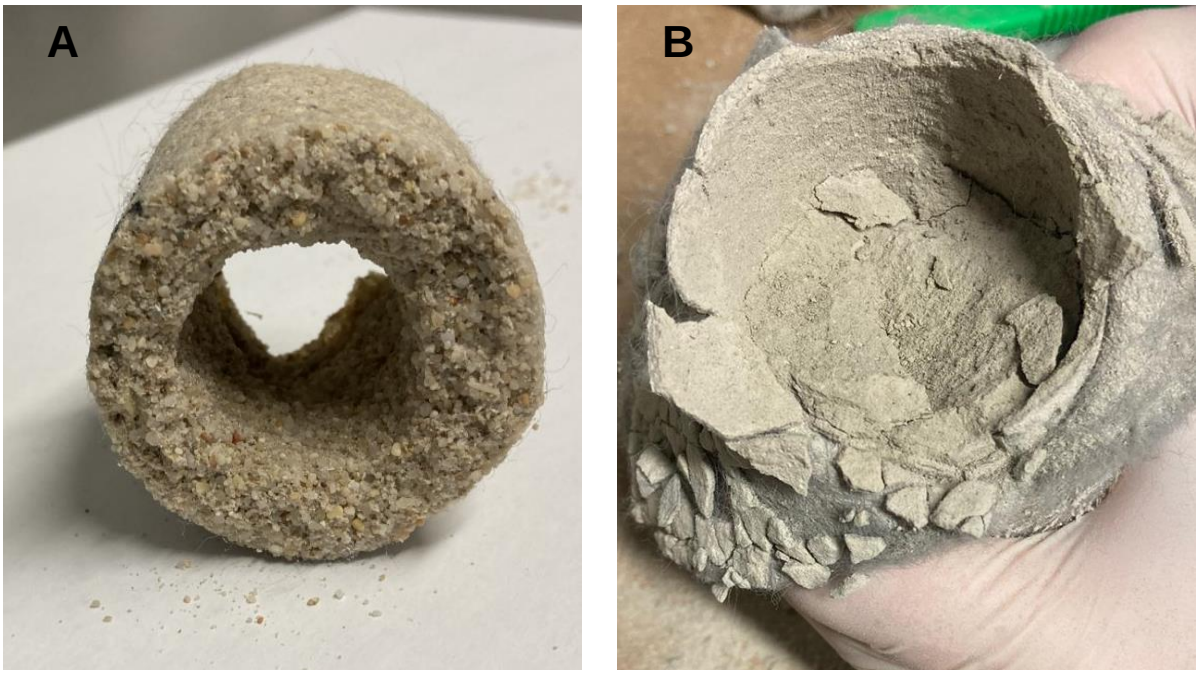


**Figure 4.6:** Image showing the solid shells formed at outer extremities of Experiment B (A) and Experiment C (B). The shell formed in Experiment B was thick (~1 cm) compared to that of Experiment C (~2 mm). Due to the formation of shells which enclosed the internal aggregated material and hence hindered the occurrence of MICP; both columns performed purely in terms of compressive strength test.

To further explain the results detailed in Figure 4.4 and Figure 4.5, a discussion is needed on the analysis of the cementation media of each experimental set. Over a period of 5-days, the 'MICP efficiency' of each experiment was determined by measuring the calcium ion concentration, ammonium ion concentration and pH of each experiments cementation media as shown in Figure 4.7. MICP efficiency was defined as the extent to which calcium ions within the cementation media precipitated to form $CaCO_3$ and, reciprocally, to what extent did the ammonium ions form from the hydrolysed urea. Both of these factors were used as proxies for measuring the rate of calcium carbonate precipitation and urea hydrolysis respectively.

The depletion of calcium ions, as they reacted with carbonate ions from enzymatically hydrolysed urea to form $CaCO_3$, is depicted in Figure 4.7A. A general decreasing trend was observed for each experiment, implying that MICP occurred in each experiment. However, when copper mine tailings (experiment C) were used significantly more calcium ions remained unconverted to $CaCO_3$ (85.6%) compared to when beach sand (experiment A) was used (55.9%). This lack of conversion of calcium ions into $CaCO_3$ for experiment C further emphasises the belief that the copper mine tailings inhibited the performance of the ureolytic bacteria and explains the poor compressive strength of the copper mine tailing bio-columns. Experiment B (the addition of 3 g/L of nutrient broth) showed the greatest depletion of calcium ions, with nearly all calcium being converted into $CaCO_3$ after only three days.

This rapid conversion, as discussed above, is believed to have been responsible for the formation of the thick shell in experiment B and hence the poor compressive strength. An interesting observation for experiment B is that, although all the calcium ions were depleted after three days, it was believed that most of it was not precipitated within the bio-column. This was due to large volumes of $CaCO_3$ forming on and around the sides and bottom of the tank containing the bio-columns. A sample of the of $CaCO_3$ formed is shown in Figure 4.8. Although this occurred in all experimental sets, this issue was particularly prominent for experiment C. Such a finding implies that the bacteria used to inoculate the aggregate for the submergent technique migrate out of the bio-columns into the cementation media; an issue which is unlikely to occur if the pumping technique is employed (see Figure 4.9A). Due to this, MICP efficiency is likely to be reduced within the bio-column as less $CaCO_3$ bridges between particles will be formed. As seen in Figure 4.9B, this is not an issue for the pumping technique as the nutrient broth is added directly to the bio-column; forcing the $CaCO_3$ to precipitate within the available pore spaces of the bio-column. Hence, while the submergent technique may be cheaper and simpler to operate, it can be expected that it will result in a reduced $CaCO_3$ precipitation efficiency compared to a pumping technique or the process will take longer to produce the same amount of $CaCO_3$.

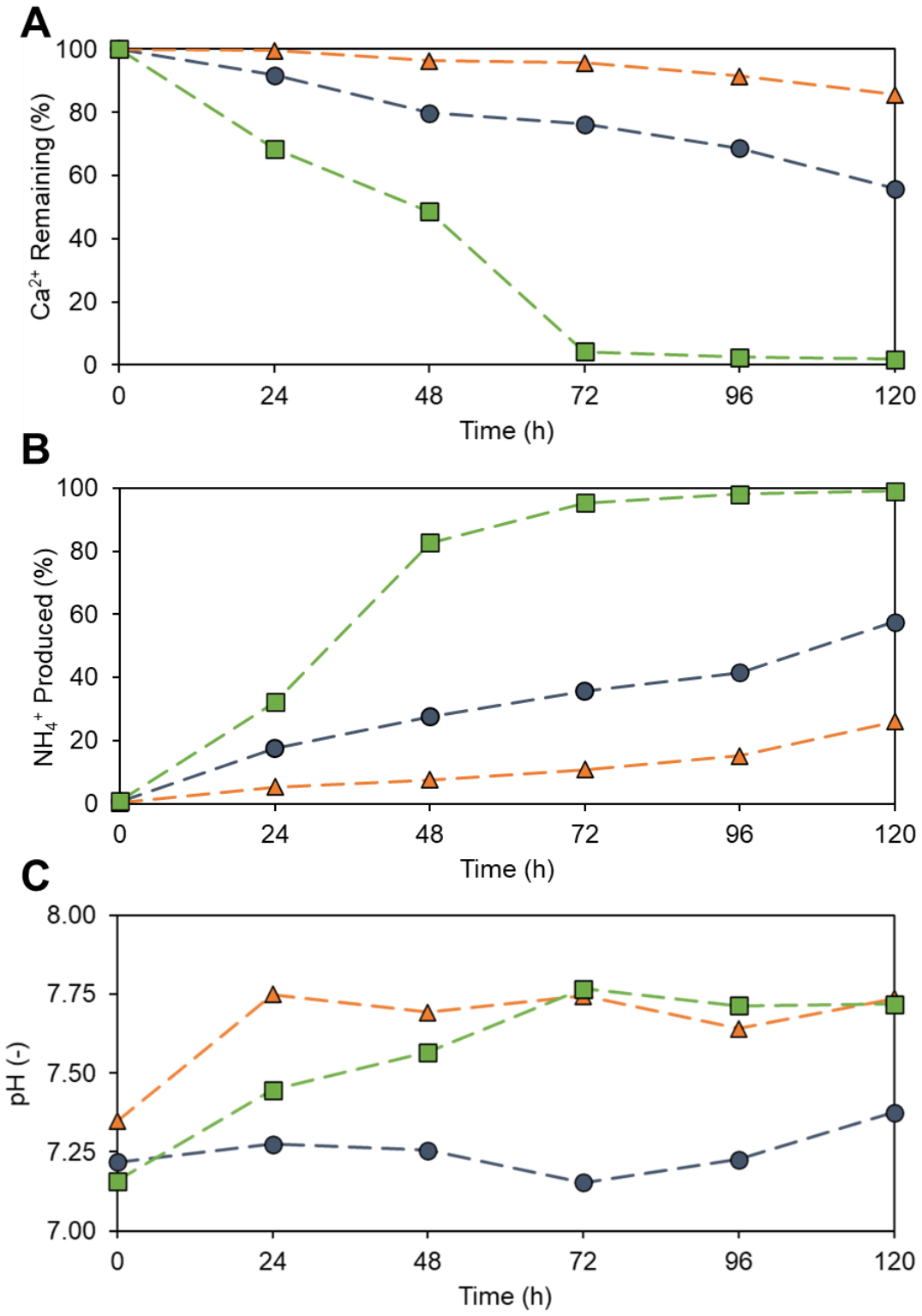


**Figure 4.7:** Changes in the chemical concentrations of the solution of Experiment A (●), Experiment B (■) and Experiment C (▲) over a period of 5-days used to determine MICP efficiency. **A:** Represents the depletion of $Ca^{2+}$ ions, as a proxy for the rate of $CaCO_3$ precipitation **B:** Represents the production of $NH_4^+$ ions, as a proxy for the rate of urea hydrolysis, where a 100% efficiency implies that all urea was degraded into $NH_4^+$ **C:** Records the change in pH for each experimental condition.

Figure 4.7B shows the extent of ammonium produced (relative to the starting mass of urea and assuming all urea hydrolysed formed ammonium) by each experiment over the course of 120-hours. As can be seen in Figure 4.7B, for each experiment, ammonium ions were produced, implying once again that MICP occurred in each experiment. As expected, and based on the compressive strength results, when copper mine tailings were employed (experiment C), the MICP reaction was inhibited, as can be seen by the fact that after 120-hours only 26% of the maximum theoretical concentration of ammonium ions were produced. This was only approximately half the amount of ammonia being produced compared to that seen in experiment A, implying that the inhibition created by the copper mine tailings is significant. Experiment B produced the largest volume of ammonium ions which was expected on the basis that it also resulted in the most calcium ions being depleted. This once again implies that the nutrient broth resulted in the rapid hydrolysis of urea.

Figure 4.7C records the change in pH for each experiment over a period of hours. Each experiment recorded an increase in pH over the duration of the experimental run due to the hydrolysis of urea into ammonium ions and carbonate ions. Previous researchers who employed the pumping technique (Henze and Randall, 2018; Lambert and Randall, 2019) have used this reaction as an indication of the extent of the MICP reaction. These ions are formed as a result of urea hydrolysis and the pH of the solution increases to the pKa of ammonia-ammonium (≈9.3). However, in neither experiment did the pH rise above 9, even in experiment B where all urea was hydrolysed.

Thus, it can be concluded that for the submergent technique, although pH can be used as indication that MICP is occurring it cannot be used as an estimate to determine when the reaction is complete. The pH of experiment C (copper mine tailings) rose more rapidly and stayed at a higher level than that of experiment A (beach sand) throughout the duration of the experiment. This was despite the fact that experiment C produced significantly less ammonium than experiment A. This occurrence was most likely attributed to the leaching of the large concentration of basic oxide compounds contained within the copper mine tailings (see Table 4.1) such as CaO and $K_2O$.

**Figure 4.8:** Image of a large piece of calcium carbonate which formed over the entirety of the bottom of cementation media container during experiment B. The formation of $CaCO_3$ along the floor of the containers was present in all experiments but the volumes formed in experiment B were particularly noticeable as was the size and thickness of the solids.

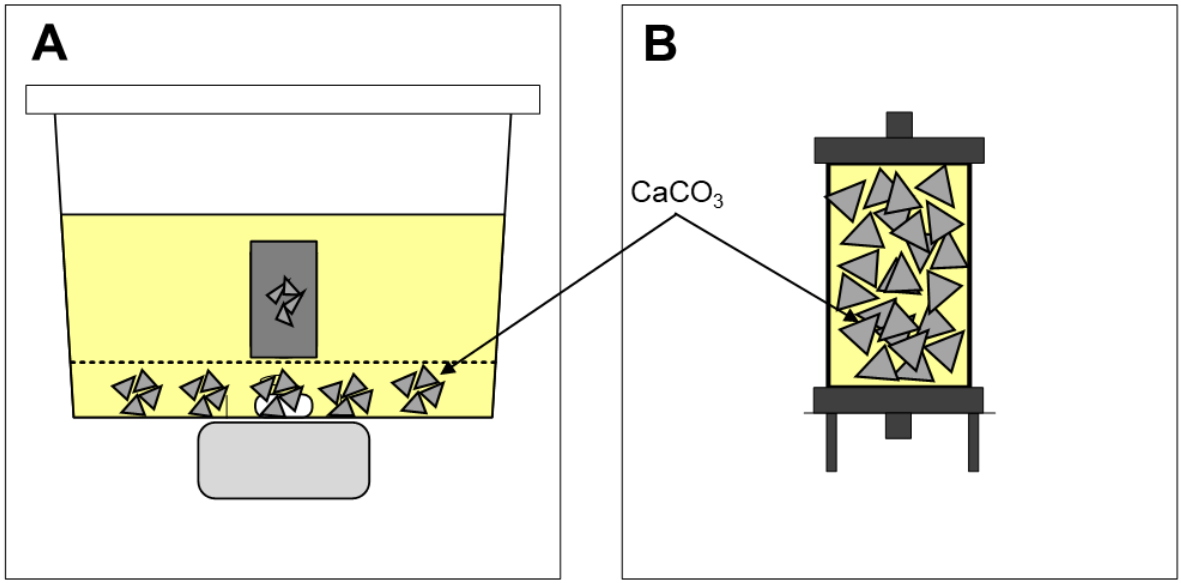


**Figure 4.9:** Schematic detailing difference in how $CaCO_3$ is deposited by MICP when applying either the submergent (A) or pumping technique (B). When the submergent technique is applied, large volumes of $CaCO_3$ are deposited outside of the columns resulting in a decrease in the overall efficiency of MICP process and a waste of raw materials. This problem is not experienced when the pumping technique is employed as $CaCO_3$ precipitation is localised and maintained within the bio-column mould. This finding implies that although the submergent technique is simpler to implement than the pumping technique, it will display a lower $CaCO_3$ precipitation efficiency within the bio-columns. This will result in increased the time being taken to produce equivalent volumes of $CaCO_3$ within the submerged bio-columns as compared to the pumped method and may thus result in increased costs.

### *4.2.1. Microstructure analysis of bio-column experiments*

To garner a greater understanding of the inner workings of each bio-column formed, a microstructure analysis was conducted to determine the distribution of calcium carbonate (see section 3.4.3) throughout each bio-column as well as an SEM analysis to determine the crystalline make-up of each bio-column (see section 3.4.4). The experimental data for these experiments can be viewed in Appendix I: Bio-column $CaCO_3$ Content Tests.

Figure 4.10 depicts the results of the $CaCO_3$ experiments conducted to determine the distribution of $CaCO_3$ precipitated throughout each bio-column formed. For each experimental set, the $CaCO_3$ content of a shard harvested from the innermost and outermost extremities of each bio-column. Experiment A was observed to have a homogeneous spread of $CaCO_3$ precipitated throughout (inner: 8.22±1.07 wt.%; outer: 8.26±0.84 wt.%) each bio-column. This even distribution of $CaCO_3$ is believed to have attributed to the high compressive strength of experiment A (1.9 MPa). Experiment D also displayed a relatively even distribution of $CaCO_3$ throughout each column; however, as no MICP occurred in this column (blank) the presence of the $CaCO_3$ in these columns must have been native to the copper mine tailings.

As expected, due to the formation of ‘shells’ as described previously, for experiment’s B and C, the ‘outer’ shards displayed a greater $CaCO_3$ content than the ‘inner’ shards. This was believed to be due to the presence of the concentration gradient established when using the submergent technique; as the outer region would be first to receive any unreacted calcium ions. The outer region of experiment C displayed the highest $CaCO_3$ content (both inner and outer) of all columns. It was hypothesised that this was due to the ureolytic bacteria present within the tailings only being able to survive at the outer most extremity of said bio-column; thus forming the main nucleation site where most precipitation would occur. Due to the copper mine tailings already natively containing $CaCO_3$, it was also predicted that the inner $CaCO_3$ content for the experiment was recorded as being too high. It is believed a more accurate value would be the experimentally measured value (6.05 wt.%) subtracted by the percentage already present (2.13 wt.%), resulting in an inner $CaCO_3$ content of 3.92 wt.%. This low inner $CaCO_3$ content of the copper mine tailings also thus further explains the reduced compressive strength of the bio-column.

Based on the results of all experiments conducted it is thus clear that when performing the MICP process using the submergent technique to form bio-columns, there seems to be a clear gradient trend in the extent of $CaCO_3$ precipitated. As experimental observation shows that $CaCO_3$ precipitation is generally concentrated at the outside extremities (in particular when copper mine tailings are employed), it is postulated that a limit exists which dictates the extent of depth which a loose aggregate can be solidified to via MICP.

This theory is deserving of further study as, based on the findings of such a study, it may reveal that MICP is a poor method for manufacturing bio-bricks as they are generally thick and require good structural integrity. Rather, based on the results discussed here, it is believed that MICP (especially when the submergent technique is employed) may be better suited to forming solids such as flooring tiles because these are thinner. Furthermore, it is postulated that the 'thin' thickness of tiles will provide less resistance to the flow of calcium ions through the tile, allowing for a more even distribution of $CaCO_3$ and hence a greater structural integrity.

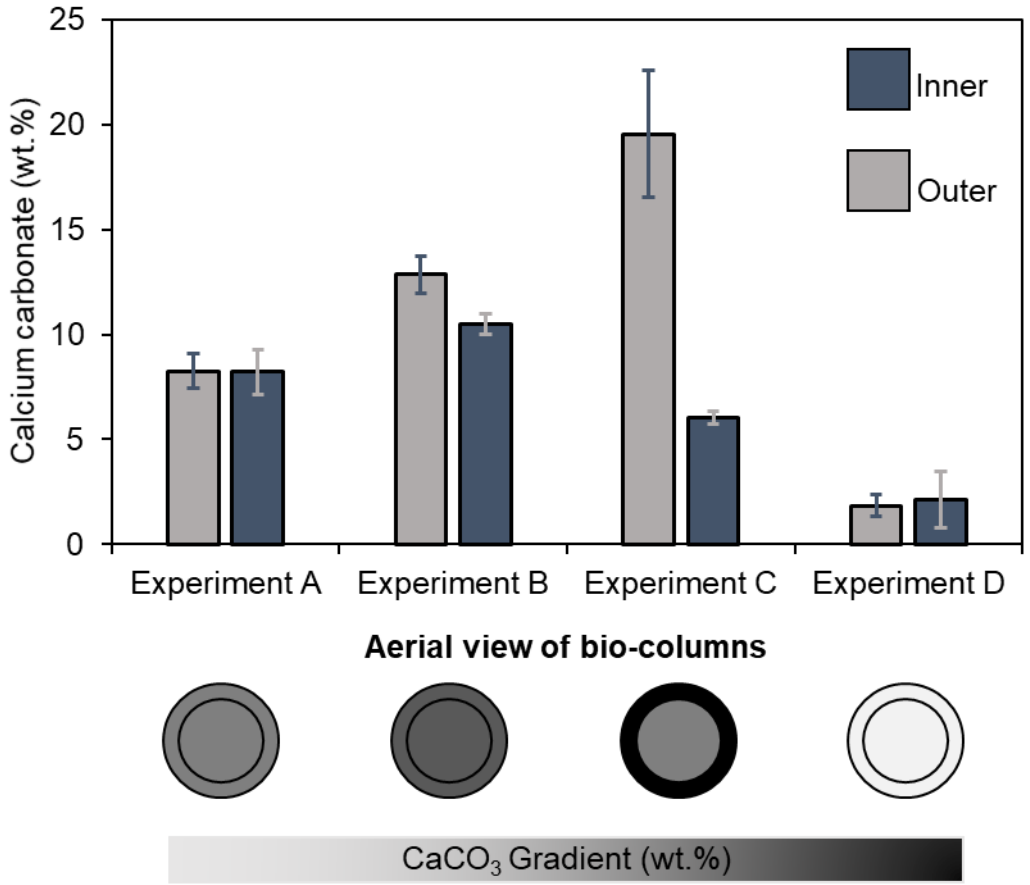


**Figure 4.10:** Graph depicting the $CaCO_3$ content of bio-column shards harvested from the inner (blue) and outermost (grey) extremities of the bio-columns from each experimental set (A-D). Below the respective data of each experiment is an aerial view schematic of the top of each bio-column; depicting the gradient distribution of $CaCO_3$ throughout each bio-column.

Displayed in Figure 4.11 are scanning electron micrographs (SEMs) of each of the MICP bio-columns (A-C) inner and outer regions. The SEMs were taken to garner a greater understanding of the crystalline structures holding each region of respective bio-columns together. Additionally, energy-dispersive X-ray spectroscopy (EDS) was used to determine the elemental composition of each region, the results of which can be viewed in Appendix J: Bio-column EDS Analysis.

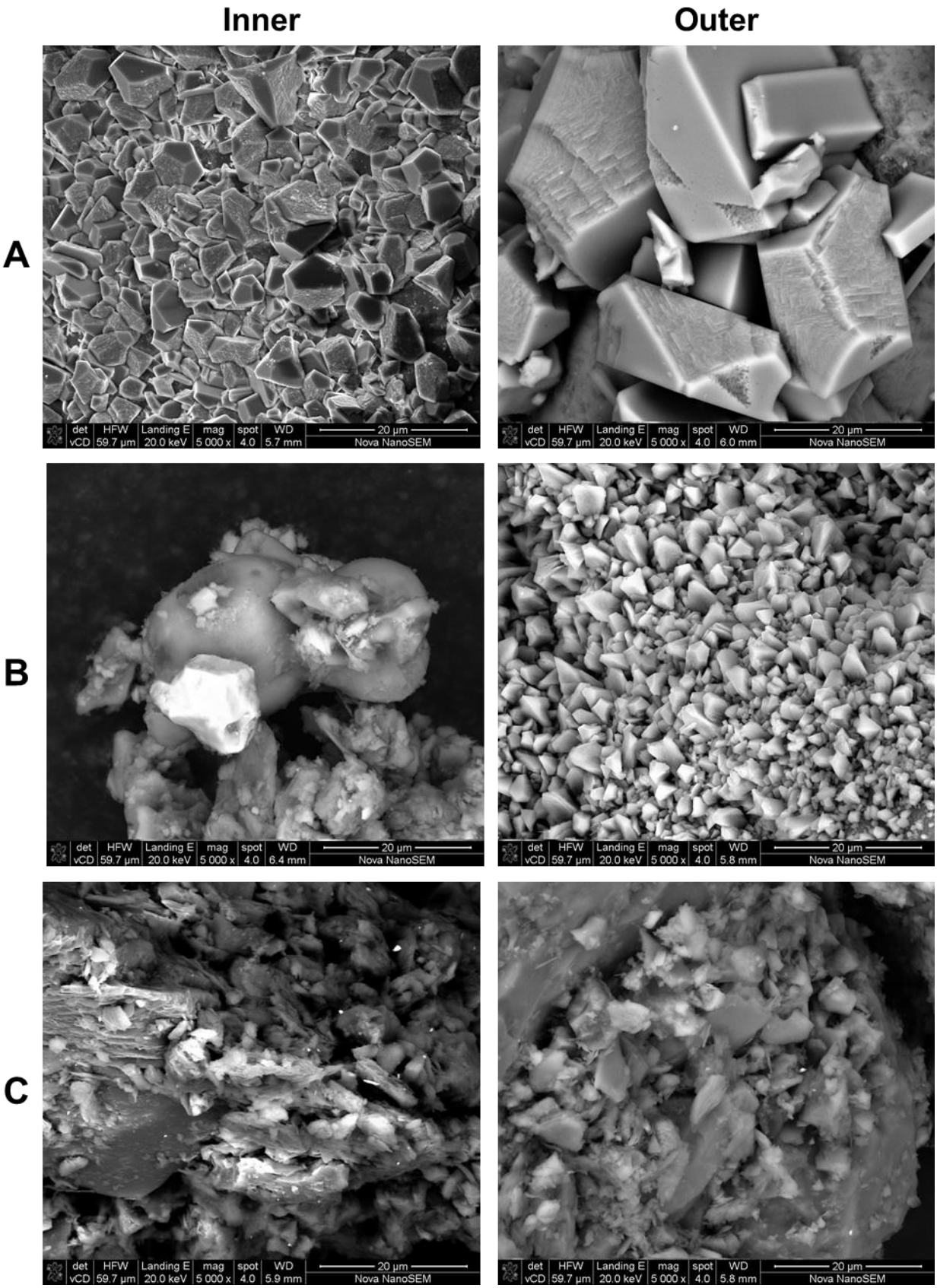


**Figure 4.11**: Scanning electron micrographs of shards harvested from the inner and outer sections of experiments A, B and C. All images viewed are at 5000 x magnification. An EDS analysis was performed on each region; the results of which can be viewed in Appendix J: Bio-column EDS Analysis.

Experiment A constituted an attempt to grow a bio-column from beach sand using the submergent technique. As can be seen in Figure 4.11A, the microscale structure of both the inner and outer section of the bio-column formed in experiment A is made up of large, rhomboidal shaped crystals. This type of crystalline structure (large and rhomboidal) is characteristic of rhomboidal calcite, which is one of the stronger morphologies of calcium carbonate (Plummer and Busenberg, 1982). Hence, the crystalline structure viewed from the SEM correlates well with experiment A displaying the highest compressive strength of all other bio-columns formed. Of further interest from this set of SEM images is the difference in rhomboidal crystal size between the inner and outer shard. As can be seen in Figure 4.11A, the outer crystals are substantially larger than those of the inner crystal. It is believed a possible reason for this is once again due to the concentration gradient which transports the chemicals needed for MICP from the cementation media to the solid being formed. It is theorised that as the outer regions are the first to come into contact with said chemicals and receive the largest concentration of chemicals; they form the main nucleation site of bio-column. Hence, by being established first and having access to the greater volume of chemicals, it is bound that these crystals will grow to a larger size. It is also believed that as these crystals grow, they reduce the pore size of the solid thus further restricting the flow of chemicals into the inner regions of the bio-column and hence further hindering the growth potential of the inner crystals. Additionally, as discussed previously, it is believed that the further restriction of the bio-column pore size by the establishment of the outer crystal wall would further starve any bacteria established within the inner area of the bio-column of oxygen. This prevents the MICP process from occurring in this location. This theory is given further credence based on the results of the EDS analysis of each region which showed on average the crystals from the inner region are constituted of 11.2 wt.% calcium, 23.7 wt.% carbon and 65.15 wt.% oxygen. This is contrasted by the outer region which is composed of 42.6 wt.% calcium, 13.9 wt.% carbon and 43.5 wt.% oxygen. As calcium carbonate is theoretically made up of 40 wt.% calcium, 12 wt.% carbon and 48 wt.% oxygen – it is clear to see that the outer region showed dominance is forming larger and more sturdy forms of calcium carbonate.

Experiment B followed on from experiment A in that it employed beach sand aggregate but additionally its cementation was supplemented with 3 g/L of nutrient broth. As can be seen in Figure 4.11B, the addition of nutrient broth had a dramatic impact on the crystalline morphologies of both the outer and inner region of the experiment B bio-column. The outer region is still dominated by rhomboidally shaped calcite crystals, but they are much smaller and more numerous than those seen in the inner region of experiment A. This is contrasted by the inner region which displayed a landscape scattered with irregular structures of calcium carbonate. The reason for the large amount of small calcite crystals formed in the outer region is believed to be directly due to the addition of nutrient broth to the cementation media.

It is postulated that the addition of nutrient broth resulted in an explosion of growth of the ureolytic bacteria in use; each which then formed a nucleation site and released large volumes of urease. The increased urease activity would have acted to rapidly break down the urea present, resulting in the formation of many, but small crystals. The large volume of crystals formed would have then restricted the flow of chemicals from the cementation media to the inner region, explaining the lack of crystal formation seen in this region. This point is further supported by the EDS analysis of the inner region, which unlike the outer region (which showed a near identical composition to that seen in experiment A), showed a high concentration of silicon being present (18.5 wt.%). This high concentration most likely originated from a silica sand particle and thus it is clear that $CaCO_3$ did not precipitate over all particles within the inner region. This was observed directly by the fact that the inner region of the bio-column from experiment B was easily removed by touch.

Experiment C, seen in Figure 4.11C, constitutes the first known attempt to grow bio-columns via MICP from copper mine tailings. As can be seen in Figure 4.11C for both the inner and outer regions, the microstructure of experiment C can generally be defined as being made-up of a loose scattering of small irregular crystals. In fact, both regions imaged are comparable to the microstructure of column made from untreated copper mine tailings (experiment D) as can be viewed in Figure 4.12.

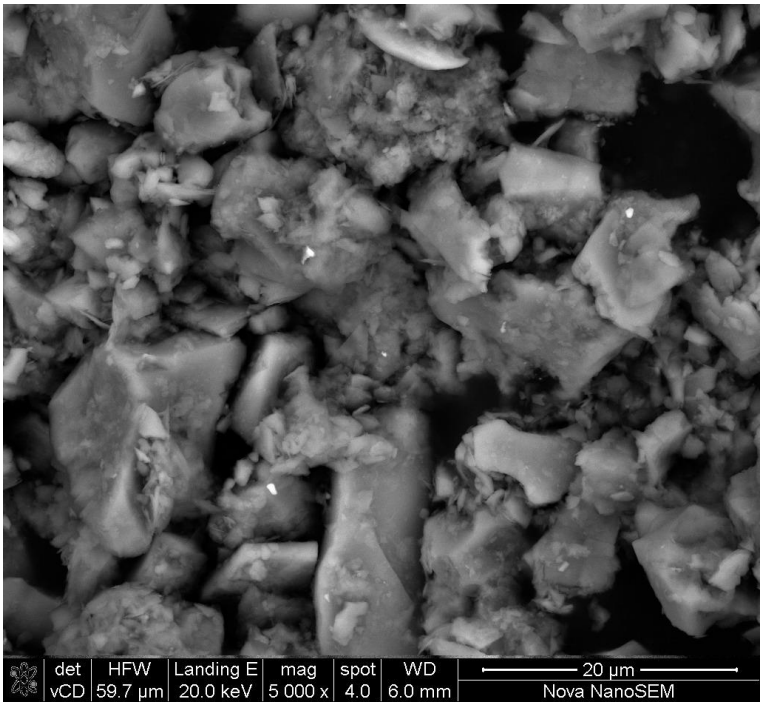


**Figure 4.12:** Scanning electron micrograph of a column formed in experiment D at 5000 x magnification. Experiment D acted as a control for experiment C and hence did not undergo MICP. Rather, it was formed by mixing deionised water to copper mine tailings and then allowing the tailings to set into the form of a bio-column naturally.

The EDS analysis recorded for the inner region was 37.5 wt.% carbon, 39.3 wt.% oxygen, 4.73 wt.% aluminium, 10.3 wt.% silicon, 3.13 wt.% potassium, 4.12 wt.% iron and 0.89 wt.% copper. The EDS analysis recorded for the outer region was recorded as 19.1 wt.% carbon, 49.8 wt.% oxygen, 5.87 wt.% aluminium, 21.98 wt.% silicon, 0.97 wt.% calcium and 2.33 wt.% iron. The presence of an amalgamation of metals was expected due to the results of the XRF and ICP analysis recorded in Table 4.1 and Figure 4.1 respectively. However, what was not expected was only 0.97 wt.% of crystal make-up in outer region being calcium. This implies that the crystals seen are not actually calcium carbonate but rather another oxide such as aluminium oxide or silica oxide. However, this is contradictory to the results shown in Figure 4.10 which calculated that approximately 19.5 wt.% of the outer region was calcium carbonate. It is speculated that this contradiction is due to spectrum where the EDS took place as this would have been on a very localised level.

However, the disorderly crystalline structure (and overall lack of crystals) seen in both the outer and inner regions of experiment C is believed to be the cause of the low compressive strength (0.54 MPa) exhibited by the columns. Besides bacterial inhibition as a result of limited nutrient transfer; the lack of calcium carbonate crystals formed was further attributed to be due to the copper within the copper mine tailings inhibiting the growth of ureolytic bacteria, a theory which was investigated in the proceeding section.

### *4.3. Overcoming heavy metal (copper) inhibition*

#### *4.3.1. Minimum inhibitory concentration of* S. pasteurii

Following the experimental method laid out in section 3.6.1 the toxicity of copper ion on *S. pasteurii* was measured by performing a basic MIC test. This allowed for both a qualitative and quantitative measure to be taken. The experimental data for the experiment performed below can be found in Appendix K: MIC Data.

Figure 4.13 shows the results of the qualitative test used to rapidly determine the MIC of copper on *S. pasteurii*. By comparing any increase in turbidity of each well in Figure 4.13B to its corresponding well in Figure 4.13A it can be seen that bacterial growth occurred throughout the 12-well microplate until the 512 mg/L well. As can be seen in the two top-left most wells of the microplate in Figure 4.13B, the turbidity of each well is almost identical to that seen in Figure 4.13A and hence it can be seen that, qualitatively, the MIC of copper on *S. pasteurii* is within the range of 128-256 mg/L. This observation was supported by the qualitative results shown Figure 4.14, which illustrates the decrease in cell density of *S. pasteurii* over ever increasing copper concentrations. Besides an initial rapid drop in cell density when copper ions are absent ($3.55x10^{-9}$ cells/mL) and the presence of 1 mg/L of copper (23.8 cells/mL), it can be observed in Figure 4.14 that cell density remained relatively constant until a copper concentration of 128 mg/L was reached. At this stage, any subsequent increase in copper concentration resulted in a rapid decrease in cell density. By defining the MIC as a 70% reduction in cell density relative to the control culture (zero metal content) (Ruggiero et al., 2004), the MIC for this experiment fell within the range of 128 – 256 mg/L of copper. Culture growth was practically non-existent at 1024 mg/L.

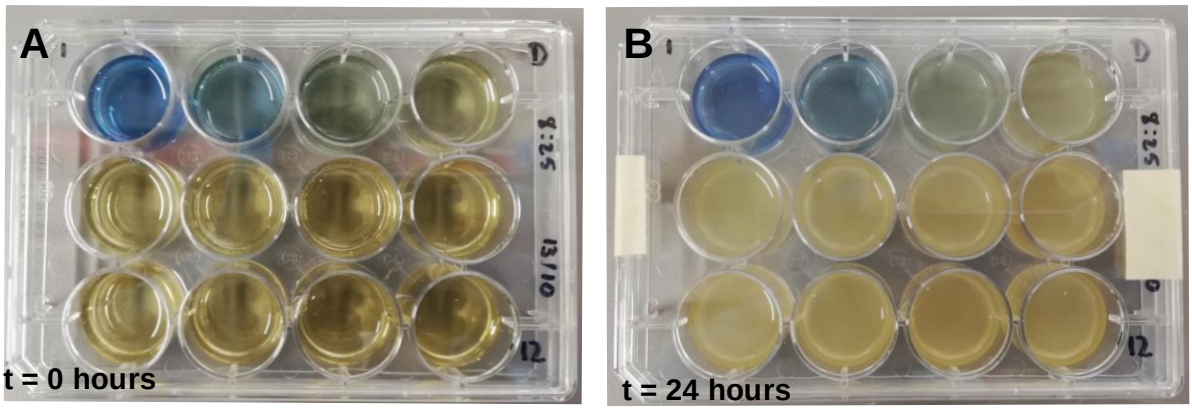


**Figure 4.13:** 12-well microplate used to perform MIC experiment before (A) and after (B) being inoculated with *S. pasteurii* and incubated overnight. Each well contained an exponential increase in copper concentration, ranging from 0 mg/L in the bottom right well to 1024 mg/L in the top left well. The extent of the growth of the bacterial culture overnight can be visually determined by viewing the turbidity of each well (B).

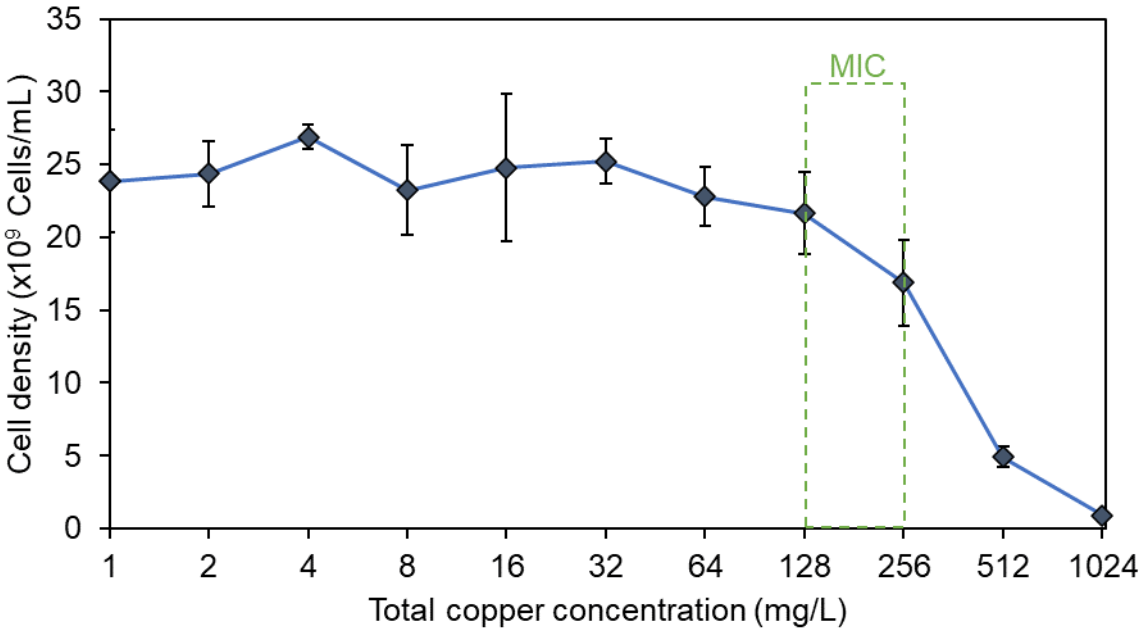


**Figure 4.14:** The effect of increasing copper concentration on the overnight growth of *S. pasteurii*. The MIC of copper on *S.* pasteurii was defined as the range of copper concentrations which resulted in a 70% reduction in cell density when compared to a culture grown in the absence of any copper (29.0 x $10^{-9}$ cells/mL), shown by the dashed green rectangle.

MIC values for *S. pasteurii* are not widely reported, however available literature showed that the MIC of copper on *Bacillus pasteurii* (which has recently been reclassified as *S. pasteurii*) is within the range of 0.2 – 1 mM (~ 13 - 64 mg/L) (Radford et al., 2003). More recently, a study focusing on the MIC for various metals on *S. pasteurii* revealed a MIC range of 0.2 – 0.5 mM (~ 13 – 32 mg/L) for copper (Mugwar and Harbottle, 2016). Both MICs are significantly lower than those reported in this study, however it must be noted that cell density for those studies were measured using optical density. This may be problematic as it measures the overall turbidity of the entire solution and hence does not differentiate between living and dead cells. Mugwar and Colleagues (2016) also used copper chloride as an alternative to copper sulphate. As mentioned previously, the impact of copper on *S. pasteurii* is poorly understood and hence this may account for the differences in MIC values reported and is deserving of further study.

Regardless, the MIC reported in this experiment is significantly lower than the copper concentration of the copper mine tailings (622 ± 158 mg/L) used in the previous experiments. The low-end MIC is thus approximately 6 times lower than the high-end copper concentration of the copper mine tailings. The MIC result from this experiment, as well as those detailed in literature, thus helps to explain the suppression of the MICP reaction seen in section 4.2 and hence the poor compressive strength of the bio-columns made from the repurposed copper mine tailings.

***4.3.2.*** *Acclimatisation of* S. pasteurii *to an increased copper concentration*

Acclimatisation experiments were performed following the establishment that the presence of copper, even found in concentrations significantly lower than that found in copper mine tailings, severely inhibited *S. pasteurii* growth and hence the formation of copper mine tailings. The setup and procedure outlined in section 3.6.2 was followed and detailed experimental data is recorded in Appendix L: Acclimatisation Experiments.

The results of the initial acclimatisation experiment, where the copper concentration was held at 50 mg/L, is shown in Figure 4.16. This initial acclimatisation phase was essential in allowing for the environmental pressure of the copper addition to genetically select for the most copper tolerant *S. pasteurii* cells. As expected, day 1 of acclimatisation resulted in the lowest cell density after 24 hours of growth. However, by the second generation of cellular growth (day 2), the culture managed to reach a cell density on-par with culture growth where copper is absent. Strong growth was once again experienced on day 3 when repeating the process once again at 50 mg/L. Based on the results described in Figure 4.16, it was deemed that a culture had been successfully selected for, which had inherited the cellular mechanisms allowing for it to survive in environments of higher copper concentrations.

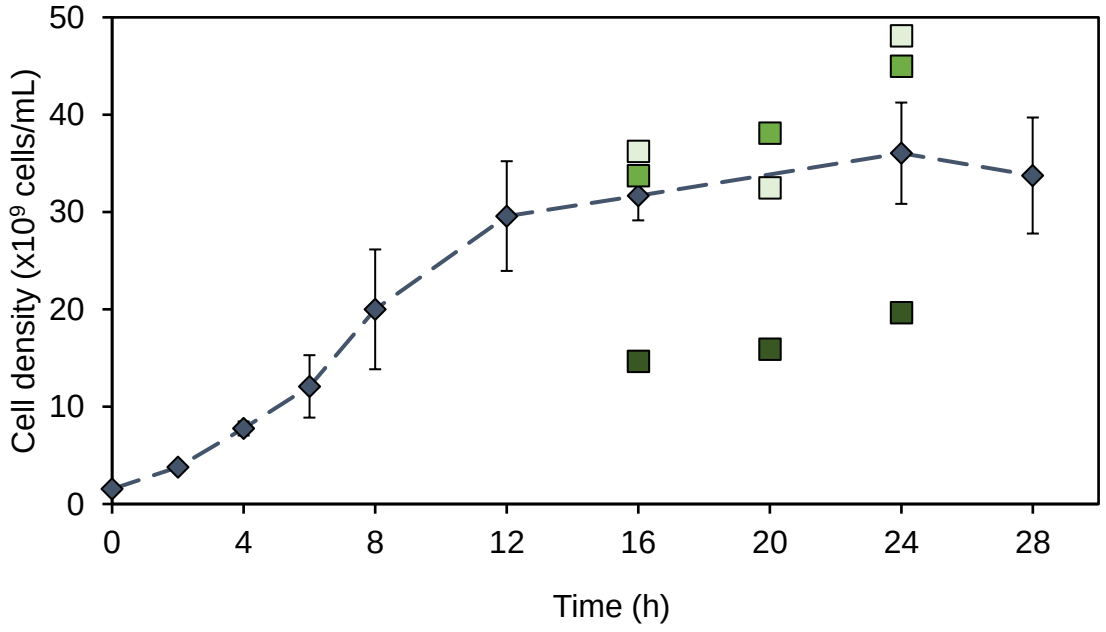


**Figure 4.15:** The effect of the addition of 50 mg/L of copper over a period of days: Day 1 (■), Day 2 (■) and Day 3 (□) on the cell density of *S. pasteurii* done in order to select for cells which are genetically predisposed to surviving in an environment of high heavy metal (copper) concentration such as copper mine tailings. The dotted blue line represents the standard growth curve of *S. pasteurii* in an environment containing 0 mg/L copper, which was used as a reference to determine if the cells were successfully acclimatised to the new environment.

As such, the second phase of acclimatisation experiments were conducted, where the environmental copper concentration of the culture was increased by 100 mg/L per day, as seen in Figure 4.16. As can be seen, the adapted culture from the initial acclimatisation responded well to each successive increase in copper concentration with the cell density of each increase falling within error of the cell density of the standard *S. pasteurii* growth curve. The only exception was for the culture grown in 500 mg/L of copper, where culture growth was strongly inhibited until the 24$^{th}$ hour. However, the cells which successfully adapted to and survived this change, performed well when subcultured into a solution containing 600 mg/L of copper.

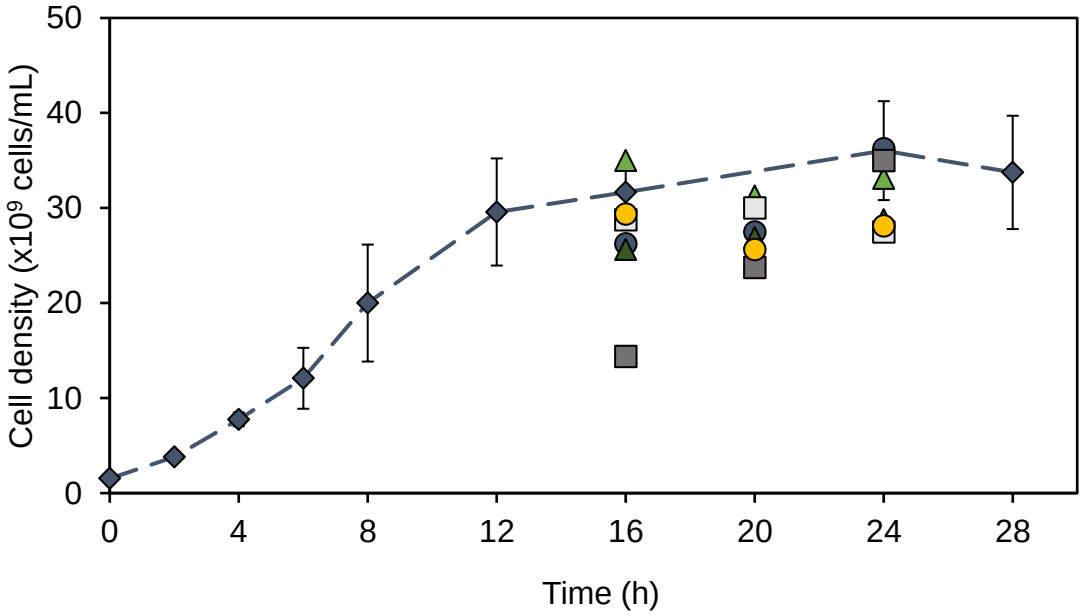


**Figure 4.16:** The response, in terms of cell density, of each successively acclimatised culture of *S. pasteurii* to a further increase in copper concentration. The copper concentrations used were: 100 mg/L (▲), 200 mg/L (□), 300 mg/L (●), 400 mg/L (▲), 500 mg/L (■) and 600 mg/L (●)

At this stage, it was thought that: 1. *S. pasteurii* could be successfully adapted to an environment of higher copper concentrations and 2. it could be grown in an environment with a copper concentration within error of the copper mine tailings (622 ± 158 mg/L). As such the experiment was ended and the bacteria culture was cryogenically stored, but it is hypothesised that the bacteria could be acclimated even further.

### *4.3.3. Results of acclimatised bacteria bio-column experiments*

The stored acclimatised bacteria culture was then used to grow a set of triplicate copper mine tailing bio-columns (Figure 4.17) following the same experimental procedure laid out in section 3.5. The results of which were compared to that of an untreated copper mine tailing column (experiment D) as well as to a column grown using a standard culture of *S. pasteurii* (experiment C), as shown in Table 4.3. The raw experimental data for the following results can be viewed in Appendix G: Gallery Measurements; Appendix H: Compressive Strength Tests; Appendix I: Bio-column $CaCO_3$ Content Tests and Appendix J: Bio-column EDS Analysis.


**Figure 4.17:** Triplicate set of copper mine tailings bio-columns grown using a culture of *S. pasteurii* acclimatised to 600 mg/L of copper. The bio-columns were brittle, with only one deemed to be suitable to undergo compressive strength testing. Like the previous set of bio-columns utilising copper mine tailings as an aggregate (experiment C), these bio-columns also displayed clear evidence of a shell forming around the outer extremities of each bio-column. However, these shells were slightly thicker and seemed to be of a sturdier nature.

As can be seen in Figure 4.18, the bio-column formed from copper mine tailings using the acclimatised bacteria once again exhibited the formation of a solid shell surrounding relatively loose tailings. The bio-columns formed were brittle, with only one maintaining enough structural integrity to undergo compressive strength testing. It must be noted however, that the shell formed around the copper mine tailings by the acclimatised bacterial culture was comparatively sturdier and more uniform than the shell formed by the standard *S. pasteurii* culture in experiment C (see Figure 4.4C).

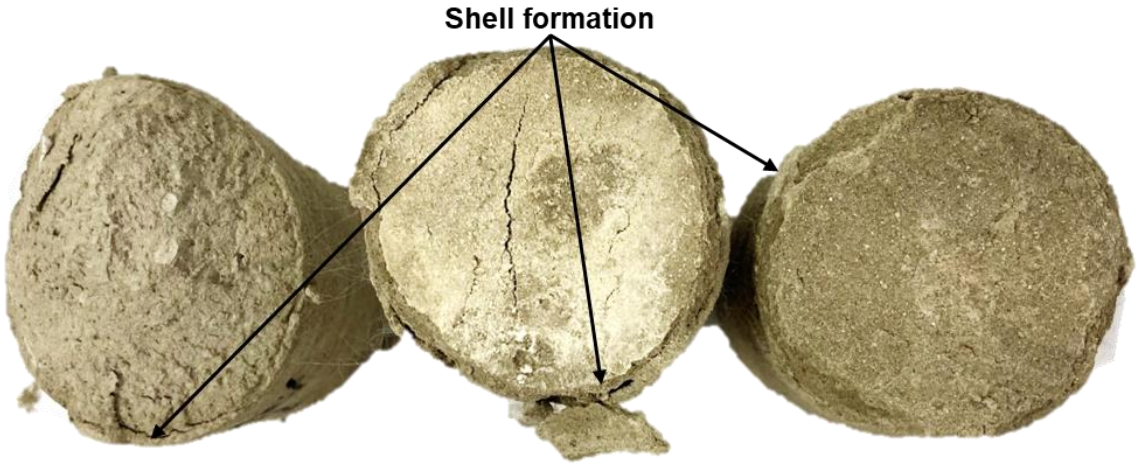


**Figure 4.18:** Aerial view of the triplicate copper mine tailing bio-columns grown from the acclimatised culture of *S. pasteurii* showing clearly defined 'shells' enclosing the material within. The white substance, which is especially prevalent on the middle column, is most likely calcium carbonate precipitated out of cementation solution by the acclimatised bacteria.

The results of the compressive strength and calcium carbonate content experiments performed on the acclimatised *S. pasteurii* bio-columns can be viewed in Table 4.3. As can be seen, the bio-columns grown from the acclimatised bacteria exhibited a lowered compressive strength to both the untreated copper mine tailing bio-columns (experiment D) as well as the bio-columns grown using a standard *S. pasteurii* culture (experiment C). Interestingly however, although the inner regions of both the acclimatised and standard bio-columns exhibited similar calcium carbonate contents; the calcium carbonate content of the outer region of the acclimatised column was higher (approximately double) than that of the standard bio-columns.

**Table 4.3:** Compressive strength and calcium carbonate content of the copper mine tailing bio-column grown using acclimatised culture of *S. pasteurii* compared to that of the standard *S. pasteurii* (experiment C) and untreated (experiment D) copper mine tailing bio-columns.

| | **Untreated (experiment D)** | | ***S. pasteurii* (experiment C)** | | ***Acclimatised S. pasteurii*** | |
|---|---|---|---|---|---|---|
| **Compressive strength (MPa)** | 0.49±0.37 | | 0.54 | | 0.11 | |
| | **Inner** | **Outer** | **Inner** | **Outer** | **Inner** | **Outer** |
| **$CaCO_3$ content (wt.%)** | 2.13±1.35 | 1.85±0.50 | 6.05±0.29 | 19.5±3.03 | 6.18±0.88 | 39.2±6.55 |

Based on this finding, it can be inferred, at least for the outer regions, that the acclimatisation procedure undertaken in section 3.6.1 resulted in the bacteria partially overcoming the inhibitive effects of the copper contained within the mine tailings. However, this impact was only noted in the outer extremities of the bio-column as the bio-column in its entirety remained structurally unsound.

The MICP efficiency for the acclimatised bio-columns, which is a measure of the depletion of calcium ions as well as the production of ammonium ions within the cementation media, is depicted in Figure 4.19. The MICP efficiency of the acclimatised copper mine tailing bio-columns was compared to that of the standard *S. pasteurii* bio-columns (experiment C). As is apparent in Figure 4.19, both bio-columns demonstrated comparable MICP efficiencies – with the standard *S. pasteurii* bio-column having depleted virtually identical concentrations of calcium ions (Figure 4.19A) as the acclimatised bio-columns but having produced slightly more ammonium ions (Figure 4.19B) by the end of the experimental run. The pH of both experiment's cementation media followed a similar pattern over the course of each experimental run. The pH of both solutions started at just above pH 7 before rapidly increasing to a pH of approximately 7.75 after 24 hours. From this point onwards the pH remained relatively constant. It was thought, due to the rapid increase of pH prior to any significant production of ammonium, that the change in pH was not due to the occurrence of MICP but rather once again due to the leaching of metal oxides from the copper mine tailing bio-columns into the cementation solution.

The results of Figure 4.19 hence shows that the MICP efficiency of the MICP process was not improved by the utilisation of the acclimatised *S. pasteurii* culture, a point which is further evident based on the fact that only one bio-column maintained structural integrity. To garner further information on the impact of the use of acclimatised bacteria on the bio-column an SEM and EDS analysis was performed on the acclimatised bio-columns, the results of which can be viewed in Figure 4.20. This was done with the aim of determining if the acclimatised bacteria employed had a direct impact on the internal microstructure of the grown bio-columns and hence provide further information as to why structurally stable bio-columns failed to form.

From the SEM of the outer region of the acclimatised bio-column, a microstructure similar to that of the outer region of the bio-column from experiment C (Figure 4.11) as well as that of the untreated bio-column (Figure 4.12) was viewed. This is unusual due to the high calcium carbonate content of the outer shell of the bio-column recorded in Table 4.3, and as such a more crystalline structure would have been expected. The results of the EDS analysis also only showed the outer region had a low average calcium concentration of 1.90±1.41 wt.%. Although a low calcium concentration is expected due to the low MICP efficiency observed in Figure 4.19A, this cannot explain for the formation of the outer shell and it is predicted that the SEM taken must have focused on area where little $CaCO_3$ precipitation occurred.

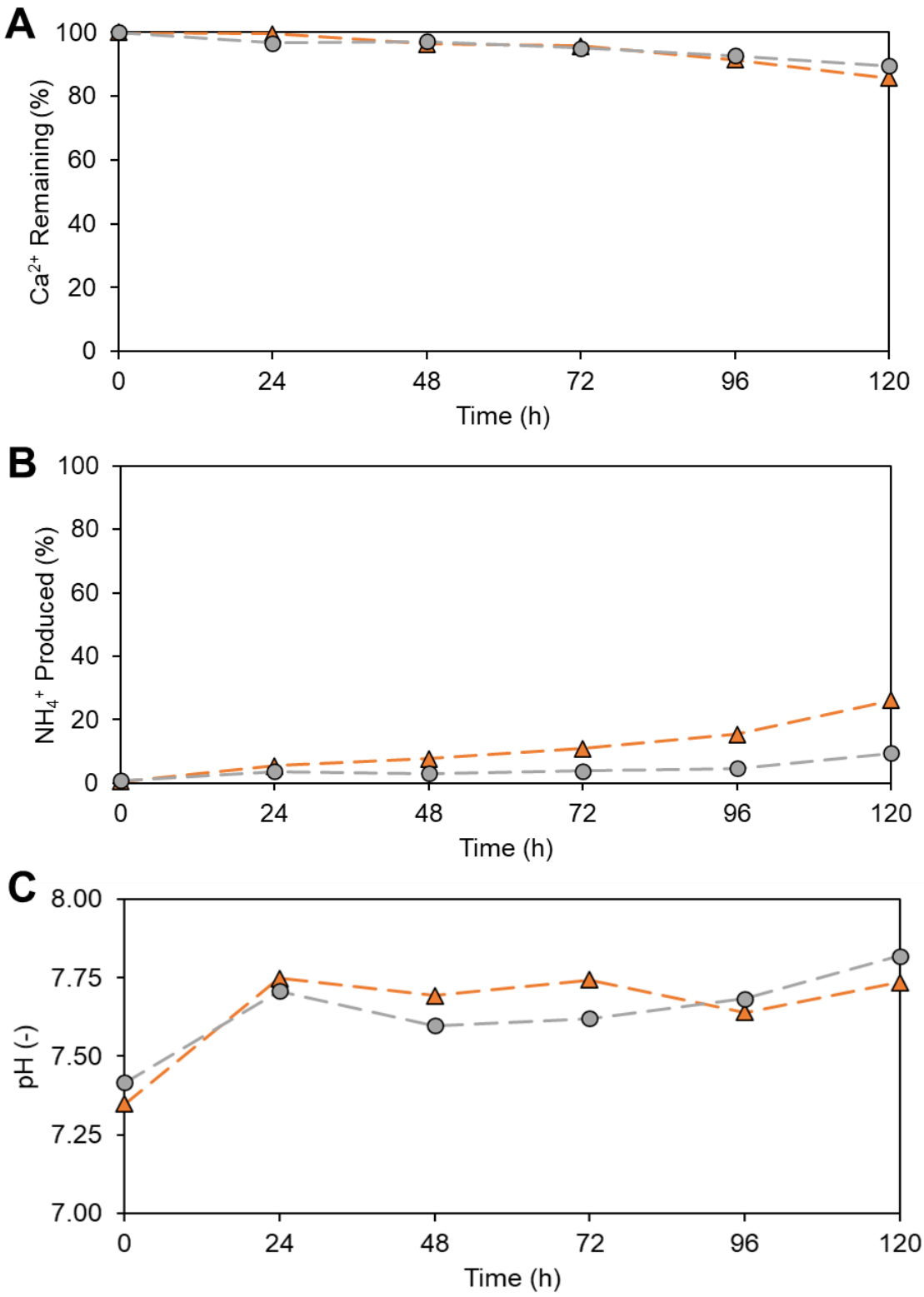


**Figure 4.19:** Comparing the changes in composition of the cementation media of the bio-columns inoculated with standard *S. pasteurii* [experiment C] (▲) and the *S.* pasteurii culture adapted 600 mg/L of copper (⊙) over a period of 5-days used to determine MICP efficiency. **A:** Represents the depletion of $Ca^{2+}$ ions, as a proxy for the rate of $CaCO_3$ precipitation **B:** Represents the production of $NH_4^+$ ions, as a proxy for the rate of urea hydrolysis **C:** Records the change in pH for each experimental condition.

The inner region of the acclimatised bio-column, however, shows different results. As can be seen in Figure 4.20, the inner region of the acclimatised column is characterised by a multitude of very small amorphous crystals. Although it is doubtful that any of these crystals are calcium carbonate, due to the EDS analysis revealing an absence of any calcium, of interest is the set of crystals circled in white. The results of the EDS analysis shows that this area of the inner region was predominantly formed of carbon (9.41 wt.%), oxygen (14.0 wt.%) and copper (75.2 wt.%). This may indicate the formation of a copper carbonate compound and hence may be the first evidence within this dissertation of the bioimmobilisation of copper. As such it can be viewed that although the acclimatised bacteria were not capable of forming a large volume of calcium carbonate crystals, they were capable of selectively entrapping free copper ions into a crystalline structure which may be useful for reducing the aqueous concentration of copper ions.

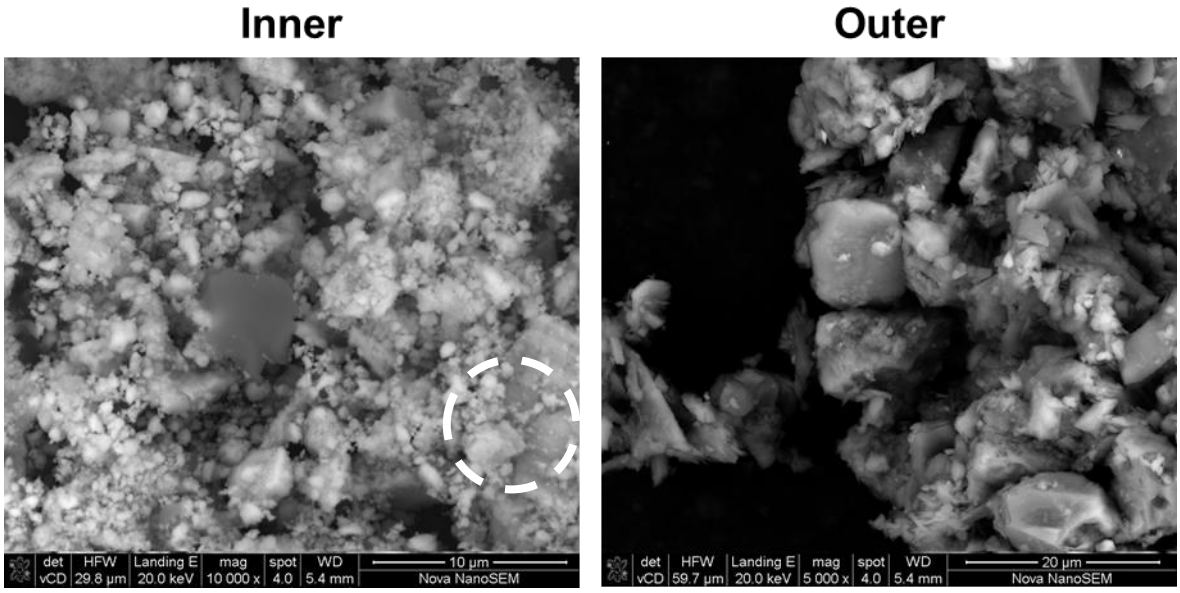


**Figure 4.20:** Scanning electron micrographs of shards extracted from the inner (10 000 x magnification) and outer (5 000 x magnification) regions of a copper mine tailing bio-column grown using a culture of *S. pasteurii* acclimatised to 600 mg/L of copper. The area of the inner region circled in white represents a possible site of copper bioimmobilisation by the acclimatised bacteria.

However, it must also be noted that at this stage it is unknown whether the copper (as chalcopyrite) within the copper tailings were leached out as copper ions during bio-column formation. It is thus suggested that a sequential extraction procedure (Tessier et al., 1979) is performed over the duration of the bio-column growth, in order to determine the bio-availability of copper to the microorganism. As such, it is also possible that the EDS results shown is in an area within the bio-column rich in copper inherent to the copper mine tailings, rather than providing evidence of the bioimmobilisation of copper ions by the acclimatised bacteria. A distinct possibility given that the entirety of this inner region shows a high copper content (24.2 wt.%).

Previously it was reasoned that a successful bio-column could not be formed from copper mine tailings was due to the inhibition of ureolytic bacteria by the high concentration of copper within the tailings. It was thus hypothesised that this inhibition could be overcome using a bacterial culture which had been previously acclimatised to high copper concentrations. The results in this section however clearly demonstrate that the use of an acclimated *S. pasteurii* culture could not form an entirely solid bio-column; although there was clear evidence of an improved outer shell formation as well as clear evidence of a differentiated internal microstructure (showing the possible bio immobilization of copper within the tailings).

Although the acclimatised culture bred in this dissertation was unable to form MICP bio-columns form the copper mine tailings, it is believed that it may hold potential in alternative scientific endeavours. Namely in the removing heavy metals from waste waters produced by tanneries and/or mining refineries as suggested by Torres-Aravena and colleagues (2018). Alternatively, the focus of creating bio-bricks from copper mine tailings could be shifted to using the ureolytic bacteria to immobilize copper within in situ within the mine tailings, thus preventing heavy metal contamination in surrounding environments. Such a potentially novel bioremediation process for copper mine tailings has already shown to be viable on a lab scale by Yang and colleagues (2016) using a ureolytic bacteria indigenous to acidic copper mine tailings. Alternatively, the acclimatised culture could be applied to growing bio-tiles, which potentially could offer a significantly higher value compared to bio-bricks, as discussed in the economic analysis found in Chapter 5.

The question, however, remains as to why viable bio-columns could not be formed from copper mine tailings using MICP. Although clear evidence was shown that *S. pasteurii* is inhibited by copper concentrations equal to and greater than 128 mg/L, it is believed that this is only partly to blame for the lack of bio-cementation seen. As shown by the fact that similar results were achieved by a *S. pasteurii* culture well acclimated to the high copper concentrations found within copper mine tailings. Due to these results and the observation that MICP did occur on the outer extremities of the copper mine tailing bio-columns (clear shell formation in all cases), it is postulated that the MICP inhibition is only partly due to the presence of copper and mainly rather a direct consequence of the small particle size distribution of the copper mine tailings. As discussed in previous sections, it is speculated that the low porosity of the tailings limits the transfer of oxygen into, and biological waste out of, the interior of the tailings. This results in a diminished rate of ureolytic bacterial growth and hence a retardation of the MICP process. Additionally, the low porosity and outer shell formation is believed to prevent essential MICP chemicals ($Ca^{2+}$ and $CO_3^{2-}$) from entering the interior of the bio-columns, further inhibiting $CaCO_3$ formation. It is thus suggested a study be undertaken to study the impact of particle size distribution on the MICP process to better understand the process.

### *4.3.4. Bioprospecting for ureolytic bacteria indigenous to copper mine tailings*

Indigenous bacteria were screened for within the copper mine tailings in order to determine if any potential candidates existed with the capability to undergo MICP within the interior of the copper mine tailing bio-columns. Following the experimental procedure detailed in section 3.6.3, a multitude of diverse bacteria were captured from the copper mine tailing enrichment onto three different nutrient agar plates. A detailed colony count was performed over a period of 48 hours, the results of which can be found in Appendix N: Bio-prospecting Experiments. The colony counts were analysed and converted into CFU/mL as seen in Table 4.4, which gave an overall indication of the number of viable bacterial cells captured from the copper tailings sample.

**Table 4.4**: The number of viable bacterial colonies, bio-prospected from the copper mine tailings, present on each type of nutrient agar after 24 and 48 hours respectively.

| Agar type | CFU/mL after 24 hours | CFU/mL after 48 hours |
|---|---|---|
| **Nutrient broth** | $7.30 \times 10^8$ | $1.09 \times 10^9$ |
| **R2A** | $3.50 \times 10^8$ | $5.3 \times 10^8$ |
| **Tailings extract** | - | $4.50 \times 10^8$ |

A diverse collection of bacteria was present on each agar plate type, with the exception of the tailings extract agar (TEA). In general, it seemed a single bacterial colony, which was small round and flat, dominated the TEA plates. The other two agar types, nutrient broth (NBA) and R2A, displayed a large diversity of bacterial colonies each of which could be isolated based on differences in morphology, shape, size and colour etc. These characteristically distinct colonies, such as those shown in Figure 4.21, were separately isolated onto new agar plates as shown in Figure 4.22. In total, approximately 16 visually distinct bacterial colonies were isolated. These colonies were then tested for urease activity on Christensen's Urea agar (CUA). The results of this experiments, as well as the description of each bacterial isolate, is recorded in Table 4.5. As shown in Table 4.5, none of the 16 bacterial isolates tested positive for urease activity on the CUA after 20 minutes.

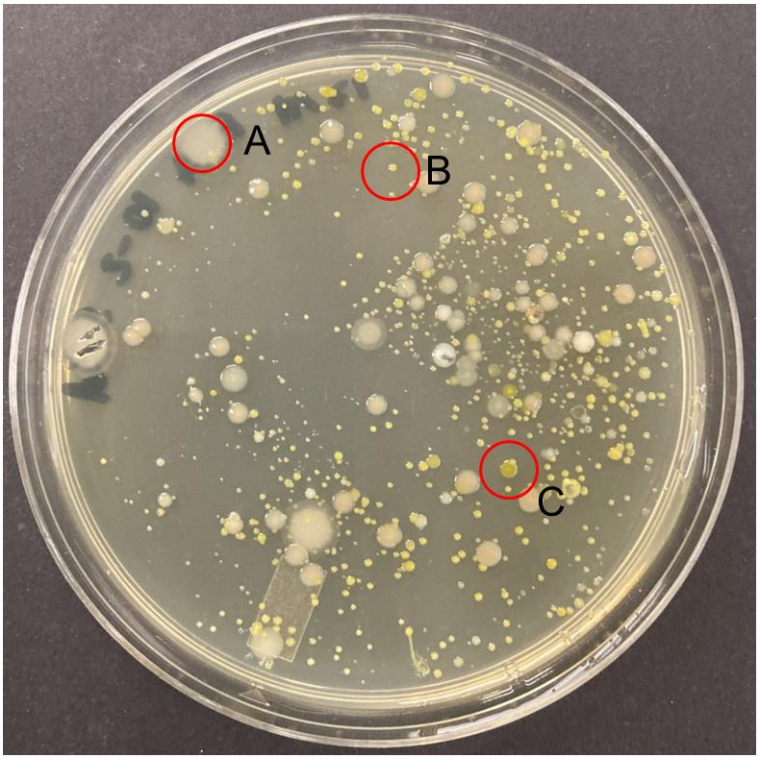


**Figure 4.21:** Sample of a R2A agar plate containing distinct bacterial colony types which were grown from a copper tailings enrichment over a period of 48 hours. Characteristically distinct colonies such as those with varying morphologies (A), sizes (B) and colour (C) were isolated onto fresh agar plates for further study.

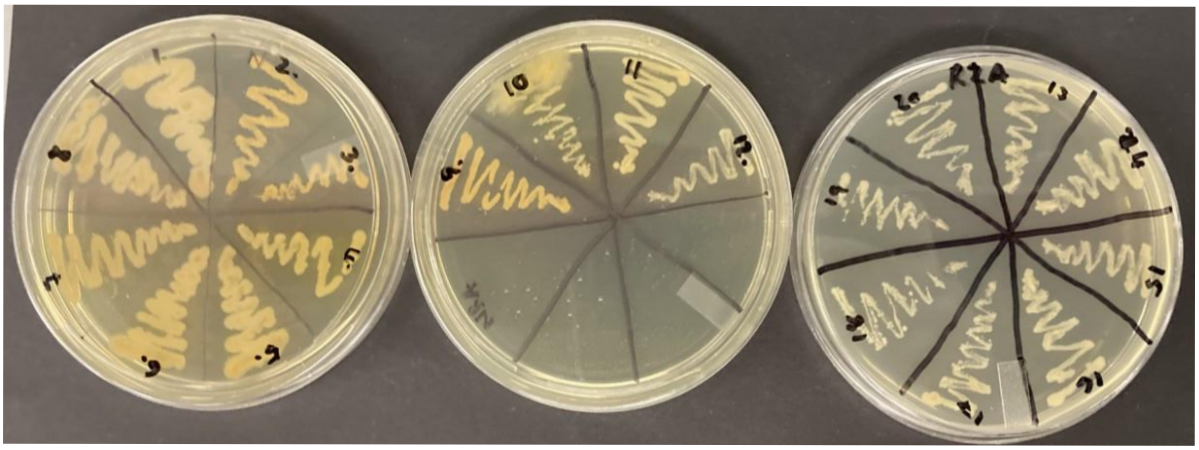

**Figure 4.22:** Sample of the bacterial colonies which were isolated, based on their distinct characteristics, onto fresh agar plates in preparation for testing for urease activity. Each segment represents a single bacterial colony, deemed to be characteristically distinct from its neighbours, incubated over a period of 48 hour

**Table 4.5:** Urease activity and morphological description of distinct bacterial colonies isolated from the copper mine tailing enrichment onto various nutrient agar plates.

| Isolate | Agar type | Urease activity✶ | Colony colour | Colony size | Colony form | Colony surface | Colony elevation | Colony margin |
|---|---|---|---|---|---|---|---|---|
| **1** | NBA | - | Milky | Large | Round | Concentric | Raised | Curled |
| **2** | NBA | - | Brown | Small | Round | Contoured | Flat | Smooth |
| **3** | NBA | - | Orange | Very small | Round | Smooth | Flat | Smooth |
| **4** | NBA | - | Milky | Large | Irregular | Smooth | Convex | Lobate |
| **5** | NBA | - | Milky | Large | Irregular | Contoured | Raised | Lobate |
| **6** | NBA | - | Opaque | Small | Irregular | Translucent | Flat | Filamentous |
| **7** | NBA | - | Milky | Large | Irregular | Wrinkled | Raised | Lobate |
| **8** | NBA | - | Milky | Very large | Filamentous | Slimy | Convex | Filamentous |
| **9** | NBA | - | Orange | Large | Round | Smooth | Flat | Smooth |
| **10** | R2A | - | Orange | Small | Irregular | Smooth | Flat | Undulated |
| **11** | R2A | - | Brown | Large | Round | Concentric | Raised | Curled |
| **12** | R2A | - | Milky | Small | Round | Smooth | Flat | Smooth |
| **13** | R2A | - | Milky | Very large | Irregular | Concentric | Umbonate | Lobate |
| **14** | R2A | - | Milky | Very Large | Round | Smooth | Flat | Filamentous |
| **15** | R2A | - | Opaque | Large | Rhizoid | Slimy | Flat | Rhizoid |
| **16** | TEA | - | White | Small | Round | Smooth | Flat | Smooth |

✶ No change in agar colour after 20 minutes inferred that the collected isolate produced no urease which was represented by '-'. An isolate which changed the agar pink after 20 minutes was defined as having tested positive for urease activity and represented by '+'

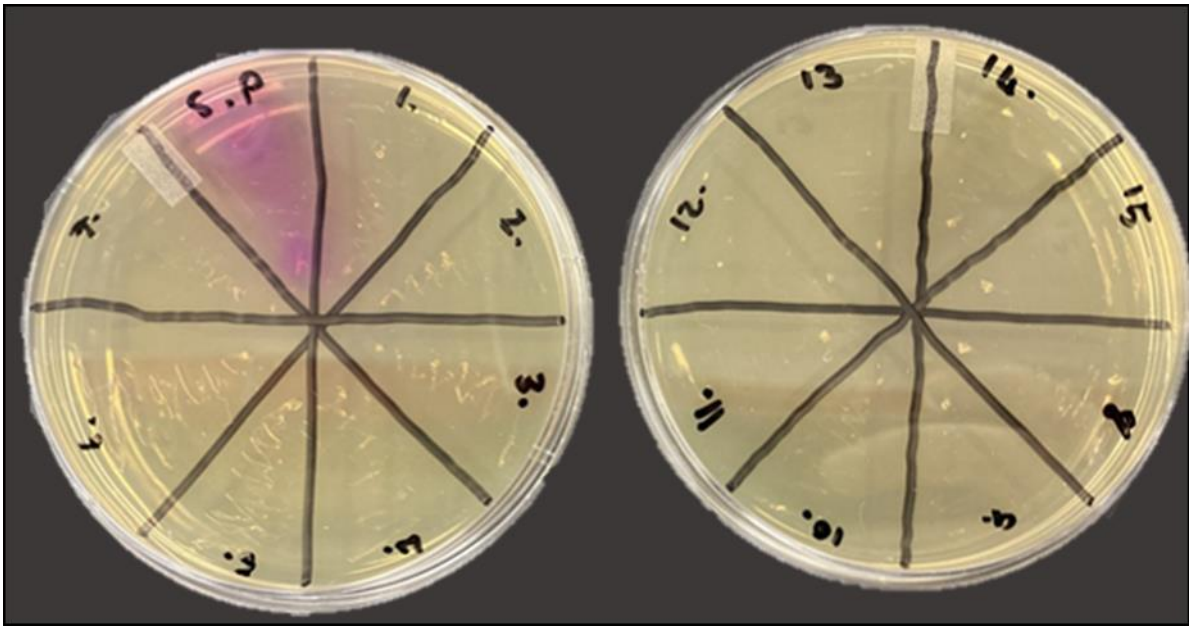


**Figure 4.23:** Results of urease activity test. None of the isolated bacterial colonies collected from the copper mine tailing enrichment tested positive for the production of urease after 20 minutes. The appearance of the pink colour on the left most CUA plate was due to *S. pasteurii* which was used as a control in testing and comparing the urease activity of the collected isolates.

Based on the discussion of the previous section, it was clear the acclimatised culture of *S. pasteurii* could not be used to form viable bio-columns. It was postulated that this was as a result of the physical characteristics (low PSD) of the copper mine tailings inhibiting the growth of the bacteria rather than due to the high copper concentration within the tailings. As postulated above, it was believed that the inability of the bacteria to undergo MICP was partly due to limited nutrient transfer. It was speculated that if this was the case and that oxygen transfer was a major inhibitor of the MICP process, then bacteria isolated from within the copper mine tailings may provide the ideal subjects to overcome this issue. This was due to the fact that not only would these bacteria be copper tolerant but there was a possibility that anaerobic bacteria could be isolated i.e. bacteria which do not require oxygen to survive.

However, as seen in the above results, despite a diverse consortium of bacteria being present in the copper mine tailing enrichment – none were shown to be capable of producing urease. This was despite using a copper mine tailing sample which was specifically enriched to favour microorganism which underwent the MICP process. This is unusual in the fact that previous researchers have shown that there is typically an abundance of urease producing bacteria present within mine tailings (Achal et al., 2011; Yang et al., 2016). This discrepancy (the lack of the presence of ureolytic bacteria) was attributed to the fact the copper tailings collected for these experiments came directly from a flotation process of a Greenfields mining project. As such the copper tailings never has a chance to ‘weather’ in an outside environment and hence lacked the opportunity to be colonised by outside urease-producing bacterial species.

On the basis if this, it is thus believed that it would be beneficial to continue the search for indigenous ureolytic bacteria and to rather focus the search on well-established/abandoned copper mine sites such as those located in Phalaborwa, Limpopo, South Africa.

# Chapter 5

# 5. Economic Analysis

An analysis was conducted to determine the economic feasibility of a potential industrial process, revolving around a mining community, capable of mass-producing bio-bricks and fertilisers. All calculations and assumptions for this economic analysis were based on the results and finding of Chapter 4, with particular focus being given to experiment's A and C. See Appendix O: Economic Analysis Assumptions for all assumptions used in developing the economic analysis.

## *5.1. Potential for a closed circular bio-economy*

This economic analysis was designed on the basis that human excreta (namely urine) and copper mine tailings could be used as integral components in forming a closed-loop circular bio-economy. This concept is explained in Figure 5.1, where it is envisioned that an entire mining community's 'waste' urine can be collected and stored in mass to form part of a value generating nitrogen nutrient cycle (shown in green). The urea contained within this urine will form one of the two main components (the other being calcium ions) of the cementation media which is needed to produce bio-bricks. As a by bio-product of bio-brick formation (and urine stabilisation) two nutrient-rich fertilisers can be manufactured: ammonium sulphate and calcium phosphate.

These fertilisers which are rich in the essential plant nutrients, nitrogen and phosphate, can be used to supplement the fertilisation requirements of local farming communities. However, the social acceptance of urine-derived fertilisers would have to be considered (Chipako and Randall, 2020) as well as the presence of pharmaceuticals and safety concerns around the products produced (Solanki and Boyer, 2017).The food grown by these farms is then used to supply food to the mining community, closing off one end on the nitrogen nutrient cycle. The other half of the nutrient cycle involves the agriculture products produced by some of the farms. Certain agriculture products, when further processed down-stream, produce nutrient-rich bio-waste streams such as lactose mother liquid, spent grains and whey. It is plausible that these waste by-products can be used as cost effective alternatives to the expensive laboratory grade nutrients currently used in cultivating the ureolytic bacteria needed for bio-brick production (Lambert and Randall, 2019). Other bio-waste streams, such as eggshells, can also be exploited further as part the nutrient cycle in this proposed process. This has recently been shown by Choi and colleagues (2016) who demonstrated that calcium produced from eggshells is as effective in forming calcium carbonate bonds via MICP as conventional sources of calcium (such as calcium chloride).

As well as a nitrogen nutrient cycle, it is also proposed that this circular economy would incorporate the upcycling of the copper mine tailings via MICP into bio-bricks (shown in blue). In this manner, this process will act as a novel means of repurposing an otherwise valueless waste (copper mine tailings) into bio-bricks which can be sold back to the community as an important construction material; whilst simultaneously mitigating the environmental damages caused by the presence of a tailings dam.

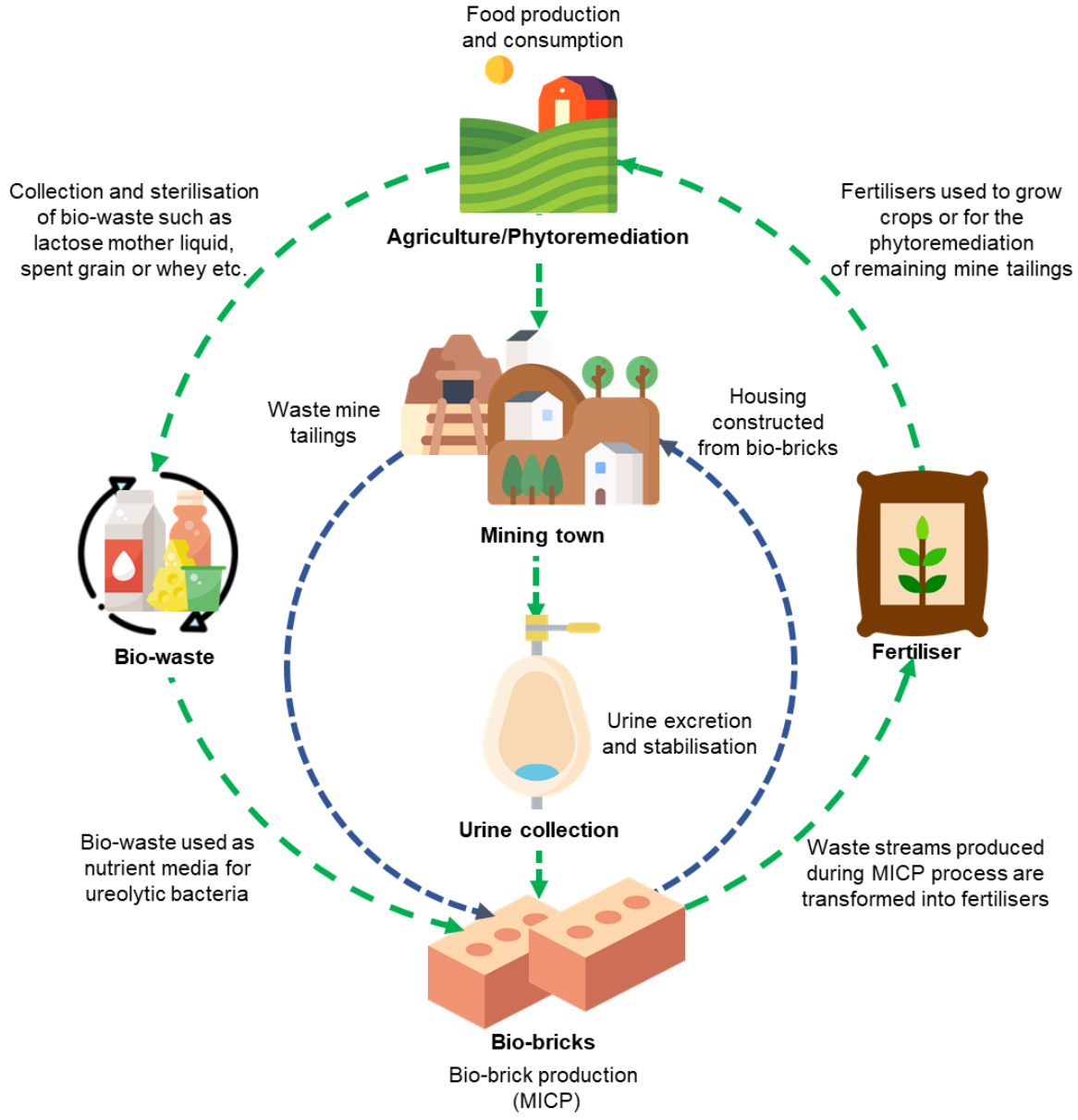


**Figure 5.1:** Proposed closed-loop resource flow in a bio-economy revolving around a mining town. The nutrient flow of nitrogen extracted from human urine is shown in green and the flow of the copper mine tailings is shown in blue. The icons for this graphic were provided by mynamepong, freepik and smashicons from www.flaticon.com. Adapted from (Simha et al., 2018).

### *5.2. Bio-brick system and mass balance assumptions*

Based on the results attained from the experiments conducted in Chapter 4, a theoretical mass balance was conducted to determine the amount of resources needed to produce a single bio-brick, as illustrated in Figure 5.2. Although it was demonstrated in this study, that at present, structurally viable bio-bricks cannot be grown from copper mine tailings it was assumed that for the purposes of this feasibility study that the inhibition issues encountered could be overcome with more research and development. As such, the chemical requirements for experiment C (see Section 3.5.1) were used for all calculations in the mass balance. As this dissertation used bio-columns as a proxy for bio-bricks, all media required was scaled up to that of a standard size South African brick (220 mm x 110 mm x 70 mm). The mass balance developed for this project can be divided into four major stages), with each stage containing the following assumptions:

**Stage 1:** Urine collection and stabilisation

Dependent on the amount of water consumed and climate conditions, an average adult person typically produces between 1 and 1.5 litres of urine per day (Richert et al., 2010). As such it is assumed for the purpose of this research that the average volume of urine produced per person per day is 1.25 litres. It is also assumed that the average concentration of urea and phosphate within the collected urine is 0.3 M and 0.014 M respectively (Henze, 2017). Collecting undiluted urine at the source of its production will significantly reduce water consumption for urinal flushing, contributing to more environmentally friendly production process (Chipako and Randall, 2019). To stabilise the collected urine for long-term storage, it is dosed with calcium hydroxide, which results in a calcium phosphate fertiliser being produced as a by-product. To ensure the long-term stabilisation of urine (pH>12.5) it has been suggested in literature by Flanagan and Randall (2018) that an excess of 10 g of calcium hydroxide is added for every litre of urine collected. As a result of this dosage it can be assumed that 11.23 g of calcium phosphate fertiliser will be produced for every litre of urine stabilised.

**Stage 2:** Cementation media preparation

As a result of the stabilisation process, the stabilised urine leaving Stage 1 has a pH of 12.5 which inhibits both the chemical and enzymatic hydrolysis of urea into the carbonate ions required for bio-brick growth. To ensure the survival of the ureolytic bacteria and that the MICP process occurs, the pH of the stabilised urine is reduced to a pH of 11.2 using a 32% concentrated hydrochloric acid solution. Work conducted by Lambert and Randall (2019) has shown that 3.5 mL of HCl per litre of stabilised urine is required to achieve a targeted pH of 11.2. To this mixture, extra calcium chloride is added until a calcium concentration of 0.3 M is reached. This resultant mixture is known as cementation media and is pumped through to Stage 3 once the mine tailings have been inoculated with the cultivated ureolytic bacteria, *S. pasteurii*.

**Stage 3:** *S. pasteurii* cultivation and bio-brick production

During experimental runs the ureolytic bacterium, *S. pasteurii, was* cultivated using ATCC®1376 (20 g/L yeast extract, 10 g/L ammonium sulphate and 15.75 g tris-base). For the purposes of the mass balance shown in Figure 5.2 it is assumed that this nutrient feed will be used for bio-brick production. However, it is noted that the use of laboratory grade reagents will not be economically feasible in the mass production of bio-bricks. A discussion which is expanded upon in the following section. Further, it is assumed that a continuous culture of *S. pasteurii* will be maintained continually to inoculate the copper mine tailings. To produce a standard size of brick (220 mm x 110 mm x 70 mm), approximately 500 mL of cultivated *S. pasteurii* is needed to inoculate 4.50 kg of copper mine tailings ($SG_{\text{Copper mine tailings}} = 2.65$). Once inoculated, it is known from experiment C conducted in Chapter 4 section 3.5.1, that 44 L of the cementation media prepared from Stage 2 will be needed to grow a single bio-brick.

Note: the bio-column grown in experiment C is approximately 9 times smaller than a bio-brick. Additionally, experiment C only achieved a calcium depletion and ammonium ion production efficiency of 14.3% (85.7% of added calcium ions remained) and 26.0% respectively (see Figure 4.7 in section 4.2). The implications of this are that the submergent technique developed in section 3.3 requires further optimisation and as such it is likely that that the volume of the cementation media can be significantly reduced. As the volume of ammonium ions produced was only 26.0% of the theoretical maximum volume that could be produced had all the urea added to the cementation media been hydrolysed, this has inhibitory implications for Stage 4, resulting in a reduced volume of fertiliser by-product being produced.

**Stage 4:** Ammonium sulphate recovery

The effluent stream produced during Stage 3 is nutrient rich, containing a high concentration of ammonium ions (theoretically equivalent to the nitrogen content of the stabilised urine entering from Stage 2). If recovered, this could serve as an additional source of fertiliser in the form of ammonium sulphate. A possible method to remove and recover the ammonium ions from the liquid effluent produced by Stage 3 is through the use of a sulfuric acid scrubber (Pradhan et al., 2017). This process is represented by equation 18, with the stoichiometry of this reaction being used to determine the amount of sulphuric acid required.

$$2NH_3 + H_2SO_4 \rightarrow (NH_4)_2SO_4 \qquad (18)$$

As no experiments were conducted to observe the efficiency or feasibility of such an acid scrubbing process, a conversion of 80% was assumed. Additionally, as mentioned in Stage 3, experiment C only exhibited an ammonium ion production efficiency of 26.0%. As such this value was used in the mass balance in formulating the volume of ammonium ions produced as well as the volume of sulphuric acid needed to convert it into by-product ammonium sulphate fertiliser.

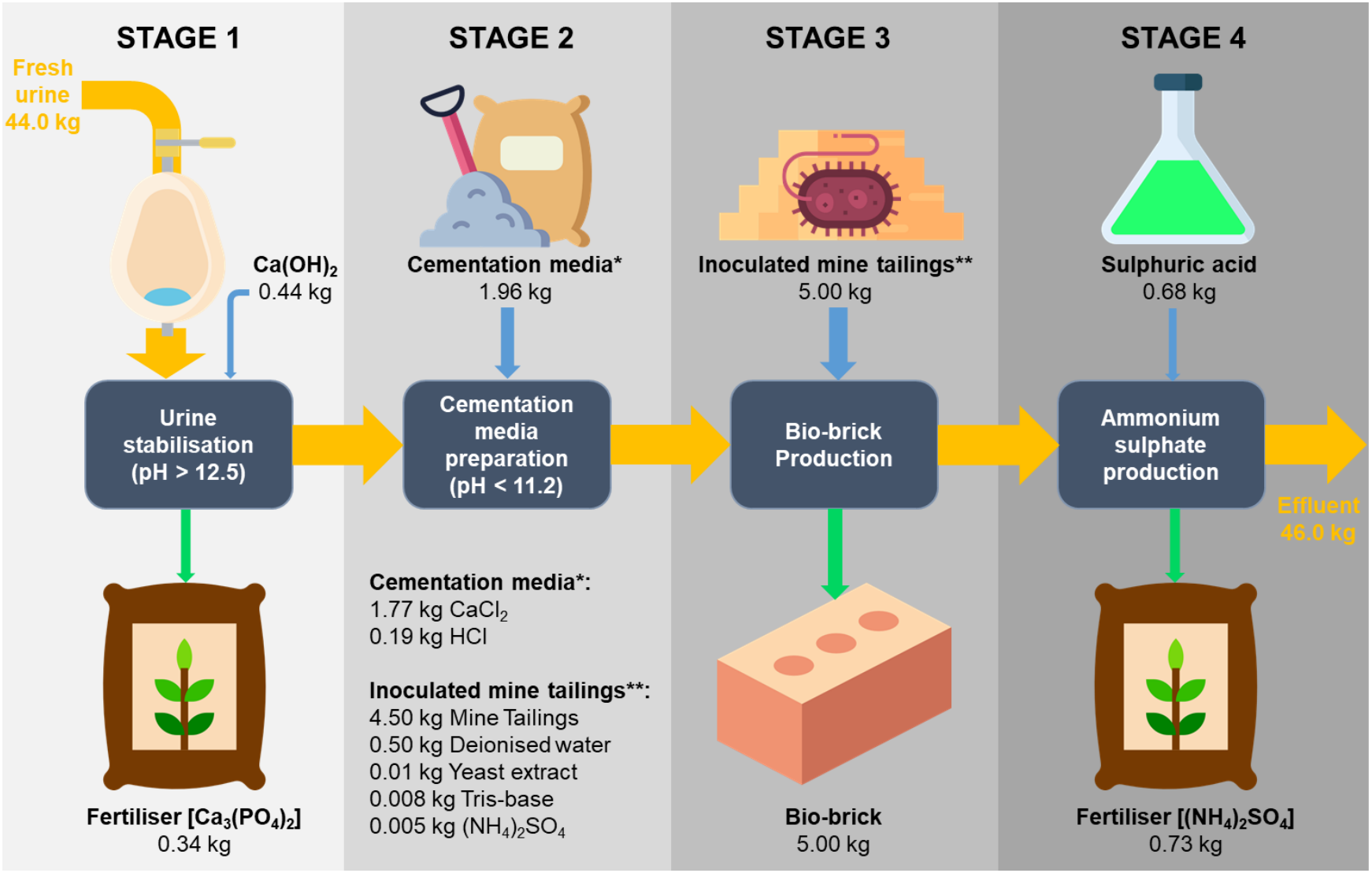


**Figure 5.2:** Theoretical process and mass balance detailing the inputs and outputs required to produce a single bio-brick from copper mine tailings usig the sumbergent technique developed in this dissertation. The above process is divided into four major stages: stabilisation of collected urine, cementation media preparation, bio-brick production and ammonium sulphate production. As a by-product of bio-brick production two nutrient-rich fertilizer can be derived, calcium phosphate [$Ca_3(PO_4)_2$] and ammonium sulphate [$(NH_4)_2SO_4$)], which may prove critical in ensuring the profitiabilty of this process. The icons for this graphic were provided by mynamepong, freepik and smashicons from www.flaticon.com. Adapted from (Lambert & Randall, 2019).

### *5.3. Economic Evaluation*

From the above mass balanced approximately 44.0 L of stabilised human urine would be required to grow a single bio-brick. Adding further value to the process is 0.73 kg of ammonium sulphate fertiliser and 0.34 kg of calcium phosphate fertiliser, both produced as by-products of the MICP and stabilisation processes, respectively. A large volume of waste effluent (46.0 L) is produced by the overall process, with the majority of it being made-up of water from the stabilised urine. As such a large volume of wastewater is produced it is suggested that its recycle and reuse potential as industrial process water in other mining processes such as beneficiation or flotation be investigated.

The large volume of stabilised urine required to produce a single bio-brick is problematic though. Besides the fact that this will result in increased costs due to the equipment needed to hold such volumes; it will also result in a high operating costs as enough calcium ions will have to be added to form a resultant cementation solution of 0.3 M $Ca^{2+}$. The collection of such volumes of urine would also prove difficult. As an average sized one story home of 200 $m^2$ requires approximately 8000 bricks (Simone Homes, 2020), to build one from copper mine tailings bio-bricks would require 352 000 L of stabilised urine. This is approximately equal to collecting the daily urine produced by 260 000 people. Thus, following this, logistically any scale-up in bio-brick production would be challenging, requiring a vast investment in repurposing existing sewage works to reroute urine to bio-brick production sites. That said it must be stated that this study only constituted a first attempt at producing bio-columns from copper mine tailings and, as can clearly be seen in Figure 4.7, not even the beach sand bio-column achieved an calcium efficiency of greater than 50% (the copper mine tailing bio-column only achieved a calcium depletion efficiency of 14.3%). As such it is suggested that future works focus on establishing the optimal volumes of cementation media needed to produce bio-bricks that improves the usage efficiency of urea above at least 90%. The logistics issue facing bio-brick production, however, is also further exacerbated by the economics of its production.

Based on the mass balance conducted in Figure 5.2, a preliminary economic evaluation was conducted to determine the profitability of producing a single bio-brick from copper mine tailings. At this stage of design only the costs of raw materials were considered with capital, labour and operating costs being ignored. It was further assumed for the purposes of this analysis that the urine would provide the entirety of urea needed for the MICP process, although as previously stated this would realistically be difficult to achieve. Besides, reducing the volume of cementation media needed, the issue of collecting human urine could be circumnavigated by using a synthetic source of urea as done in this dissertation. However, this would add additional operating costs to a process which is already expensive. It was assumed that for bio-bricks to be competitive in the market they would have to sell for a price on-par with traditional masonry bricks.

The detailed cost calculations of producing copper mine tailings from copper mine tailings, based off the mass balance illustrated in Figure 5.2, is displayed in Table 5.1.

**Table 5.1:** Table displaying the costs required to produce a single bio-brick as well as the potential earnings which could be achieved from selling said bio-bricks and by-product fertilisers. The major costs displayed in this table are due to the use of laboratory grade reagents, which must be replaced if this process is to be economically viable. (Exchange rate: US$ 1 = R 14.99). See Appendix O: Economic Analysis Assumptions for assumptions used.

| | Amount per bio-brick | Value (USD) | Total Value (USD) |
|---|---|---|---|
| **Expenses** | | | **(3.06)** |
| **Calcium hydroxide** [kg] | 0.44 | 0.29[1] | 0.13 |
| **Calcium chloride** [kg] | 1.77 | 0.27[1] | 0.48 |
| **Hydrochloric acid** [kg] | 0.19 | 0.33[1] | 0.06 |
| **Yeast extract** [kg] | 0.01 | 53.4[2] | 0.53 |
| **Ammonium sulphate** [kg] | 0.005 | 40.8[2] | 0.20 |
| **Tris-base** [kg] | 0.008 | 184[2] | 1.47 |
| **Sulphuric acid [kg]** | 0.68 | 0.31[1] | 0.21 |
| **Incomes** | | | **0.71** |
| **Calcium phosphate** fertiliser [kg] | 0.50 | 0.75[3] | 0.38 |
| **Ammonium sulphate fertiliser [kg]** | 0.73 | 0.14[3] | 0.10 |
| **Bio-brick** [per unit] | 1.00 | 0.23[4] | 0.23 |
| **Profit/Loss** | | | **-2.35** |

[1.] Kemcore, February 2021
[2.] Merk, February 2021
[3.] Alibaba, February 2021
[4.] Builders, February 2021

As can be seen in Table 5.1, the expenses (US$ 3.06) are high compared to the income (US$ 0.71) which can be earned from bio-brick production. As such, the process is, as of now, unprofitable with a negative margin of US$ 2.35. It is also of interest to note that the main source of revenue for the process is generated the by-product fertilisers, which account for just under 70% of the total income. The majority of production expenses seen in Table 5.1, 72% of total expenses, is as a consequence of using laboratory grade reagents in growing the ureolytic bacteria.

A large decrease in costs can thus be expected by replacing the bacterial media with other, cheaper nutrient resources. Lambert and Randall (2019) have previously shown that alternative agriculture waste streams such as spent wheat and lactose mother liquor to have much potential in cultivating *S. pasteurii*. Thus, these agriculture waste streams, as discussed previously in Figure 5.1, have the potential to significantly reduce or even eliminate the cost of culture medium in the bio-brick production process. However, even if the bacterial media could be replaced in its entirety by a waste-stream for free, the bio-brick process would remain unprofitable with every brick produced resulting in a net loss of US$ 0.16. Although, this results in significant margin increase (93%), more would need to be done in making such a process profitable, with particular focus being placed on reducing the $CaCl_2$ requirements.

The volume of cementation media was large (44.0 L) but the MICP efficiency in experiment C was low with only 14.3% of added calcium ions being precipitated as $CaCO_3$. If equivalent volumes of $CaCO_3$ being precipitated were to constitute a process at a 100% efficiency, the cementation media volume could thus be reduced to 6.29 L (under the assumption that the copper mine tailing bio-brick process could be fully optimised). However, even if full optimisation were to occur (including the complete hydrolysis of all urea into ammonium ions), the bio-brick process remains unprofitable with the operating expenses only being decreased by 23.5%. In fact, any reduction applied to the volume of cementation media used has an inhibitory impact on the income of the process. This is due to the resultant impact of significantly less by-product fertilisers being produced (86.0% less calcium phosphate and 72.6% less ammonium sulphate compared to the base case.), which as previously stated, accounted for more than double of the income that could be made by selling a bio-brick. The results of this sensitivity analysis are shown in Figure 5.3.

It must also be further noted that the cost of producing ammonium sulphate from sulphuric acid via acid stripping is approximately double that of the income it generates; hence the economic viability of Stage 4 of the bio-brick has to be investigated further. Particular focus should also be placed in analysing the environmental benefits of Stage 4 against the cost of its operation. Alternatively, the nitrogen-rich solution from the bio-brick process could be concentrated using reverse osmosis and sold as a niche liquid fertiliser (Chipako and Randall, 2020b). A detailed analysis of which type of fertiliser (ammonium sulphate or liquid nitrogen) should be investigated further.

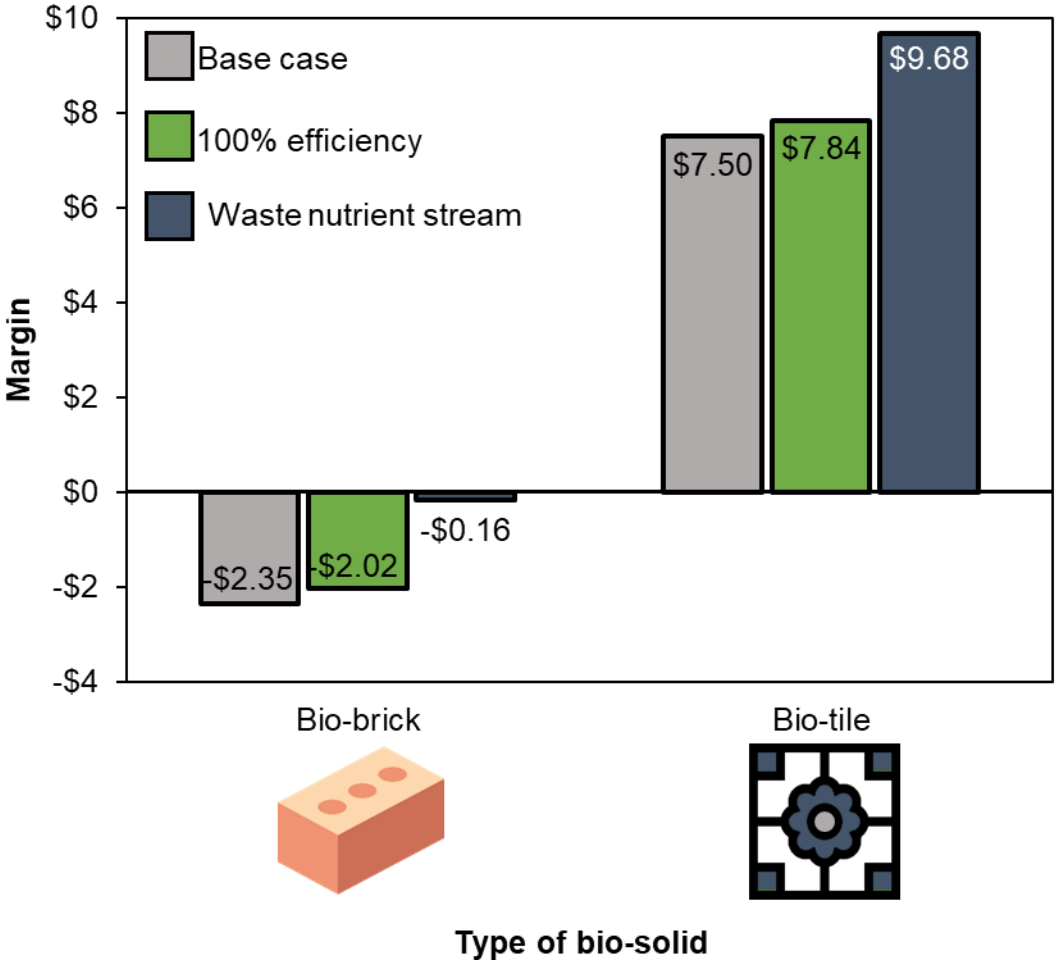


**Figure 5.3:** Comparison of the profit margin which can be achieved depending on which MICP bio-solid is produced (brick/tile) as well as a sensitivity analysis comparing the margins of each bio-solid if (1) the base case is used; (2) if a 100% MICP efficiency were to be achieved and (3) if the laboratory grade bacterial nutrient media were to be replaced with a cost-free agriculture nutrient waste stream. The above margins consider the sale of each of the fertiliser by-products produced. The cost comparison is between a single bio-brick of similar volume to a single bio-tile. The icons for this graphic were provided by freepik from www.flaticon.com

An interesting proposal to increase the profitability of said the proposed process is to switch from producing bio-bricks to producing niche bio-tiles. Not only would these sell for a greater unit price, but this proposal is made more intriguing by what was observed in the technical analysis of this study. It was observed that although copper mine tailings bio-columns could not be solidified completely by MICP, a 2 mm ‘shell’ was formed around the mine tailing aggregate of the bio-column. As discussed in the technical analysis, this was thought to be due to the low porosity of the copper mine tailings which prevented the transfer of essential nutrients into the interior of the bio-columns. As bio-tiles would be thinner than both bio-columns and bio-bricks, it is believed that this nutrient transport inhibition would not be as apparent. Hence, making bio-tiles a good alternative product for a MICP process when copper mine tailings are used as aggregate.

As a 2 mm shell was formed around the entire radius of the bio-columns grown in experiment C, it was postulated that a bio-tile of at least 4 mm thick could be theoretically grown using the submergent technique discussed in section 3.3. As the vast majority of porcelain tiles are approximately 6 – 10 mm thick (Beaumont Tiles, 2021), it is believed that with slight improvement, MICP bio-tiles could theoretically be grown to meet these standards. A porcelain wall tile of dimensions 600 mm x 600 mm x 10 mm, which would require only a slightly larger volume of copper mine tailings compared to a bio-brick (1.79 L vs 1.69 L) can achieve a market value of approximately US$ 10.8 (Beaumont Tiles, 2021). This is higher than the income which can be achieved from selling a bio-brick (US$ 0.23), correlating to an over 4300% increase in price for the same volume of tailings. Additionally, it must be noted that this price just represents the price of a single large wall tile and other potential tile types (and sizes) could be used to increase the margin further. This increase in sale price drastically increases the profitably of such a process, as can be seen in Figure 5.3. This is despite the cost laboratory grade reagents for the bacteria growth medium still being included in the costs of the bio-tiles (base case). If a waste agriculture stream were to be used to replace this cost for free, it can be expected that the profitability of producing bio-tiles would increase by approximately a third. Additionally, if this process were to be 100% efficient, the profit margin would increase slightly by 4.5% as seen in Figure 5.3.

As such, it is believed bio-tiles, unlike bio-bricks, can be used to establish an industry which profitably repurposes otherwise waste copper mine tailings into a valuable product. In this manner, not only will the environmental impact of mining activities be mitigated, but a lucrative source of income will become available to surrounding communities.

# Chapter 6

# 6. Conclusions and Recommendations

## 6.1. Research overview

A detailed review on the existing literature on MICP theory as well as the inhibition created by copper mine tailings on *S. pasteurii* was conducted. This review was used to both guide the formulation of the key objectives and the hypothesis of this report, which in turn were used to establish the methodology used in this dissertation.

This dissertation was the first known attempt to repurpose copper mine tailings into bio-solids via MICP. The major experiments conducted involved characterising said copper mine tailings physiochemical makeup; developing a submergent technique for MICP processes involving very fine aggregates; establishing if copper mine tailings could be used to form bio-solids via MICP; determining the toxicity of copper ions on *S. pasteurii*; acclimating *S. pasteurii* to a copper concentration mimicking those found in copper mine tailings and the isolation of urease-producing bacteria indigenous to copper mine tailings. These technical experimental findings were used to inform an economic analysis revolving around determining the economic feasibility of producing bio-bricks via MICP from repurposed copper mine tailings and human urine.

## 6.2. Research conclusions

The key finding of this research was that copper mine tailings could not be repurposed into bio-columns (and hence bio-bricks) by microbial induced calcium carbonate precipitation using *S. pasteurii*, both from a technical and economical point of view, but that the potential exists to repurpose them into thinner material solids such as wall tiles. However, the possibility remains that the technical challenges faced in repurposing copper mine tailings into bio-bricks may be overcome by isolating an anaerobic ureolytic bacteria which is indigenous to the copper mine tailings.

Based on the physicochemical characterisation of the copper mine tailings undertaken within this dissertation, it was noted that fine aggregate materials (such as copper mine tailings) could not be used in MICP systems where cementation media is directly pumped through the aggregate. This is due to the low porosity of such aggregates providing too large of a resistance to the flow of fluid within an enclosed area, resulting in pump failure. Consequently, this work expanded on existing submergent guidelines to establish a process of growing bio-columns via submergence in a cementation media mimicking the 0.3 M urea concentration of human urine (supplemented with an equimolar concentration of calcium ions). Although the submergent technique developed in this dissertation was deemed to be simpler to implement compared to the pumping technique; it came at the cost of a reduced $CaCO_3$ precipitation efficiency.

As $CaCO_3$ precipitation was no longer forced to occur in the confines of the bio-column mould (as in the case of the pumping method), $CaCO_3$ precipitation in the submergent technique occurred undesirably in large volumes outside of the submerged bio-columns. This resulted in the wasteful use of calcium ions and most likely contributed to a slower formation of the submerged bio-columns.

Using the submergent technique developed in this dissertation, a bio-column was grown, using beach sand as an aggregate, exhibiting a compressive strength of 1.85±0.39 MPa. This was 2.1x greater than the compressive strength of a bio-column with beach sand and applying a pumping technique as well as 1.4x greater than a bio-column grown with Ottawa silica sand but using a similar submergent technique. However, when the beach sand aggregate was replaced with copper mine tailings, this MICP submergent technique only managed to form a bio-column with a compressive strength of 0.541 MPa. As the compressive strength of untreated copper mine tailings columns, which were formed only by the addition of deionised water, was 0.54±0.31 MPa it can be seen that the addition of ureolytic bacteria to the copper mine tailings did not result adequate levels of MICP being induced and hence had no impact on the solidification of the bio-columns. This point is further illustrated by the MICP efficiency of each bio-column grown. Whereas the beach sand bio-column depleted 44.1% of added calcium ions (55.9% of calcium ions remained in the cementation media) and produced 57.6% of theoretically possible ammonium ions; the copper mine tailing bio-columns only depleted 14.3% of added calcium ions and produced 26.0% of theoretically possible ammonium ions.

A MIC analysis was conducted to determine the toxicity of copper ions on *S. pasteurii*. From this it was noted that the MIC of copper on *S. pasteurii* was in the region of 128-256 mg/L at which concentrations less than 70% of optimal growth was achieved. As the copper mine tailings used in this dissertation contained a copper concentration of approximately 622 mg/L; it was believed that this was the main source of inhibition resulting in the reduced compressive strength of the copper mine tailing bio-column. However, this was shown to be only partly true based on the finding that even a bio-column grown using a culture acclimated to a copper concentration of 600 mg/L achieved a reduced compressive strength of 0.11 MPa.

Rather, due to the observation that a ‘MICP shell’ formed around the outer edges of both the copper mine tailing bio-columns (standard and acclimated *S. pasteurii* cultures), it was theorised that the reduced compressive strength displayed was not due entirely to copper inhibition but rather due to limited nutrient transfer throughout the bio-column due to the low particle size (and hence porosity) of the copper mine tailings. This theory was based on the premise that past literature has shown that limited oxygen and waste transfer occurs in fine aggregates, resulting in a decrease of bacterial growth as well as reduced bacterial activity and movement.

SEM imaging of the copper mine tailings bio-columns further substantiated this hypothesis by showing that $CaCO_3$ crystal formation was concentrated around the outer extremities of the bio-columns. This was also supported by $CaCO_3$ content measurements which showed that $CaCO_3$ was not precipitated homogenously throughout the grown copper mine tailing bio-columns but rather increased radially from the centre. It was speculated that the lack of oxygen transfer into the interior of the copper mine tailing bio-columns could be overcome by using an anaerobic, ureolytic bacteria which was tolerant of high copper concentrations. An attempt was made to isolate an indigenous bacterium to the copper mine tailings, matching these criteria. However, despite isolating numerous variant colonies of bacteria, none tested positive for urease activity and hence this hypothesis could not be tested.

An economic analysis was conducted which envisioned the production of bio-bricks in by mining community as an essential part of a circular economy. Where human urine, waste agriculture streams and copper mine tailings are all ‘upcycled’ to produce bio-bricks and related by-product fertilisers. The fertiliser would be used to grow crops for the mining community, which would supply urine for the production of bio-bricks, which in turn could be used in the construction industry. Additionally, any waste agriculture produced by the harvested crops could be used to grow the ureolytic bacteria needed to grow the bio-bricks. It was however shown, using the experimental data established in this dissertation, that a single bio-brick would cost US$ 3.06 but only achieved an income of US$ 0.71 (which includes the sale of the by-product fertilisers). This correlates to a loss of US$ 2.35 per bio-brick produced. The major cost of this process is due to the bacterial media (US$ 2.18), which is laboratory grade. As such a significant cost reduction (71.6%) can be achieved by using waste agriculture products to replace this cost but even complete exclusion of this cost still results in a loss (-US$ 0.16). This is mainly due to the low selling price of bricks. A more lucrative product to sell would be bio-tiles, which can sell for up to US$ 10.8 and achieve a profit of US$7.50 per bio-tile sold (base case). The profitability can be significantly improved by approximately a third (US$ 9.68) if a waste agriculture stream is used to replace the laboratory grade bacteria nutrient media. The switch to bio-tiles is also supported by the nutrient transfer limit observed in the technical analysis of this work.

### *6.3. Recommendations*

Based on these conclusions, several recommendations for future research have been made:

1. Continued attempts should be made to isolate an anaerobic, copper tolerant, ureolytic bacteria which may hold the potential to overcome the limitations placed on the MICP process by very fine aggregates in forming bio-bricks.
2. MIC analyses should be performed on the other heavy metals (such as barium and chromium) contained within the copper mine tailings used in this dissertation. As heavy metal toxicity on *S. pasteurii* is poorly reported, it is believed that understanding the interactions the ureolytic bacteria has with the heavy metals contained within the copper mine tailings will greatly help in future attempts to repurpose copper mine tailings into bio-solids.
3. A study should be carried out determining the impact aggregates of varying particle size distribution have on the MICP process when the submergent technique is applied.
4. Further, the limit (or depth) where MICP can effectively and satisfactorily solidify fine aggregate particles such as copper mine tailings should be determined. This limit can be used as further evidence to determine the future feasibility of repurposing copper mine tailings in bio-bricks, or if a switch to bio-solids of alternative thickness (such as bio-tiles) should be made. Following from this, an in-depth study should be conducted to determine the impact that fine aggregates have on limiting nutrient and waste transfer on ureolytic bacteria as well as means of overcoming this limitation.
5. An attempt should be made to grow bio-tiles, as described in the economic analysis, using the submergent technique developed in this report.
6. Attempts should also be made to improve the MICP efficiency of the submergent technique such as by determining means of preventing $CaCO_3$ precipitation form occurring outside of the bio-column mould.
7. A study should be conducted to determine the impact of either reducing the volume of cementation media or alternatively of increasing/decreasing the molarity of the urea-calcium constituents of the cementation media.
8. If technically feasible, a more detailed economic analysis should be conducted on the profitably of MICP bio-tiles. This economic analysis should make provisions for capital costs as well as operating cost.
9. Alternative industrial uses of the copper acclimated *S. pasteurii* culture grown in this dissertation should be investigated. This includes, use in both in situ prevention of copper mine tailing dust dispersion as well as application in the bioremediation of heavy metals contained within industrial waste waters.

## *Reference List*


Achal, V., Mukerjee, A., Sudhakara Reddy, M., 2013. Biogenic treatment improves the durability and remediates the cracks of concrete structures. Constr. Build. Mater. 48, 1–5. https://doi.org/10.1016/j.conbuildmat.2013.06.061

Achal, V., Pan, X., Fu, Q., Zhang, D., 2012. Biomineralization based remediation of As(III) contaminated soil by Sporosarcina ginsengisoli. J. Hazard. Mater. 201–202, 178–184. https://doi.org/10.1016/j.jhazmat.2011.11.067

Achal, V., Pan, X., Zhang, D., 2011. Remediation of copper-contaminated soil by Kocuria flava CR1, based on microbially induced calcite precipitation. Ecol. Eng. 37, 1601–1605. https://doi.org/10.1016/j.ecoleng.2011.06.008

Albéric, M., Bertinetti, L., Zou, Z., Fratzl, P., Habraken, W., Politi, Y., 2018. The Crystallization of Amorphous Calcium Carbonate is Kinetically Governed by Ion Impurities and Water. Adv. Sci. 5, 1701000. https://doi.org/10.1002/advs.201701000

Asabonga, M., Cecilia, B., Mpundu, M.C., Vincent, N.M.D., 2017. The physical and environmental impacts of sand mining. Trans. R. Soc. South Afr. 72, 1–5. https://doi.org/10.1080/0035919X.2016.1209701

Barbière, C., 2017. French urban development expert: “In 2050, 3 billion people will live in slums.” www.euractiv.com. URL https://www.euractiv.com/section/development-policy/interview/french-urban-development-expert-in-2050-3-billion-people-will-live-in-slums/ (accessed 4.13.20).

Bartos, P.J., Garcia, C., Gil, J., 2017. The Nuevo Chaquiro Cu-Au-(Mo) Porphyry Deposit, Middle Cauca Belt, Colombia: Geology, Alteration, Mineralization. Econ. Geol. 112, 275–294. https://doi.org/10.2113/econgeo.112.2.275

Beaumont Tiles, 2021. Ice Pietra Charcoal Polished Tiles [WWW Document]. URL https://www.beaumont-tiles.com.au/product/tile/1006653?postcode=5067 (accessed 2.4.21).

Bernardi, D., DeJong, J.T., Montoya, B.M., Martinez, B.C., 2014. Bio-bricks: Biologically cemented sandstone bricks. Constr. Build. Mater. 55, 462–469. https://doi.org/10.1016/j.conbuildmat.2014.01.019

Boivin-Jahns, V., Ruimy, R., Bianchi, A., Daumas, S., Christen, R., 1996. Bacterial diversity in a deep-subsurface clay environment. Appl. Environ. Microbiol. 62, 3405–3412. https://doi.org/10.1128/AEM.62.9.3405-3412.1996

Broughton, W., 2012. Testing the Mechanical, Thermal and Chemical Properties of Adhesives for Marine Environments, in: Adhesives in Marine Engineering. https://doi.org/10.1016/B978-1-84569-452-4.50006-0

Bu, C., Wen, K., Liu, S., Ogbonnaya, U., Li, L., 2018. Development of bio-cemented constructional materials through microbial induced calcite precipitation. Mater. Struct. 51, 30. https://doi.org/10.1617/s11527-018-1157-4

Buikema, N.D., 2015. STABILIZATION OF IRON MINE TAILINGS THROUGH MICROBIALLY INDUCED CALCITE PRECIPITATION (Master). Michigan Technoligal University.

Cheng, L., Kobayashi, T., Shahin, M.A., 2020. Microbially induced calcite precipitation for production of “bio-bricks” treated at partial saturation condition. Constr. Build. Mater. 231, 117095. https://doi.org/10.1016/j.conbuildmat.2019.117095

Chilamkurthy, K., Marckson, A.V., Chopperla, S.T., Santhanam, M., 2016. A statistical overview of sand demand in Asia and Europe. 16.

Chipako, T., Randall, D., 2019. Urinals for water savings and nutrient recovery: a feasibility study. Water SA 45. https://doi.org/10.4314/wsa.v45i2.14
Chipako, T.L., Randall, D.G., 2020. Urine treatment technologies and the importance of pH. J. Environ. Chem. Eng. 8, 103622. https://doi.org/10.1016/j.jece.2019.103622
Chipako, T.L., Randall, D.G., 2020b. Investigating the feasibility and logistics of a decentralized urine treatment and resource recovery system. J. Water Process Eng. 37, 101383. https://doi.org/10.1016/j.jwpe.2020.101383
Choi, S.-G., Wu, S., Chu, J., 2016. Biocementation for Sand Using an Eggshell as Calcium Source. J. Geotech. Geoenvironmental Eng. 142, 06016010. https://doi.org/10.1061/(ASCE)GT.1943-5606.0001534
de Leeuw, J., Shankman, D., Wu, G., de Boer, W.F., Burnham, J., He, Q., Yesou, H., Xiao, J., 2010. Strategic assessment of the magnitude and impacts of sand mining in Poyang Lake, China. Reg. Environ. Change 10, 95–102. https://doi.org/10.1007/s10113-009-0096-6
de Oliveira, D., Fahn, K., 2019. Overcoming ionic strength for the production of urine bio-bricks (Honours). University of Cape Town, Cape Town.
DeJong, J.T., Mortensen, B.M., Martinez, B.C., Nelson, D.C., 2010. Bio-mediated soil improvement. Ecol. Eng. 36, 197–210. https://doi.org/10.1016/j.ecoleng.2008.12.029
Desprez, M., 2000. Physical and biological impact of marine aggregate extraction along the French coast of the Eastern English Channel: short- and long-term post-dredging restoration. ICES J. Mar. Sci. 57, 1428–1438. https://doi.org/10.1006/jmsc.2000.0926
Dhami, N.K., 2013. Biomineralization of Calcium Carbonate Polymorphs by the Bacterial Strains Isolated from Calcareous Sites. J. Microbiol. Biotechnol. 23, 707–714. https://doi.org/10.4014/jmb.1212.11087
Diaz-Zorita, M., Grosso, G.A., 2000. Effect of soil texture, organic carbon and water retention on the compactability of soils from the Argentinean pampas 6.
Dickinson, S., McGrath, K., 2004. Aqueous Precipitation of Calcium Carbonate Modified by Hydroxyl-Containing Compounds. Cryst. Growth Des. 4. https://doi.org/10.1021/cg049843i
Dosier, G., 2017. Production of masonry with bacteria. US 9 ,796,626 B2.
Duruibe, O.J., Ogwuegbu, M.O.C., Egwurugwu, J.N., 2007. Heavy metal pollution and human biotoxic effects. Int. J. Phys. Sci. 2, 112–118.
Eriksen, L., Andreasen, P., Ilsøe, B., 1996. Inactivation of Ascaris suum eggs during storage in lime treated sewage sludge. Water Res. 30, 1026–1029. https://doi.org/10.1016/0043-1354(95)00258-8
Esterhuysen, A., Knight, J., Keartland, T., 2018. Mine waste: The unseen dead in a mining landscape. Prog. Phys. Geogr. Earth Environ. 42, 650–666. https://doi.org/10.1177/0309133318793581
Flanagan, C.P., Randall, D.G., 2018. Development of a novel nutrient recovery urinal for on-site fertilizer production. J. Environ. Chem. Eng. 6, 6344–6350. https://doi.org/10.1016/j.jece.2018.09.060
Fredrickson, J.K., Balkwill, D.L., Zachara, J.M., Li, S.-M.W., Brockman, F.J., Simmons, M.A., 1991. Physiological Diversity and Distributions of Heterotrophic Bacteria in Deep Cretaceous Sediments of the Atlantic Coastal Plain. Appl. Environ. Microbiol. 57, 402–411. https://doi.org/10.1128/AEM.57.2.402-411.1991

Fujita, Y., Ferris, F.G., Lawson, R.D., Colwell, F.S., Smith, R.W., 2000. Subscribed Content Calcium Carbonate Precipitation by Ureolytic Subsurface Bacteria. Geomicrobiol. J. 17, 305–318. https://doi.org/10.1080/782198884

Gadd, G.M., 2010. Metals, minerals and microbes: geomicrobiology and bioremediation. Microbiology 156, 609–643. https://doi.org/10.1099/mic.0.037143-0

Hammes, F., Boon, N., de Villiers, J., Verstraete, W., Siciliano, S.D., 2003. Strain-Specific Ureolytic Microbial Calcium Carbonate Precipitation. Appl. Environ. Microbiol. 69, 4901–4909. https://doi.org/10.1128/AEM.69.8.4901-4909.2003

Henze, J., 2017. A nature inspired approach for producing bio-solids from urine (Master). ETH Zurich.

Henze, J., Randall, D.G., 2018. Microbial induced calcium carbonate precipitation at elevated pH values (>11) using Sporosarcina pasteurii. J. Environ. Chem. Eng. 6, 5008–5013. https://doi.org/10.1016/j.jece.2018.07.046

Hu, B., Liang, D., Liu, J., Lei, L., Yu, D., 2014. Transformation of heavy metal fractions on soil urease and nitrate reductase activities in copper and selenium co-contaminated soil. Ecotoxicol. Environ. Saf. 110, 41–48. https://doi.org/10.1016/j.ecoenv.2014.08.007

Ikematsu, M., Kaneda, K., Iseki, M., Yasuda, M., 2007. Electrochemical Treatment of Human Urine for Its Storage and Reuse as Flush Water. Sci. Total Environ. 382, 159–64. https://doi.org/10.1016/j.scitotenv.2007.03.028

Jabri, E., Carr, M., Hausinger, R., Karplus, P., 1995. The crystal structure of urease from Klebsiella aerogenes. Science 268, 998–1004. https://doi.org/10.1126/science.7754395

Jackson, A.P., Vincent, J.F.V., Turner, R.M., 1988. The mechanical design of nacre. Proc. R. Soc. Lond. B Biol. Sci. 234, 415–440. https://doi.org/10.1098/rspb.1988.0056

Kamhi, S.R., 1963. On the structure of vaterite $CaCO_3$. Acta Crystallogr. 16, 770–772. https://doi.org/10.1107/S0365110X63002000

Kistiakowsky, G.B., Shaw, W.H.R., 1953. Ureolytic Activity of Urease at pH 8.9 [1]. J. Am. Chem. Soc. 75, 2751–2754. https://doi.org/10.1021/ja01107a061

Kondolf, G.M., 1997. PROFILE: Hungry Water: Effects of Dams and Gravel Mining on River Channels. Environ. Manage. 21, 533–551. https://doi.org/10.1007/s002679900048

Koroneos, C., Dompros, A., 2007. Environmental assessment of brick production in Greece. Build. Environ. 42, 2114–2123. https://doi.org/10.1016/j.buildenv.2006.03.006

Kossoff, D., Dubbin, W.E., Alfredsson, M., Edwards, S.J., Macklin, M.G., Hudson-Edwards, K.A., 2014. Mine tailings dams: Characteristics, failure, environmental impacts, and remediation. Appl. Geochem. 51, 229–245. https://doi.org/10.1016/j.apgeochem.2014.09.010

Krajewska, B., 2009. Ureases I. Functional, catalytic and kinetic properties: A review. J. Mol. Catal. B Enzym. 59, 9–21. https://doi.org/10.1016/j.molcatb.2009.01.003

Krishna, K., Philip, L., 2005. Bioremediation of Cr(VI) in contaminated soils. J. Hazard. Mater. 121, 109–117. https://doi.org/10.1016/j.jhazmat.2005.01.018

Kumari, D., Qian, X.-Y., Pan, X., Achal, V., Li, Q., Gadd, G.M., 2016. Microbially-induced Carbonate Precipitation for Immobilization of Toxic Metals, in: Advances in Applied Microbiology. Elsevier, pp. 84–87. https://doi.org/10.1016/bs.aambs.2015.12.001

Lambert, S.E., Randall, D.G., 2019. Manufacturing bio-bricks using microbial induced calcium carbonate precipitation and human urine. Water Res. 160, 158–166. https://doi.org/10.1016/j.watres.2019.05.069
Le Bot, S., Lafite, R., Fournier, M., Baltzer, A., Desprez, M., 2010. Morphological and sedimentary impacts and recovery on a mixed sandy to pebbly seabed exposed to marine aggregate extraction (Eastern English Channel, France). Estuar. Coast. Shelf Sci. 89, 221–233. https://doi.org/10.1016/j.ecss.2010.06.012
Li, Q., Csetenyi, L., Gadd, G.M., 2014. Biomineralization of Metal Carbonates by *Neurospora crassa*. Environ. Sci. Technol. 48, 14409–14416. https://doi.org/10.1021/es5042546
Lin, H., Suleiman, M.T., Brown, D.G., Kavazanjian, E., 2016. Mechanical Behavior of Sands Treated by Microbially Induced Carbonate Precipitation. J. Geotech. Geoenvironmental Eng. 142, 04015066. https://doi.org/10.1061/(ASCE)GT.1943-5606.0001383
Lippiatt, B.C., 2007. Building for Environmental and Economic Sustainability Technical Manual and User Guide. Natl. Institure Stand. Technol. 327.
Mitchell, A.C., Dideriksen, K., Spangler, L.H., Cunningham, A.B., Gerlach, R., 2010. Microbially Enhanced Carbon Capture and Storage by Mineral-Trapping and Solubility-Trapping. Environ. Sci. Technol. 44, 5270–5276. https://doi.org/10.1021/es903270w
Mortensen, B.M., Haber, M.J., DeJong, J.T., Caslake, L.F., Nelson, D.C., 2011. Effects of environmental factors on microbial induced calcium carbonate precipitation. J. Appl. Microbiol. 111, 338–349. https://doi.org/10.1111/j.1365-2672.2011.05065.x
Mugwar, A.J., Harbottle, M.J., 2016. Toxicity effects on metal sequestration by microbially-induced carbonate precipitation. J. Hazard. Mater. 314, 237–248. https://doi.org/10.1016/j.jhazmat.2016.04.039
Müller, N., Harnisch, J., 2008. A blueprint for a climate friendly cement industry. World Wildlife Fund.
Nordstrom, D.K., Blowes, D.W., Ptacek, C.J., 2015. Hydrogeochemistry and microbiology of mine drainage: An update. Appl. Geochem. 57, 3–16. https://doi.org/10.1016/j.apgeochem.2015.02.008
Ogino, T., Suzuki, T., Sawada, K., 1987. The formation and transformation mechanism of calcium carbonate in water. \gca 51, 2757–2767. https://doi.org/10.1016/0016-7037(87)90155-4
Owens, G., 2013. Sustainable Concrete, in: Fundamentals of Concrete. The Concrete Institute, Midrand, South Africa, p. 10.
Pancorbo, O.C., Overman, A.R., 1988. Poliovirus Retention in Soil Columns after Application of Chemical- and Polyelectrolyte-Conditioned Dewatered Sludges. APPL Env. MICROBIOL 54, 6.
Pedersen, O., Colmer, T.D., Sand-Jensen, K., 2013. Underwater Photosynthesis of Submerged Plants – Recent Advances and Methods. Front. Plant Sci. 4. https://doi.org/10.3389/fpls.2013.00140
Plummer, L.N., Busenberg, E., 1982. The solubilities of calcite, aragonite and vaterite in CO2-H2O solutions between 0 and 90°C, and an evaluation of the aqueous model for the system CaCO3-CO2-H2O. Geochim. Cosmochim. Acta 46, 1011–1040. https://doi.org/10.1016/0016-7037(82)90056-4
Pradhan, S.K., Mikola, A., Vahala, R., 2017. Nitrogen and Phosphorus Harvesting from Human Urine Using a Stripping, Absorption, and Precipitation Process.

Environ. Sci. Amp Technol. 51, 5165—5171. https://doi.org/10.1021/acs.est.6b05402
Putnam, D.F., 1971. Composition and Concentrative Properties of Human Urine.
Radford, D.S., Kihlken, M.A., Borrelly, G.P.M., Harwood, C.R., Brun, N.E.L., Cavet, J.S., 2003. CopZ from Bacillus subtilis interacts in vivo with a copper exporting CPx-type ATPase CopA. FEMS Microbiol. Lett. 220, 105–112. https://doi.org/10.1016/S0378-1097(03)00095-8
Ramachandran, S.K., Ramakrishnan, V., Bang, S.S., 2001. Remediation of concrete using micro-organisms. ACI Mater. J. 98, 3–9. https://doi.org/10.14359/10154
Randall, D.G., Krähenbühl, M., Köpping, I., Larsen, T.A., Udert, K.M., 2016. A novel approach for stabilizing fresh urine by calcium hydroxide addition. Water Res. 95, 361–369. https://doi.org/10.1016/j.watres.2016.03.007
Randall, D.G., Naidoo, V., 2018. Urine: The liquid gold of wastewater. J. Environ. Chem. Eng. 6, 2627–2635. https://doi.org/10.1016/j.jece.2018.04.012
Razon, L.F., 2014. Life cycle analysis of an alternative to the haber-bosch process: Non-renewable energy usage and global warming potential of liquid ammonia from cyanobacteria. Environ. Prog. Sustain. Energy 33, 618–624. https://doi.org/10.1002/ep.11817
Rebata-Landa, V., 2007. Microbial Activity in Sediments: Effects on Soil Behavior.
Reddy, B., Lal, R., Kenkere, N., 2007. Enhancing Bond Strength and Characteristics of Soil-Cement Block Masonry. J. Mater. Civ. Eng. - J MATER Civ. ENG 19. https://doi.org/10.1061/(ASCE)0899-1561(2007)19:2(164)
Richert, A., Gensch, R., Jönsson, H., Stenström, T.-A., Dagerskog, L., 2010. Practical Guidance on the Use of Urine in Crop Production. Stockh. Environ. Inst. 70.
Ruggiero, C.E., Boukhalfa, H., Forsythe, J.H., Lack, J.G., Hersman, L.E., Neu, M.P., 2004. Actinide and metal toxicity to prospective bioremediation bacteria. Environ. Microbiol. 10.
Simha, P., Friedrich, C., Randall, D.G., Vinnerås, B., 2021. Alkaline Dehydration of Human Urine Collected in Source-Separated Sanitation Systems Using Magnesium Oxide. Front. Environ. Sci. 8, 286. https://doi.org/10.3389/fenvs.2020.619901
Simha, P., Zabaniotou, A., Ganesapillai, M., 2018. Continuous urea–nitrogen recycling from human urine: A step towards creating a human excreta based bio–economy. J. Clean. Prod. 172, 4152–4161. https://doi.org/10.1016/j.jclepro.2017.01.062
Simone Homes, 2020. How many bricks does it take to build a house? [WWW Document]. Home Des. URL https://www.simonehomes.com.au/how-many-bricks/ (accessed 2.3.21).
Solanki, A., Boyer, T.H., 2017. Pharmaceutical removal in synthetic human urine using biochar. Environ. Sci. Water Res. Technol. 3, 553–565. https://doi.org/10.1039/C6EW00224B
Sonak, S., Pangam, P., Sonak, M., Mayekar, D., 2006. Impact of sand mining on local ecology, in: Sonak, S. (Ed.), Multiple Dimensions of Global Environmental Change. pp. 100–105.
Soon, N.W., Lee, L.M., Khun, T.C., Ling, H.S., 2014. Factors Affecting Improvement in Engineering Properties of Residual Soil through Microbial-Induced Calcite Precipitation. J. Geotech. Geoenvironmental Eng. 140, 04014006. https://doi.org/10.1061/(ASCE)GT.1943-5606.0001089
Sreebha, S., Padmalal, D., 2011. Environmental Impact Assessment of Sand Mining from the Small Catchment Rivers in the Southwestern Coast of India: A Case

Study. Environ. Manage. 47, 130–140. https://doi.org/10.1007/s00267-010-9571-6
Tessier, A., Campbell, P.G.C., Bisson, M., 1979. Sequential extraction procedure for the speciation of particulate trace metals. Anal. Chem. 51, 844–851. https://doi.org/10.1021/ac50043a017
Torres-Aravena, Á., Duarte-Nass, C., Azócar, L., Mella-Herrera, R., Rivas, M., Jeison, D., 2018. Can Microbially Induced Calcite Precipitation (MICP) through a Ureolytic Pathway Be Successfully Applied for Removing Heavy Metals from Wastewaters? Crystals 8, 438. https://doi.org/10.3390/cryst8110438
UNEP 2019, 2019. Sand and Sustainability: Finding new solutions for environmental governance of global sand resources: 2019. United Nations Environment Programme, Geneva, Switzerland.
Venkatarama Reddy, B.V., Jagadish, K.S., 2003. Embodied energy of common and alternative building materials and technologies. Energy Build. 35, 129–137. https://doi.org/10.1016/S0378-7788(01)00141-4
Wellsbury, P., Mather, I., Parkes, R.J., 2002. Geomicrobiology of deep, low organic carbon sediments in the Woodlark Basin, Pacific Ocean. FEMS Microbiol. Ecol. 42, 59–70. https://doi.org/10.1111/j.1574-6941.2002.tb00995.x
Wilsenach, J., van Loosdrecht, M., 2003. Impact of Seperate Urine Collection on Wastewater Treatment Systems. Water Sci. Technol. J. Int. Assoc. Water Pollut. Res. 48, 103–10. https://doi.org/10.2166/wst.2003.0027
Yang, J., Pan, X., Zhao, C., Mou, S., Achal, V., Al-Misned, F.A., Mortuza, M.G., Gadd, G.M., 2016. Bioimmobilization of Heavy Metals in Acidic Copper Mine Tailings Soil. Geomicrobiol. J. 33, 261–266. https://doi.org/10.1080/01490451.2015.1068889
Zaborska, W., Krajewska, B., Olech, Z., 2004. Heavy Metal Ions Inhibition of Jack Bean Urease: Potential for Rapid Contaminant Probing. J. Enzyme Inhib. Med. Chem. 19, 65–69. https://doi.org/10.1080/14756360310001650237
Zhao, Q., Li, L., Li, C., Li, M., Amini, F., Zhang, H., 2014. Factors Affecting Improvement of Engineering Properties of MICP-Treated Soil Catalyzed by Bacteria and Urease. J. Mater. Civ. Eng. 26, 04014094. https://doi.org/10.1061/(ASCE)MT.1943-5533.0001013
Zinjarde, S., Apte, M., Mohite, P., Kumar, A.R., 2014. Yarrowia lipolytica and pollutants: Interactions and applications. Biotechnol. Adv. 32, 920–933. https://doi.org/10.1016/j.biotechadv.2014.04.008

# *Appendix A: Standard Growth Curve Preparation*

**Table A.0.1:** Raw data of direct cell counts over a period of 28 hours used to determine standard growth curve of *S. pasteurii.*

| Direct cell counts | | | | |
|---|---|---|---|---|
| **Time (h)** | **A** | **B** | **C** | **Dilution** |
| **0** | 447 | 507 | 522 | 1 |
| **2** | 24 | 23 | 26 | 50 |
| **4** | 55 | 47 | 47 | 50 |
| **6** | 36 | 30 | 50 | 100 |
| **8** | 58 | 48 | 86 | 100 |
| **12** | 38 | 56 | 48 | 200 |
| **16** | 53 | 53 | 46 | 200 |
| **24** | 55 | 67 | 51 | 200 |
| **28** | 63 | 44 | 55 | 200 |

**Table A.0.2:** Raw data of cell density over a period of 28 hours used to illustrate growth curve of *S. pasteurii.*

| Cell density (x$10^9$ cells/mL) | | | | | |
|---|---|---|---|---|---|
| **Time (h)** | **A** | **B** | **C** | **Avg.** | **Std dev.** |
| **0** | 1.40 | 1.58 | 1.63 | 1.54 | 0.12 |
| **2** | 3.75 | 3.59 | 4.06 | 3.80 | 0.24 |
| **4** | 8.59 | 7.34 | 7.34 | 7.76 | 0.72 |
| **6** | 11.3 | 9.4 | 15.6 | 12.1 | 3.21 |
| **8** | 18.1 | 15.0 | 26.9 | 20.0 | 6.16 |
| **12** | 23.8 | 35.0 | 30.0 | 29.6 | 5.64 |
| **16** | 33.1 | 33.1 | 28.8 | 31.7 | 2.53 |
| **24** | 34.4 | 41.9 | 31.9 | 36.0 | 5.20 |
| **28** | 39.4 | 27.5 | 34.4 | 33.8 | 5.96 |

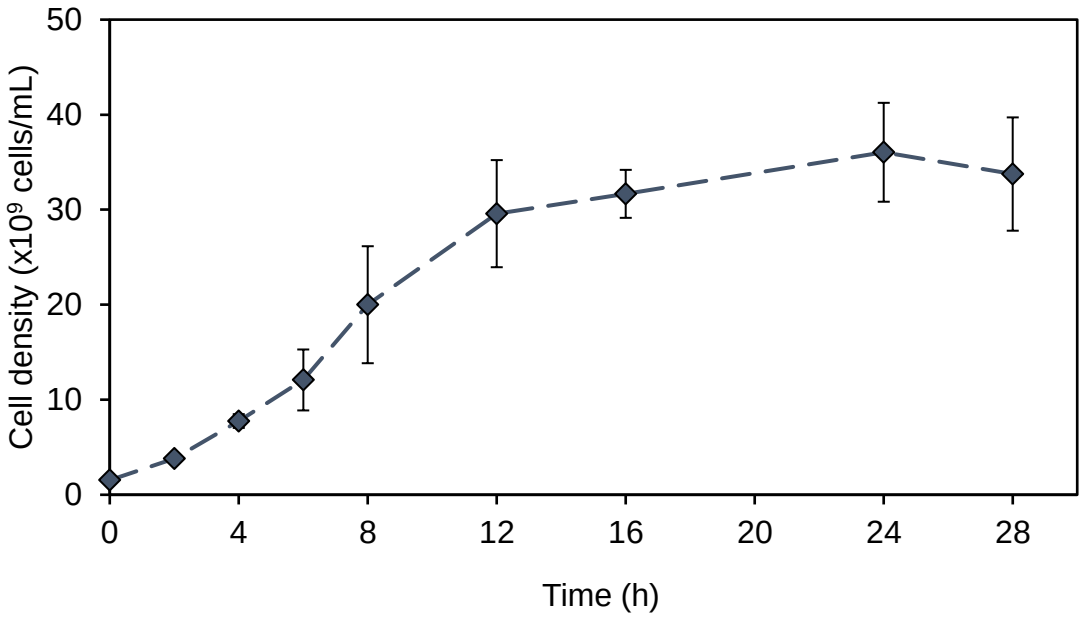


**Figure A.0.1:** Growth curve of *S. pasteurii* over a period of 28 hours determined using direct cell counts. The growth of the culture could be divided into three distinct phases: Lag phase (0 to ~4 hours) where the starter culture acclimatised to its new environment; exponential growth (4 to ~16 hours) where rapid cell division occurred and maintenance phase (16 to ~18 hours) where cellular growth was mainly stationary.

# *Appendix B: ICP Data*

**Table B.0.1:** Experimental ICP data obtained from the ICP-MS Laboratory located within the Central Analytical Facility at University of Stellenbosch detailing the heavy metal concentration of a triplicate set of copper mine tailings.

| | Heavy metal concentration (mg/kg) | | | | | | | | | | | | | | | | | | |
|---|---|---|---|---|---|---|---|---|---|---|---|---|---|---|---|---|---|---|---|
| | **V** | **Cr** | **Mn** | **Co** | **Ni** | **Cu** | **Zn** | **As** | **Se** | **Sr** | **Mo** | **Cd** | **Sn** | **Sb** | **Ba** | **Hg** | **Pb** | **Al** | **Fe** | **B** |
| **A** | 147 | 174 | 388 | 6.68 | 11.2 | 676 | 106 | 14.7 | 0.44 | 59.2 | 10.3 | 0.44 | 3.72 | 0.12 | 192 | 0.04 | 22.3 | 31.2 | 42.4 | BDL |
| **B** | 119 | 134 | 292 | 6.06 | 8.25 | 746 | 87.8 | 11.4 | 1.74 | 44.3 | 10.6 | 0.31 | 3.07 | 0.12 | 141 | 0.03 | 35.2 | 30.4 | 44.7 | BDL |
| **C** | 131 | 148 | 342 | 5.86 | 10.7 | 445 | 94.1 | 11.4 | 0.40 | 50.6 | 10.2 | 0.39 | 3.67 | BDL | 171 | 0.01 | 22.0 | 35.6 | 44.6 | BDL |
| **Avg.** | 133 | 152 | 341 | 6.20 | 10.1 | 622 | 95.8 | 12.5 | 0.86 | 51.4 | 10.4 | 0.38 | 3.49 | 0.12 | 168 | 0.03 | 26.5 | 32.4 | 43.9 | - |
| **Std Dev.** | 14.0 | 20.5 | 47.9 | 0.43 | 1.58 | 158 | 9.03 | 1.93 | 0.76 | 7.47 | 0.25 | 0.06 | 0.36 | 0.00 | 26.0 | 0.02 | 7.51 | 2.81 | 1.29 | - |

*BDL =Below detection limits

# *Appendix C: XRF Data*

**Table C.0.1:** Experimental XRF data obtained from the ICP-MS Laboratory located within the Central Analytical Facility at University of Stellenbosch detailing the weight percentage of the compounds making up the copper mine tailings.

| | Compound (wt.%) | | | | | | | | | | | | | |
|---|---|---|---|---|---|---|---|---|---|---|---|---|---|---|
| | **Al2O3** | **CaO** | **Cr2O3** | **Fe2O3** | **K2O** | **MgO** | **MnO** | **Na2O** | **P2O5** | **SiO2** | **TiO2** | **S** | **P** | **L.O.I.*** |
| **A** | 13.2 | 2.53 | 0.01 | 5.93 | 3.77 | BDL* | BDL | 1.66 | 0.22 | 68.8 | 0.55 | 0.15 | 0.10 | 2.36 |
| **B** | 13.2 | 2.50 | 0.01 | 6.29 | 3.72 | BDL | BDL | 1.70 | 0.22 | 68.7 | 0.54 | 0.18 | 0.10 | 2.24 |
| **C** | 14.7 | 2.65 | 0.02 | 6.33 | 4.12 | BDL | BDL | 1.71 | 0.23 | 65.9 | 0.60 | 0.18 | 0.11 | 2.77 |
| **Avg.** | 13.7 | 2.56 | 0.01 | 6.18 | 3.87 | BDL | BDL | 1.69 | 0.23 | 67.8 | 0.56 | 0.17 | 0.10 | 2.46 |
| **Std Dev.** | 0.87 | 0.08 | 0.01 | 0.22 | 0.22 | - | - | 0.03 | 0.00 | 1.66 | 0.04 | 0.02 | 0.01 | 0.27 |

*BDL = Below detection limits

**L.O.I. = Weight loss/gain at 1000°C

## *Appendix D: PSD Data*

**Table D.0.1:** Experimental data detailing the PSD (in terms of volume) of copper mine tailing samples over a range of 0.02 – 2000 µm.

| **Size (µm)** | **0.02** | **0.03** | **0.03** | **0.03** | **0.04** | **0.04** | **0.04** | **0.05** | **0.06** | **0.06** | **0.07** | **0.08** | **0.09** | **0.10** | **0.11** | **0.13** | **0.14** |
|---|---|---|---|---|---|---|---|---|---|---|---|---|---|---|---|---|---|
| **A** | 0.00 | 0.00 | 0.00 | 0.00 | 0.00 | 0.00 | 0.00 | 0.00 | 0.00 | 0.00 | 0.00 | 0.00 | 0.00 | 0.00 | 0.00 | 0.00 | 0.00 |
| **B** | 0.00 | 0.00 | 0.00 | 0.00 | 0.00 | 0.00 | 0.00 | 0.00 | 0.00 | 0.00 | 0.00 | 0.00 | 0.00 | 0.00 | 0.00 | 0.00 | 0.00 |
| **C** | 0.00 | 0.00 | 0.00 | 0.00 | 0.00 | 0.00 | 0.00 | 0.00 | 0.00 | 0.00 | 0.00 | 0.00 | 0.00 | 0.00 | 0.00 | 0.00 | 0.00 |
| **Avg. vol. (%)** | 0.00 | 0.00 | 0.00 | 0.00 | 0.00 | 0.00 | 0.00 | 0.00 | 0.00 | 0.00 | 0.00 | 0.00 | 0.00 | 0.00 | 0.00 | 0.00 | 0.00 |
| **Std dev.** | 0.00 | 0.00 | 0.00 | 0.00 | 0.00 | 0.00 | 0.00 | 0.00 | 0.00 | 0.00 | 0.00 | 0.00 | 0.00 | 0.00 | 0.00 | 0.00 | 0.00 |
| **Size (µm)** | 0.16 | 0.18 | 0.20 | 0.22 | 0.25 | 0.28 | 0.32 | 0.36 | 0.40 | 0.45 | 0.50 | 0.56 | 0.63 | 0.71 | 0.80 | 0.89 | 1.00 |
| **A** | 0.00 | 0.00 | 0.00 | 0.00 | 0.00 | 0.00 | 0.02 | 0.12 | 0.22 | 0.35 | 0.45 | 0.57 | 0.68 | 0.79 | 0.90 | 1.02 | 1.15 |
| **B** | 0.00 | 0.00 | 0.00 | 0.00 | 0.00 | 0.00 | 0.02 | 0.26 | 0.45 | 0.65 | 0.86 | 1.06 | 1.26 | 1.46 | 1.66 | 1.87 | 2.09 |
| **C** | 0.00 | 0.00 | 0.00 | 0.00 | 0.00 | 0.00 | 0.03 | 0.16 | 0.29 | 0.44 | 0.57 | 0.71 | 0.84 | 0.97 | 1.09 | 1.23 | 1.36 |
| **Avg. vol. (%)** | 0.00 | 0.00 | 0.00 | 0.00 | 0.00 | 0.00 | 0.02 | 0.18 | 0.32 | 0.48 | 0.63 | 0.78 | 0.93 | 1.07 | 1.22 | 1.37 | 1.53 |
| **Std dev.** | 0.00 | 0.00 | 0.00 | 0.00 | 0.00 | 0.00 | 0.00 | 0.07 | 0.12 | 0.15 | 0.21 | 0.25 | 0.30 | 0.35 | 0.40 | 0.45 | 0.50 |

**Table D.0.2:** Experimental data detailing the PSD) of copper mine tailing samples over a particle size range of 0.02 – 2000 µm (continued).

| Size (µm) | 1.12 | 1.26 | 1.42 | 1.59 | 1.78 | 2.00 | 2.24 | 2.52 | 2.83 | 3.17 | 3.56 | 3.99 | 4.48 | 5.02 | 5.64 | 6.32 | 7.10 |
|---|---|---|---|---|---|---|---|---|---|---|---|---|---|---|---|---|---|
| **A** | 1.29 | 1.44 | 1.61 | 1.79 | 1.97 | 2.16 | 2.35 | 2.54 | 2.74 | 2.93 | 3.13 | 3.32 | 3.52 | 3.70 | 3.88 | 4.03 | 4.14 |
| **B** | 2.33 | 2.59 | 2.86 | 3.14 | 3.41 | 3.67 | 3.89 | 4.08 | 4.22 | 4.31 | 4.35 | 4.32 | 4.24 | 4.10 | 3.91 | 3.67 | 3.40 |
| **C** | 1.51 | 1.67 | 1.85 | 2.04 | 2.24 | 2.45 | 2.66 | 2.89 | 3.12 | 3.35 | 3.58 | 3.81 | 4.02 | 4.20 | 4.34 | 4.42 | 4.44 |
| **Avg. vol. (%)** | 1.71 | 1.90 | 2.11 | 2.32 | 2.54 | 2.76 | 2.97 | 3.17 | 3.36 | 3.53 | 3.68 | 3.82 | 3.93 | 4.00 | 4.04 | 4.04 | 3.99 |
| **Std dev.** | 0.55 | 0.61 | 0.66 | 0.72 | 0.77 | 0.80 | 0.82 | 0.81 | 0.77 | 0.71 | 0.62 | 0.50 | 0.37 | 0.26 | 0.26 | 0.37 | 0.54 |
| **Size (µm)** | 8.00 | 8.90 | 10.0 | 11.2 | 12.6 | 14.2 | 15.9 | 17.8 | 20.0 | 22.4 | 25.2 | 28.3 | 31.7 | 35.6 | 39.9 | 44.8 | 50.2 |
| **A** | 4.22 | 4.24 | 4.20 | 4.11 | 3.94 | 3.72 | 3.43 | 3.11 | 2.75 | 2.39 | 2.03 | 1.70 | 1.39 | 1.13 | 0.91 | 0.74 | 0.60 |
| **B** | 3.10 | 2.80 | 2.50 | 2.21 | 1.94 | 1.70 | 1.47 | 1.27 | 1.08 | 0.91 | 0.75 | 0.62 | 0.52 | 0.45 | 0.42 | 0.42 | 0.45 |
| **C** | 4.39 | 4.26 | 4.08 | 3.82 | 3.52 | 3.17 | 2.79 | 2.40 | 2.01 | 1.65 | 1.32 | 1.06 | 0.84 | 0.69 | 0.58 | 0.51 | 0.46 |
| **Avg. vol. (%)** | 3.90 | 3.77 | 3.59 | 3.38 | 3.13 | 2.86 | 2.56 | 2.26 | 1.95 | 1.65 | 1.37 | 1.13 | 0.92 | 0.76 | 0.64 | 0.55 | 0.50 |
| **Std dev.** | 0.70 | 0.84 | 0.95 | 1.02 | 1.05 | 1.04 | 1.00 | 0.93 | 0.84 | 0.74 | 0.64 | 0.54 | 0.44 | 0.35 | 0.25 | 0.16 | 0.08 |

**Table D.0.3:** Experimental data detailing the PSD) of copper mine tailing samples over a particle size range of 0.02 – 2000 µm (continued).

| Size (µm) | 56.4 | 63.2 | 71.0 | 79.6 | 89.3 | 100 | 113 | 126 | 142 | 159 | 178 | 200 | 224 | 252 | 283 | 317 | 355 |
|---|---|---|---|---|---|---|---|---|---|---|---|---|---|---|---|---|---|
| **A** | 0.49 | 0.41 | 0.36 | 0.31 | 0.28 | 0.25 | 0.21 | 0.17 | 0.09 | 0.03 | 0.00 | 0.00 | 0.00 | 0.00 | 0.00 | 0.00 | 0.00 |
| **B** | 0.49 | 0.52 | 0.54 | 0.52 | 0.45 | 0.37 | 0.24 | 0.09 | 0.02 | 0.00 | 0.00 | 0.00 | 0.00 | 0.00 | 0.00 | 0.00 | 0.00 |
| **C** | 0.42 | 0.38 | 0.34 | 0.30 | 0.25 | 0.21 | 0.16 | 0.10 | 0.06 | 0.02 | 0.00 | 0.00 | 0.00 | 0.00 | 0.00 | 0.00 | 0.00 |
| **Avg. vol. (%)** | 0.47 | 0.44 | 0.41 | 0.38 | 0.33 | 0.28 | 0.20 | 0.12 | 0.05 | 0.02 | 0.00 | 0.00 | 0.00 | 0.00 | 0.00 | 0.00 | 0.00 |
| **Std dev.** | 0.04 | 0.08 | 0.11 | 0.12 | 0.11 | 0.09 | 0.04 | 0.04 | 0.03 | 0.02 | 0.00 | 0.00 | 0.00 | 0.00 | 0.00 | 0.00 | 0.00 |

| Size (µm) | 399 | 448 | 502 | 564 | 632 | 710 | 796 | 893 | 1000 | 1130 | 1260 | 1420 | 1590 | 1780 | 2000 |
|---|---|---|---|---|---|---|---|---|---|---|---|---|---|---|---|
| **A** | 0.00 | 0.00 | 0.00 | 0.00 | 0.00 | 0.00 | 0.00 | 0.00 | 0.00 | 0.00 | 0.00 | 0.00 | 0.00 | 0.00 | 0.00 |
| **B** | 0.00 | 0.00 | 0.00 | 0.00 | 0.00 | 0.00 | 0.00 | 0.00 | 0.00 | 0.00 | 0.00 | 0.00 | 0.00 | 0.00 | 0.00 |
| **C** | 0.00 | 0.00 | 0.00 | 0.00 | 0.00 | 0.00 | 0.00 | 0.00 | 0.00 | 0.00 | 0.00 | 0.00 | 0.00 | 0.00 | 0.00 |
| **Avg. vol. (%)** | 0.00 | 0.00 | 0.00 | 0.00 | 0.00 | 0.00 | 0.00 | 0.00 | 0.00 | 0.00 | 0.00 | 0.00 | 0.00 | 0.00 | 0.00 |
| **Std dev.** | 0.00 | 0.00 | 0.00 | 0.00 | 0.00 | 0.00 | 0.00 | 0.00 | 0.00 | 0.00 | 0.00 | 0.00 | 0.00 | 0.00 | 0.00 |

# *Appendix E: Void Ratio Calculation*

**Table E.0.1:** Experimental data obtained from 'Density Bottle Method' used to determine the specific gravity, void ratio and porosity of the copper mine tailings utilised throughout the course of this experiment.

| | A | B | C | Avg. | Std dev. |
|---|---|---|---|---|---|
| **Weight of bottle [W1] (g)** | 35.0 | 37.5 | 35.5 | 36.0 | 1.31 |
| **Weight of bottle + Dry tailings [W2] (g)** | 45.1 | 47.5 | 45.5 | 46.0 | 1.29 |
| **Weight of bottle + Dry tailings + Water [W3] (g)** | 93.8 | 94.8 | 93.6 | 94.1 | 0.64 |
| **Weight of bottle + Water [W4] (g)** | 87.5 | 88.6 | 87.3 | 87.8 | 0.68 |
| **Specific Gravity** | 2.67 | 2.65 | 2.70 | 2.68 | 0.02 |
| | **A** | **B** | **C** | **Avg.** | **Std dev.** |
| **Measured volume of dry tailings [1] (mL)** | 25.0 | 25.0 | 25.0 | 25.00 | 0.00 |
| **Theoretical volume of dry tailings [2] (mL)** | 14.9 | 14.7 | 14.4 | 14.68 | 0.23 |
| **Volume of void [1] - [2]** | 10.1 | 10.3 | 10.6 | 10.32 | 0.23 |
| **Void ratio** | 0.41 | 0.41 | 0.42 | 0.41 | 0.00 |
| **Porosity** | 0.29 | 0.29 | 0.29 | 0.29 | 0.00 |

# *Appendix F: Pumping Experiment Data*

**Table F.0.1:** Experimental data obtained from pump experiments, detailing the mass of effluent which was pumped through each ratio of copper mine tailings to beach sand.

| **Mass of beaker (g) [A]** | | | | |
|---|---|---|---|---|
| **Tailing Percentage** | **1** | **2** | **3** | **Avg.** |
| **100%** | 0.00 | 0.00 | 0.00 | 0.00 |
| **80%** | 0.00 | 0.00 | 0.00 | 0.00 |
| **60%** | 76.4 | 76.5 | 76.8 | 76.5 |
| **40%** | 78.5 | 78.5 | 78.6 | 78.5 |
| **20%** | 76.2 | 77.5 | 76.7 | 76.8 |
| **0%** | 78.7 | 78.9 | 79.1 | 78.9 |
| **Mass of beaker and effluent (g) [B]** | | | | |
| **Tailing Percentage** | **1** | **2** | **3** | **Avg.** |
| **100%** | 0.00 | 0.00 | 0.00 | 0.00 |
| **80%** | 0.00 | 0.00 | 0.00 | 0.00 |
| **60%** | 80.3 | 79.3 | 77.8 | 79.1 |
| **40%** | 88.8 | 86.7 | 83.7 | 86.4 |
| **20%** | 144 | 140 | 149 | 144 |
| **0%** | 177 | 177 | 184 | 179 |
| **Difference (g) [A] - [B]** | | | | |
| **Tailing Percentage** | **1** | **2** | **3** | **Avg.** |
| **100%** | 0.00 | 0.00 | 0.00 | 0.00 |
| **80%** | 0.00 | 0.00 | 0.00 | 0.00 |
| **60%** | 3.84 | 2.88 | 1.07 | 2.60 |
| **40%** | 10.3 | 8.15 | 5.13 | 7.85 |
| **20%** | 68.0 | 62.4 | 72.1 | 67.5 |
| **0%** | 98.3 | 98.2 | 105 | 100 |

**Table F.0.2:** Experimental data obtained from pump experiments, detailing the mass flow rate of fluid through each respective ratio of copper mine tailings to beach sand.

| Mass Flow Rate (g/s) ([A] - [B])/210 | | | | | |
|---|---|---|---|---|---|
| **Tailing Percentage** | **1** | **2** | **3** | **Avg.** | **Std dev.** |
| **100%** | 0.00 | 0.00 | 0.00 | 0.00 | 0.00 |
| **80%** | 0.00 | 0.00 | 0.00 | 0.00 | 0.00 |
| **60%** | 0.02 | 0.01 | 0.01 | 0.01 | 0.01 |
| **40%** | 0.05 | 0.04 | 0.02 | 0.04 | 0.01 |
| **20%** | 0.32 | 0.30 | 0.34 | 0.32 | 0.02 |
| **0%** | 0.47 | 0.47 | 0.50 | 0.48 | 0.02 |

# *Appendix G: Gallery Measurements*

**Table G.0.1:** Experimental data showing the change in calcium ion content of the cementation media of each bio-column experiment over a five-day period.

| | **$Ca^{2+}$ concentration (mg/L) after given time (h)** | | | | | |
|---|---|---|---|---|---|---|
| **Experiment** | **0** | **24** | **48** | **72** | **96** | **120** |
| A | 0 | 24 | 48 | 72 | 96 | 120 |
| B | 11852 | 10881 | 9459 | 9037 | 8139 | 6626 |
| C | 10478 | 7176 | 5098 | 443 | 259 | 189 |
| Acclimatised | 11740 | 11688 | 11318 | 11238 | 10739 | 10056 |

**Table G.0.2:** Experimental data showing the change in ammonium ion concentration of the cementation media of each bio-column experiment over a five-day period.

| | **$NH_4^+$ concentration (mg/L) after given time (h)** | | | | | |
|---|---|---|---|---|---|---|
| **Experiment** | **0** | **24** | **48** | **72** | **96** | **120** |
| A | 88 | 1921 | 3033 | 3925 | 4572 | 6326 |
| B | 106 | 3610 | 9257 | 10669 | 10980 | 11092 |
| C | 43 | 593 | 842 | 1204 | 1684 | 2871 |
| Acclimatised | 73 | 380 | 313 | 397 | 489 | 979 |

**Table G.0.3:** Experimental data showing the change in pH of the cementation media of each bio-column experiment over a five-day period.

| | **pH of cementation media after given time (h)** | | | | | |
|---|---|---|---|---|---|---|
| **Experiment** | **0** | **24** | **48** | **72** | **96** | **120** |
| A | 7.22 | 7.28 | 7.26 | 7.15 | 7.23 | 7.38 |
| B | 7.16 | 7.57 | 7.45 | 7.77 | 7.71 | 7.72 |
| C | 7.35 | 7.75 | 7.69 | 7.74 | 7.64 | 7.74 |
| Acclimatised | 7.42 | 7.71 | 7.60 | 7.62 | 7.68 | 7.82 |

**Table G.0.4:** Experimental data showing the initial urea concertation of the cementation media of each experimental bio-column run as well as the maximum theoretical ammonium which could be produced if all urea was hydrolysed.

| Experiment | Initial urea concentration (mg/L) | Maximum theoretical ammonium concentration (mg/L)* |
|---|---|---|
| **A** | 19331 | 10974 |
| **B** | 11196 | 11196 |
| **C** | 19422 | 11025 |
| **Acclimatised** | 18424 | 10459 |

*It was assumed all urea, if broken down completely, would be converted into ammonium. Following Equation 6, every one mole of urea would break down to produce 2 moles of ammonium.

# *Appendix H: Compressive Strength Tests*

**Table H.0.1:** Results of compressive strength test for Experiment A showing load applied (kN) by the Proline Z100 onto bio-column specimens which was converted into compressive strength (MPa).

| Experiment A | Applied load (kN) | Compressive strength (MPa) |
|---|---|---|
| 1 | 2.24 | 1.41 |
| 2 | 3.29 | 2.07 |
| 3 | 3.32 | 2.09 |
| **Average** | 2.95 | 1.85 |
| **Std dev.** | 0.62 | 0.39 |

**Table H.0.2:** Results of compressive strength test for Experiment B showing load applied (kN) by the Proline Z100 onto bio-column specimens which was converted into compressive strength (MPa).

| Experiment B | Applied load (kN) | Compressive strength (MPa) |
|---|---|---|
| 1 | 0.49 | 0.31 |
| 2 | - | - |
| 3 | - | - |
| **Average** | N/A | N/A |
| **Std dev.** | N/A | N/A |

**Table H.0.3:** Results of compressive strength test for Experiment C showing load applied (kN) by the Proline Z100 onto bio-column specimens which was converted into compressive strength (MPa).

| Experiment C | Applied load (kN) | Compressive strength (MPa) |
|---|---|---|
| 1 | 0.86 | 0.54 |
| 2 | - | - |
| 3 | - | - |
| **Average** | N/A | N/A |
| **Std dev.** | N/A | N/A |

**Table H.0.4:** Results of compressive strength test for Experiment D showing load applied (kN) by the Proline Z100 onto bio-column specimens which was converted into compressive strength (MPa).

| Experiment D | Applied load (kN) | Compressive strength (MPa) |
|---|---|---|
| 1 | 0.14 | 0.09 |
| 2 | 1.32 | 0.83 |
| 3 | 0.86 | 0.54 |
| **Average** | 0.77 | 0.49 |
| **Std dev.** | 0.59 | 0.37 |

**Table H.0.5:** Results of compressive strength test for the acclimatised bio-columns showing load applied (kN) by the Proline Z100 onto bio-column specimens which was converted into compressive strength (MPa).

| Acclimatised | Applied load (kN) | Compressive strength (MPa) |
|---|---|---|
| 1 | 0.18 | 0.11 |
| 2 | - | - |
| 3 | - | - |
| **Average** | N/A | N/A |
| **Std dev.** | N/A | N/A |

**Note:** If a compressive strength was not recorded it was due to the respective bio-column breaking on removal from fabric mould before compressive strength testing could take place.

**Note:** Flatwise area of all bio-columns = 0.00159 $m^2$

# *Appendix I: Bio-column $CaCO_3$ Content Tests*

**Table I.0.1:** Data collected to determine the $CaCO_3$ content of both the outer and inner regions of Experiment A.

| **Outer:** | **1** | **2** | **3** | **Avg.** | **Std dev.** |
|---|---|---|---|---|---|
| Mass Container (g) | 44.7 | 74.7 | 45.5 | 55.0 | 17.1 |
| Mass Total (g) | 47.8 | 77.3 | 49.3 | 58.1 | 16.6 |
| Mass After Acid Wash (g) | 47.5 | 77.1 | 49.0 | 57.9 | 16.6 |
| Mass Solid (g) | 3.01 | 2.60 | 3.84 | 3.15 | 0.63 |
| Mass $CaCO_3$ (g) | 0.26 | 0.23 | 0.28 | 0.26 | 0.03 |
| **$CaCO_3$ (%)** | **8.64** | **8.85** | **7.29** | **8.26** | **0.84** |
| **Inner:** | **1** | **2** | **3** | **Avg.** | **Std dev.** |
| Mass Container (g) | 44.8 | 45.72 | 47.64 | 46.0 | 1.46 |
| Mass Total (g) | 47.2 | 49.15 | 49.53 | 48.6 | 1.25 |
| Mass After Acid Wash (g) | 47.0 | 48.91 | 49.36 | 48.4 | 1.26 |
| Mass Solid (g) | 2.42 | 3.43 | 1.89 | 2.58 | 0.78 |
| Mass $CaCO_3$ (g) | 0.21 | 0.24 | 0.17 | 0.21 | 0.04 |
| **$CaCO_3$ (%)** | **8.68** | **7.00** | **8.99** | **8.22** | **1.07** |

**Table I.0.2:** Data collected to determine the CaCO3 content of both the outer and inner regions of Experiment B.

| **Outer:** | **1** | **2** | **3** | **Avg.** | **Std dev.** |
|---|---|---|---|---|---|
| Mass Container (g) | 74.6 | 45.7 | 47.7 | 56.0 | 16.2 |
| Mass Total (g) | 77.4 | 49.7 | 50.8 | 59.3 | 15.7 |
| Mass After Acid Wash (g) | 77.1 | 49.3 | 50.4 | 58.9 | 15.7 |
| Mass Solid (g) | 2.78 | 4.02 | 3.09 | 3.30 | 0.65 |
| Mass $CaCO_3$ (g) | 0.38 | 0.48 | 0.40 | 0.42 | 0.05 |
| **$CaCO_3$ (%)** | **13.7** | **11.9** | **12.9** | **12.8** | **0.87** |
| **Inner:** | **1** | **2** | **3** | **Avg.** | **Std dev.** |
| Mass Container (g) | 44.7 | 45.5 | 47.6 | 45.9 | 1.51 |
| Mass Total (g) | 47.3 | 48.1 | 50.9 | 48.8 | 1.89 |
| Mass After Acid Wash (g) | 47.1 | 47.8 | 50.6 | 48.5 | 1.84 |
| Mass Solid (g) | 2.60 | 2.59 | 3.27 | 2.82 | 0.39 |
| Mass CaCO3 (g) | 0.27 | 0.26 | 0.36 | 0.30 | 0.06 |
| **$CaCO_3$ (%)** | **10.4** | **10.0** | **11.0** | **10.5** | **0.49** |

**Table I.0.3:** Data collected to determine the CaCO3 content of both the outer and inner regions of Experiment C.

| **Outer:** | **1** | **2** | **3** | **Avg.** | **Std dev.** |
|---|---|---|---|---|---|
| Mass Container (g) | 44.7 | 74.7 | 45.5 | 55.0 | 17.1 |
| Mass Total (g) | 46.0 | 75.6 | 47.1 | 56.2 | 16.8 |
| Mass After Acid Wash (g) | 45.8 | 75.4 | 46.8 | 56.0 | 16.8 |
| Mass Solid (g) | 1.28 | 0.90 | 1.62 | 1.27 | 0.36 |
| Mass $CaCO_3$ (g) | 0.21 | 0.20 | 0.32 | 0.24 | 0.07 |
| **$CaCO_3$ (%)** | **16.4** | **22.4** | **19.8** | **19.5** | **3.03** |
| **Inner:** | **1** | **2** | **3** | **Avg.** | **Std dev.** |
| Mass Container (g) | 44.8 | 45.7 | 47.7 | 46.1 | 1.47 |
| Mass Total (g) | 47.2 | 49.1 | 51.5 | 49.3 | 2.16 |
| Mass After Acid Wash (g) | 47.1 | 48.8 | 51.3 | 49.1 | 2.11 |
| Mass Solid (g) | 2.44 | 3.33 | 3.86 | 3.21 | 0.72 |
| Mass CaCO3 (g) | 0.14 | 0.21 | 0.23 | 0.19 | 0.05 |
| **$CaCO_3$ (%)** | **5.74** | **6.31** | **6.10** | **6.05** | **0.29** |

**Table I.0.4:** Data collected to determine the CaCO3 content of both the outer and inner regions of Experiment D.

| **Outer:** | **1** | **2** | **3** | **Avg.** | **Std dev.** |
|---|---|---|---|---|---|
| Mass Container (g) | 40.2 | 39.2 | 39.5 | 39.7 | 0.50 |
| Mass Total (g) | 41.9 | 40.6 | 41.9 | 41.5 | 0.75 |
| Mass After Acid Wash (g) | 41.8 | 40.6 | 41.9 | 41.4 | 0.73 |
| Mass Solid (g) | 1.66 | 1.37 | 2.39 | 1.81 | 0.53 |
| Mass $CaCO_3$ (g) | 0.04 | 0.02 | 0.04 | 0.03 | 0.01 |
| **$CaCO_3$ (%)** | **2.41** | **1.46** | **1.67** | **1.85** | **0.50** |
| **Inner:** | **1** | **2** | **3** | **Avg.** | **Std dev.** |
| Mass Container (g) | 29.0 | 36.9 | 28.7 | 31.5 | 4.62 |
| Mass Total (g) | 30.4 | 37.7 | 30.4 | 32.9 | 4.21 |
| Mass After Acid Wash (g) | 30.4 | 37.7 | 30.4 | 32.8 | 4.24 |
| Mass Solid (g) | 1.44 | 0.87 | 1.71 | 1.34 | 0.43 |
| Mass CaCO3 (g) | 0.03 | 0.01 | 0.06 | 0.03 | 0.03 |
| **$CaCO_3$ (%)** | **2.08** | **0.80** | **3.51** | **2.13** | **1.35** |

**Table I.0.5**: Data collected to determine the CaCO3 content of both the outer and inner regions of the Acclimatised bio-columns.

| **Outer:** | **1** | **2** | **3** | **Avg.** | **Std dev.** |
|---|---|---|---|---|---|
| Mass Container (g) | 35.1 | 36.7 | 38.8 | 36.9 | 1.86 |
| Mass Total (g) | 36.0 | 38.2 | 39.4 | 37.9 | 1.72 |
| Mass After Acid Wash (g) | 35.6 | 37.7 | 39.2 | 37.5 | 1.81 |
| Mass Solid (g) | 0.92 | 1.53 | 0.62 | 1.02 | 0.46 |
| Mass $CaCO_3$ (g) | 0.43 | 0.54 | 0.22 | 0.40 | 0.16 |
| **$CaCO_3$ (%)** | 46.7 | 35.3 | 35.5 | 39.2 | 6.55 |
| **Inner:** | **1** | **2** | **3** | **Avg.** | **Std dev.** |
| Mass Container (g) | 35.5 | 37.8 | 41.0 | 38.1 | 2.75 |
| Mass Total (g) | 38.9 | 39.5 | 43.9 | 40.8 | 2.71 |
| Mass After Acid Wash (g) | 38.8 | 39.4 | 43.7 | 40.6 | 2.67 |
| Mass Solid (g) | 3.46 | 1.70 | 2.93 | 2.70 | 0.90 |
| Mass CaCO3 (g) | 0.19 | 0.10 | 0.21 | 0.17 | 0.06 |
| **$CaCO_3$ (%)** | **5.49** | **5.88** | **7.17** | **6.18** | **0.88** |

# *Appendix J: Bio-column EDS Analysis*

| Experiment A (Inner) | | | |
|---|---|---|---|
| **Spectrum** | **C** | **O** | **Ca** |
| **1** | 21.1 | 60.67 | 18.2 |
| **2** | 24.5 | 67.6 | 7.86 |
| **3** | 24.5 | 65.35 | 10.1 |
| **4** | 24.5 | 66.96 | 8.58 |
| **Avg.** | 23.7 | 65.2 | 11.2 |
| **Std dev.** | 1.7 | 3.13 | 4.77 |

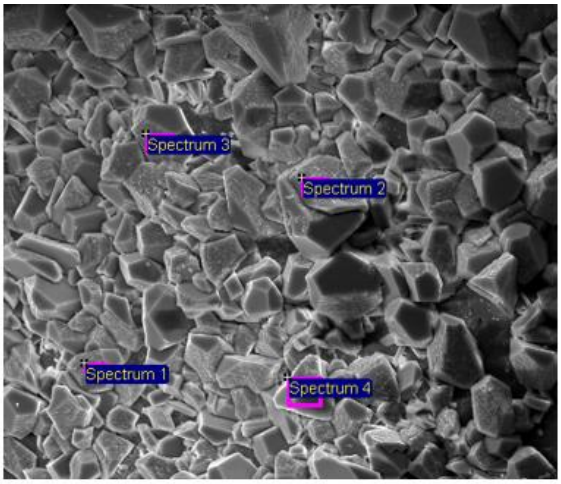


**Figure J.0.1:** EDS results for the inner bio-column region of Experiment A.

| Experiment A (Outer) | | | |
|---|---|---|---|
| **Spectrum** | **C** | **O** | **Ca** |
| **1** | 4.35 | 9.27 | 86.4 |
| **2** | 19.5 | 62.3 | 18.2 |
| **3** | 17.0 | 55.5 | 27.5 |
| **4** | 18.2 | 58.1 | 23.7 |
| **5** | 10.3 | 32.5 | 57.2 |
| **Avg.** | 13.9 | 43.5 | 42.6 |
| **Std dev.** | 6.38 | 22.4 | 28.8 |

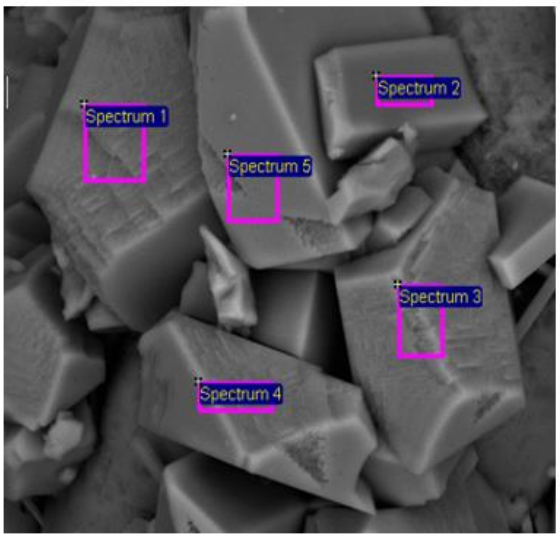


**Figure J.0.2:** EDS results for the outer bio-column region of Experiment A.

| Experiment B (Inner) | | | | | | |
|---|---|---|---|---|---|---|
| **Spec** | **C** | **O** | **Cl** | **Si** | **Ca** | **Fe** |
| **1** | 18.1 | 52.6 | 0.51 | 1.56 | 26.7 | 0.50 |
| **2** | 22.1 | 59.5 | 4.65 | 1.22 | 12.3 | 0.29 |
| **3** | 10.8 | 37.6 | 2.57 | 0.21 | 0.53 | 48.3 |
| **4** | 20.9 | 54.2 | 21.4 | 0.67 | 0.74 | 2.11 |
| **5** | 20.0 | 39.1 | 1.65 | 2.25 | 36.2 | 0.89 |
| **Avg.** | 18.4 | 48.6 | 6.16 | 1.18 | 15.3 | 10.4 |
| **Std dev.** | 4.48 | 9.71 | 8.67 | 0.79 | 15.85 | 21.2 |

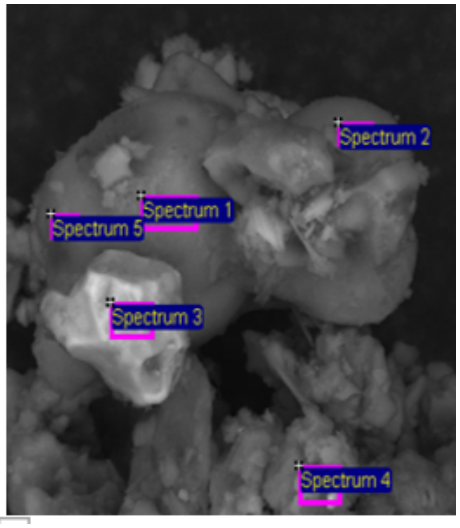


**Figure J.0.3:** EDS results for the inner bio-column region of Experiment B.

| Experiment B (Outer) | | | | |
|---|---|---|---|---|
| **Spectrum** | **C** | **O** | **Si** | **Ca** |
| **1** | 11.3 | 50.6 | 0.33 | 37.8 |
| **2** | 10.5 | 47.0 | 0.78 | 41.8 |
| **3** | 19.2 | 61.0 | 0.38 | 19.4 |
| **4** | 17.6 | 57.7 | 0.53 | 24.2 |
| **5** | 12.4 | 49.0 | 0.37 | 38.3 |
| **Avg.** | 14.2 | 53.1 | 0.48 | 32.3 |
| **Std dev.** | 3.97 | 6.0 | 0.18 | 9.85 |

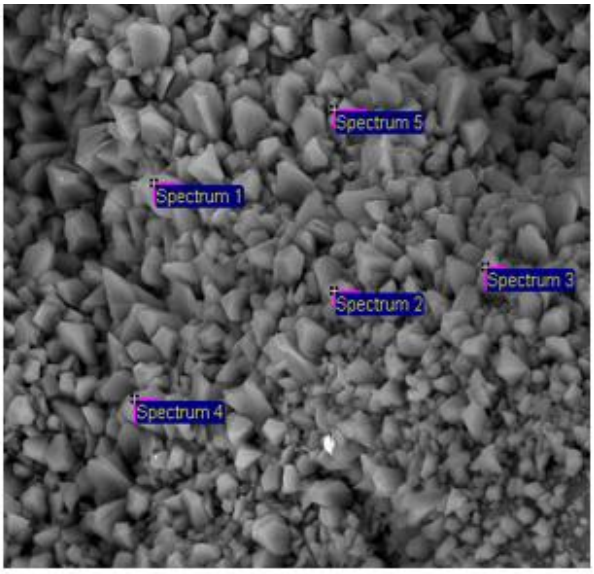


**Figure J.0.4:** EDS results for the outer bio-column region of Experiment B.

| Experiment C (Inner) | | | | | | |
|---|---|---|---|---|---|---|
| **Spec.** | **C** | **O** | **Al** | **Si** | **Fe** | **Cu** |
| **1** | 35.0 | 47.7 | 5.42 | 9.01 | 1.11 | 0.00 |
| **2** | 45.6 | 22.1 | 2.26 | 12.4 | 9.73 | 2.68 |
| **3** | 32.0 | 48.1 | 6.50 | 9.45 | 1.50 | 0.00 |
| **Avg.** | 37.5 | 39.3 | 4.73 | 10.3 | 4.12 | 0.89 |
| **Std dev.** | 7.18 | 14.9 | 2.20 | 1.85 | 4.87 | 1.55 |

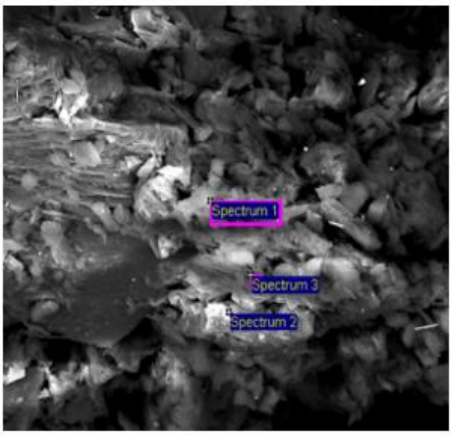


**Figure J.0.5:** EDS results for the inner bio-column region of Experiment C.

| Experiment C (Outer) | | | | | |
|---|---|---|---|---|---|
| **Spec.** | **C** | **O** | **Al** | **Si** | **Fe** |
| **1** | 19.0 | 48.2 | 8.8 | 23.1 | 1.01 |
| **2** | 17.1 | 49.2 | 6.7 | 19.1 | 6.45 |
| **3** | 20.8 | 51.4 | 5.9 | 19.5 | 1.50 |
| **4** | 23.2 | 52.1 | 6.7 | 13.6 | 2.30 |
| **5** | 15.4 | 47.9 | 1.3 | 34.7 | 0.37 |
| **Avg.** | 19.1 | 49.8 | 5.9 | 22.0 | 2.33 |
| **Std dev.** | 3.05 | 1.92 | 2.76 | 7.87 | 2.41 |

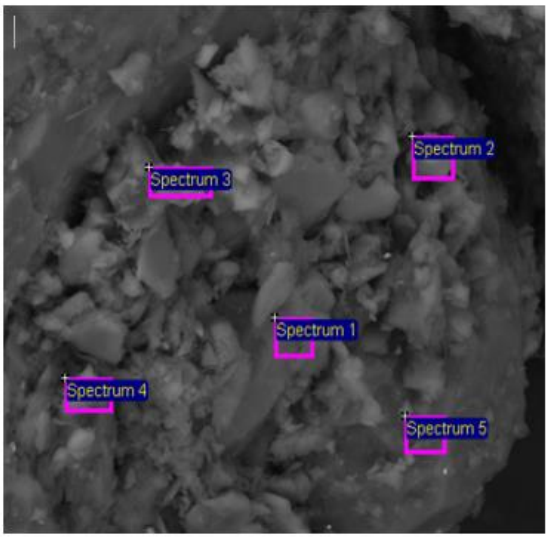


**Figure J.0.6:** EDS results for the outer bio-column region of Experiment C.

| Experiment D | | | | | |
|---|---|---|---|---|---|
| **Spec.** | **C** | **O** | **Al** | **Si** | **Fe** |
| **1** | 14.2 | 52.6 | 10.0 | 18.0 | 0.74 |
| **2** | 18.8 | 14.9 | 4.40 | 11.7 | 50.1 |
| **3** | 13.7 | 58.0 | 1.33 | 26.4 | 0.36 |
| **4** | 12.7 | 11.3 | 6.99 | 18.9 | 42.0 |
| **5** | 16.4 | 37.9 | 8.08 | 18.2 | 19.0 |
| **Avg.** | 15.2 | 34.9 | 6.17 | 18.6 | 22.4 |
| **Std dev.** | 2.44 | 21.3 | 3.38 | 5.20 | 23.0 |

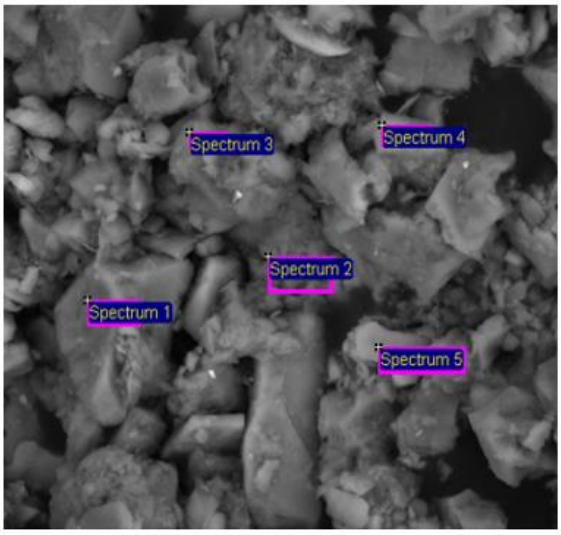


**Figure J.0.7:** EDS results of a shard of bio-column harvested from Experiment D.

| Acclimatised (Inner) | | | | |
|---|---|---|---|---|
| **Spectrum** | **C** | **O** | **Fe** | **Cu** |
| **1** | 19.3 | 22.6 | 0.59 | 57.5 |
| **2** | 9.41 | 14.0 | 1.37 | 75.2 |
| **3** | 74.1 | 11.5 | 0.00 | 14.5 |
| **4** | 14.6 | 22.2 | 0.49 | 62.8 |
| **5** | 11.8 | 17.0 | 0.76 | 70.4 |
| **Avg.** | 25.8 | 17.5 | 0.64 | 56.1 |
| **Std dev.** | 27.2 | 4.92 | 0.50 | 24.2 |

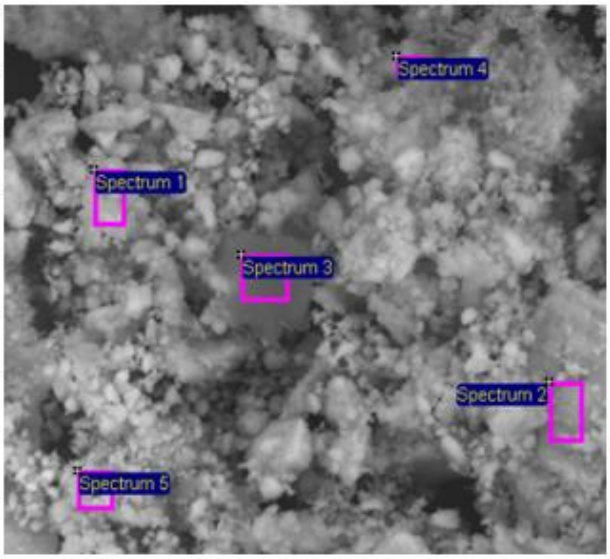


**Figure J.0.8:** EDS results for the inner region of the bio-column grown using a culture of *S. pasteurii* acclimatised to 600 mg/L of copper.

| Acclimatised (Outer) | | | | | | | | |
|---|---|---|---|---|---|---|---|---|
| **Spec** | **C** | **O** | **Al** | **Si** | **Cl** | **K** | **Ca** | **Fe** |
| **1** | 43.8 | 28.0 | 5.25 | 8.07 | 1.04 | 4.94 | 2.54 | 6.32 |
| **2** | 15.5 | 42.1 | 9.09 | 25.5 | 0.00 | 5.05 | 2.88 | 0.00 |
| **3** | 16.9 | 45.5 | 6.95 | 22.0 | 0.23 | 8.15 | 0.29 | 0.00 |
| **Avg.** | 25.4 | 38.6 | 7.10 | 18.5 | 0.42 | 6.05 | 1.90 | 2.11 |
| **Std dev.** | 16.0 | 9.28 | 1.92 | 9.19 | 0.55 | 1.82 | 1.41 | 3.65 |

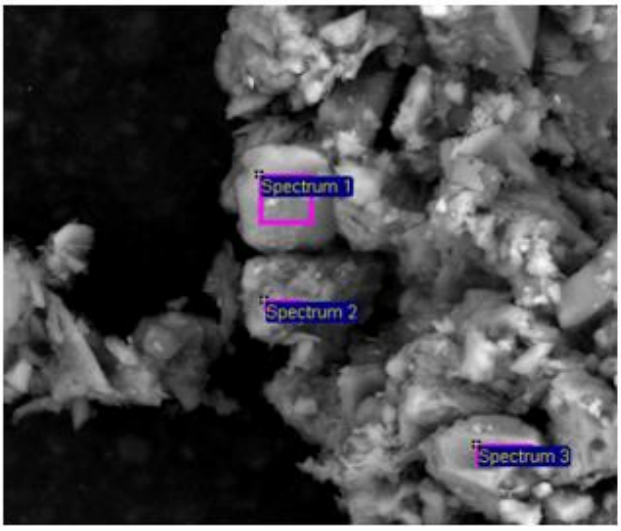


**Figure J.0.9:** EDS results for the outer region of the bio-column grown using a culture of *S. pasteurii* acclimatised to 600 mg/L of copper.

# *Appendix K: MIC Data*

**Table K.0.1:** Raw data of direct cell counts of *S. pasteurii* after 24 hours of growth in various concentration of $Cu^{2+}$ (1024 – 0 mg/L).

| Direct cell counts | | | | |
|---|---|---|---|---|
| **$Cu^{2+}$ (mg/L)** | **A** | **B** | **C** | **Dilution** |
| **1024** | 27 | 29 | 31 | 10 |
| **512** | 132 | 35 | 33 | 50 |
| **256** | 91 | 128 | 105 | 100 |
| **128** | 61 | 79 | 68 | 100 |
| **64** | 80 | 67 | 72 | 100 |
| **32** | 75 | 83 | 84 | 100 |
| **16** | 72 | 98 | 68 | 100 |
| **8** | 63 | 81 | 79 | 100 |
| **4** | 84 | 89 | 85 | 100 |
| **2** | 86 | 72 | 76 | 100 |
| **1** | 79 | 64 | 86 | 100 |
| **0** | 80 | 102 | 96 | 100 |

**Table K.0.2:** Raw data of cell density of S. pasteurii after 24 hours of growth in various concentration of Cu2+ (1024 – 0 mg/L) used to construct MIC curve.

| Cell density (x$10^9$ cells/mL) | | | | | |
|---|---|---|---|---|---|
| **$Cu^{2+}$ (mg/L)** | **A** | **B** | **C** | **Avg.** | **Std dev.** |
| **1024** | 0.84 | 0.91 | 0.97 | 0.9 | 0.06 |
| **512** | 4.13 | 5.47 | 5.16 | 4.9 | 0.70 |
| **256** | 14.2 | 20.0 | 16.4 | 16.9 | 2.92 |
| **128** | 19.1 | 24.7 | 21.3 | 21.7 | 2.84 |
| **64** | 25.0 | 20.9 | 22.5 | 22.8 | 2.05 |
| **32** | 23.4 | 25.9 | 26.3 | 25.2 | 1.54 |
| **16** | 22.5 | 30.6 | 21.3 | 24.8 | 5.09 |
| **8** | 19.7 | 25.3 | 24.7 | 23.2 | 3.08 |
| **4** | 26.3 | 27.8 | 26.6 | 26.9 | 0.83 |
| **2** | 26.9 | 22.5 | 23.8 | 24.4 | 2.25 |
| **1** | 24.7 | 20.0 | 26.9 | 23.9 | 3.51 |
| **0** | 25.0 | 31.9 | 30.0 | 29.0 | 3.55 |

# *Appendix L: Acclimatisation Experiments*

**Table L.0.1:** Raw data of direct cell counts of bacteria grown in the presence of 50 mg/L (Day 1) of copper over a period of 24 hours in order to acclimatise the overall culture to an environment of increased copper concentration.

| | 50 mg/L $Cu^{2+}$ (Day 1) | | |
|---|---|---|---|
| **Time (h)** | **Cell Count** | **Dilution** | **Cells/ml** |
| **16** | 47 | 100 | 14.7 |
| **20** | 51 | 100 | 15.9 |
| **24** | 63 | 100 | 19.7 |

**Table L.0.2:** Raw data of direct cell counts of bacteria grown in the presence of 50 mg/L (Day 2) of copper over a period of 24 hours in order to acclimatise the overall culture to an environment of increased copper concentration.

| | 50 mg/L $Cu^{2+}$ (Day 2) | | |
|---|---|---|---|
| **Time (h)** | **Cell Count** | **Dilution** | **Cells/ml** |
| **16** | 54 | 200 | 33.8 |
| **20** | 61 | 200 | 38.1 |
| **24** | 72 | 200 | 45.0 |

**Table L.0.3:** Raw data of direct cell counts of bacteria grown in the presence of 50 mg/L (Day 3) of copper over a period of 24 hours in order to acclimatise the overall culture to an environment of increased copper concentration.

| | 50 mg/L $Cu^{2+}$ (Day 3) | | |
|---|---|---|---|
| **Time (h)** | **Cell Count** | **Dilution** | **Cells/ml** |
| **16** | 58 | 200 | 36.3 |
| **20** | 52 | 200 | 32.5 |
| **24** | 77 | 200 | 48.1 |

**Table L.0.4:** Raw data of direct cell counts of acclimatised bacteria grown in the presence of 100 mg/L of copper.

| | | 100 mg/L $Cu^{2+}$ | |
|---|---|---|---|
| **Time (h)** | **Cell Count** | **Dilution** | **Cells/ml** |
| **16** | 56 | 200 | 35.0 |
| **20** | 50 | 200 | 31.3 |
| **24** | 53 | 200 | 33.1 |

**Table L.0.5:** Raw data of direct cell counts of acclimatised bacteria grown in the presence of 200 mg/L of copper.

| | | 200 mg/L $Cu^{2+}$ | |
|---|---|---|---|
| **Time (h)** | **Cell Count** | **Dilution** | **Cells/ml** |
| **16** | 46 | 200 | 28.8 |
| **20** | 48 | 200 | 30.0 |
| **24** | 44 | 200 | 27.5 |

**Table L.0.6:** Raw data of direct cell counts of acclimatised bacteria grown in the presence of 300 mg/L of copper.

| | | 300 mg/L $Cu^{2+}$ | |
|---|---|---|---|
| **Time (h)** | **Cell Count** | **Dilution** | **Cells/ml** |
| **16** | 42 | 200 | 26.3 |
| **20** | 44 | 200 | 27.5 |
| **24** | 58 | 200 | 36.3 |

**Table L.0.7:** Raw data of direct cell counts of acclimatised bacteria grown in the presence of 400 mg/L of copper.

| | 400 mg/L $Cu^{2+}$ | | |
|---|---|---|---|
| **Time (h)** | **Cell Count** | **Dilution** | **Cells/ml** |
| **16** | 41 | 200 | 25.6 |
| **20** | 43 | 200 | 26.9 |
| **24** | 46 | 200 | 28.8 |

**Table L.0.8:** Raw data of direct cell counts of acclimatised bacteria grown in the presence of 500 mg/L of copper.

| | 500 mg/L $Cu^{2+}$ | | |
|---|---|---|---|
| **Time (h)** | **Cell Count** | **Dilution** | **Cells/ml** |
| **16** | 23 | 200 | 14.4 |
| **20** | 38 | 200 | 23.8 |
| **24** | 56 | 200 | 35.0 |

**Table L.0.9:** Raw data of direct cell counts of acclimatised bacteria grown in the presence of 600 mg/L of copper.

| | 600 mg/L $Cu^{2+}$ | | |
|---|---|---|---|
| **Time (h)** | **Cell Count** | **Dilution** | **Cells/ml** |
| **16** | 47 | 200 | 29.4 |
| **20** | 41 | 200 | 25.6 |
| **24** | 45 | 200 | 28.1 |

# *Appendix M: Agar Plate Recipes*

**Nutrient broth agar:**

In 1 L of deionised water:

15 g of bacteriological agar (Sigma-Aldrich, St Louis, United States)

16 g of nutrient broth (Sigma-Aldrich, St Louis, United States)

Supplement with 0.39 g of copper sulphate pentahydrate (Sigma-Aldrich, St Louis, United States) to get a 100 mg/L solution of $Cu^{2+}$.

Autoclave solution and pour into petri dishes before the solution cools.

**R2A agar:**

In 1 L of deionised water:

18.2 g R2A agar (Sigma-Aldrich, St Louis, United States)

Supplement with 0.39 g of copper sulphate pentahydrate (Sigma-Aldrich, St Louis, United States) to get a 100 mg/L solution of $Cu^{2+}$.

Autoclave solution and pour into petri dishes before the solution cools.

**Tailings extract agar (adapted from a soil extract medium):**

In 1 L of tap water:

400g of oven-dried copper mine tailings

Autoclave solution and allow sediment to settle overnight. Centrifuge the supernatant and add 15 g of bacteriological agar per 1000 mL of supernatant obtained. Autoclave the solution again and pour into petri dishes before the solution cools.

**Christensen's urea agar (CUA):**

In 950 mL of deionised water:

24 g Christensen's Urea agar base (Sigma-Aldrich, St Louis, United States)

Autoclave above solution.

In 50 mL of deionised water:

10 g Urea (Sigma-Aldrich, St Louis, United States)

Filter sterilise the urea solution using 0.2 µm sterile syringe filter as urea rapidly breaks down if heated. Once the autoclaved solution has cooled to 50°C, aseptically mix both solutions together and pour into petri dishes.

# *Appendix N: Bio-prospecting Experiments*

**Table N.0.1:** Raw data of colony counts of enriched copper mine tailing solution grown on three different nutrient agar plates after 24 and 48 hours.

| | Dilution (24 hours) | | | | | | | |
|---|---|---|---|---|---|---|---|---|
| **Agar Type** | **$10^{-1}$** | **$10^{-2}$** | **$10^{-3}$** | **$10^{-4}$** | **$10^{-5}$** | **$10^{-6}$** | **$10^{-7}$** | **$10^{-8}$** |
| **Nutrient Broth** | TMTC | TMTC | TMTC | TMTC | TMTC | TMTC | TMTC | 73 |
| **R2A** | TMTC | TMTC | TMTC | TMTC | TMTC | TMTC | TMTC | 35 |
| **Tailings Extract** | TMTC | TMTC | TMTC | TMTC | TMTC | TMTC | TMTC | 0 |
| | **Dilution (48 hours)** | | | | | | | |
| **Agar Type** | **$10^{-1}$** | **$10^{-2}$** | **$10^{-3}$** | **$10^{-4}$** | **$10^{-5}$** | **$10^{-6}$** | **$10^{-7}$** | **$10^{-8}$** |
| **Nutrient Broth** | TMTC | TMTC | TMTC | TMTC | TMTC | TMTC | TMTC | 109 |
| **R2A** | TMTC | TMTC | TMTC | TMTC | TMTC | TMTC | TMTC | 53 |
| **Tailings Extract** | TMTC | TMTC | TMTC | TMTC | TMTC | TMTC | TMTC | 45 |

*TMTC = Too many to count

Conversion of colony count into CFU/mL:

$$\frac{\text{CFU}}{\text{mL}} = (\text{colony count})(\text{dilution})(\text{volume of sample plated})$$

Only colony counts which showed statistical significance were utilised.

# *Appendix O: Economic Analysis Assumptions*

**Mass Balance Assumptions:**

- Dependent on the amount of water consumed and climate conditions, an average adult person typically produces between 1 and 1.5 litres of urine per day (Richert et al., 2010). As such it was assumed for the purpose of this research that the average volume of urine produced per person per day is 1.25 litres
- It was also assumed that the average concentration of urea and phosphate within the collected urine is 0.3 M and 0.014 M respectively (Henze, 2017).
- An equimolar concentration of urea and calcium ions were used to match the experimental methodology used in experiment C.
- To stabilise the collected urine for long-term storage, it is dosed with calcium hydroxide, which results in a calcium phosphate fertiliser being produced as a by-product. To ensure the long-term stabilisation of urine (pH>12.5) it has been suggested in literature by Flanagan and Randall (2018) that an excess of 10 g of calcium hydroxide is added for every litre of urine collected.
- To ensure the survival of the ureolytic bacteria and that the MICP process occurs, the pH of the stabilised urine is reduced to a pH of 11.2 using a 32% concentrated hydrochloric acid solution. Work conducted by Lambert and Randall (2019) has shown that 3.5 mL of HCl per litre of stabilised urine is required to achieve a targeted pH of 11.2.
- During experimental runs the ureolytic bacterium, *S. pasteurii, was* cultivated using ATCC®1376 (20 g/L yeast extract, 10 g/L ammonium sulphate and 15.75 g tris-base). For the purposes of the mass balance, it was assumed that this nutrient feed will be used for bio-brick production. However, it is noted that the use of laboratory grade reagents will not be economically feasible in the mass production of bio bricks.
- To produce a standard size of brick (220 mm x 110 mm x 70 mm), approximately 500 mL of cultivated *S. pasteurii* is needed to inoculate 4.50 kg of copper mine tailings ($SG_{Copper\ mine\ tailings}$ = 2.65 and porosity = 0.29).
- Based on the results of experiment C, 44.0 L of cementation media would be needed to grow a bio-brick based on the volume ratio (1:9) of the grown bio-columns (0.19 L) to the theoretical bio-bricks (1.69 L).
- Experiment C only achieved a calcium depletion and ammonium ion production efficiency of 14.3% and 26.0% respectively.
- As the volume of ammonium ions produced was only 26.0% of the theoretical maximum volume that could be produced had all the urea added to the cementation media been hydrolysed, this resulted reduced volume of fertiliser by-product being produced.

- It was assumed that a sulfuric acid scrubber could serve as a possible method to remove and recover the ammonium ions from the liquid effluent produced by Stage 3 (Pradhan et al., 2017).
- This process is represented by the equation: $2NH_3 + H_2SO_4 \rightarrow (NH_4)_2SO_4$, with the stoichiometry of this reaction being used to determine the amount of sulphuric acid required (assuming an 80% conversion):

**Economic Analysis Assumptions:**

- This economic analysis only considered material operation costs and as such no capital nor wage nor overhead costs were reviewed.
- $CaCl_2$ was chosen as the source of calcium ions due to it being cheap and widely available.
- Calcium hydroxide is an effective base to increase the pH of a solution because it is cheap and widely available (Randall et al., 2016) and hence it was used to stabilize the collected urine**.**
- Collected urine was assumed to be free and no transportation costs were associated to its collection and transport to the bio-brick production site.
- Copper mine tailings were assumed to be free.
- A bio-tile of near equivalent volume (6% larger) to the bio-brick was used in the economic comparison of bio-solids.
- The sale price of both the bio-brick and bio-tile was assumed to be on-par with the current sale price of traditional masonry units of similar dimensions and utility.
- The base case of the sensitivity analysis (for both the bio-brick and bio-tile) was defined as using the scale-up chemical inputs and resulting outputs of experiment C. Experiment C was chosen despite only 14.3% of calcium ions being depleted as this experiment involved the use of actual copper mine tailings as well as allowing for the 'extreme' limits of MICP efficiency to be reviewed in the economic sensitivity analysis.
- It was assumed that agriculture waste streams used as an alternative to the ATCC®1376 in the sensitivity analysis would be provided by surrounding dairy producers for free.
- It was assumed that 100% efficiency could be achieved for both calcium ion depletion and ammonium ion production efficiency in the sensitivity analysis.

The excel spread sheets used to determine the mass balance and perform the economic analysis can be found here.

# *Appendix P: Ethics Approval*

Application for Approval of Ethics in Research (EiR) Projects
Faculty of Engineering and the Built Environment, University of Cape Town

## ETHICS APPLICATION FORM

**Please Note:**
Any person planning to undertake research in the Faculty of Engineering and the Built Environment (EBE) at the University of Cape Town is required to complete this form **before** collecting or analysing data. The objective of submitting this application *prior* to embarking on research is to ensure that the highest ethical standards in research, conducted under the auspices of the EBE Faculty, are met. Please ensure that you have read, and understood the **EBE Ethics in Research Handbook** (available from the UCT EBE, Research Ethics website) prior to completing this application form: http://www.ebe.uct.ac.za/ebe/research/ethics1

| **APPLICANT'S DETAILS** | | |
|---|---|---|
| Name of principal researcher, student or external applicant | | Daniel de Oliveira |
| Department | | Civil Engineering |
| Preferred email address of applicant: | | DLVDAN002 @myuct.ac.za |
| If Student | Your Degree: e.g., MSc, PhD, etc. | MSc |
| | Credit Value of Research: e.g., 60/120/180/360 etc. | 180 |
| | Name of Supervisor (if supervised): | Dyllon Randall |
| If this is a researchcontract, indicate the source of funding/sponsorship | | AngloGold Ashante; Columbia / WRC |
| Project Title | | Production of Bio-bricks via microbial induced calcium carbonate precipitation, human urine & mine tai |

**I hereby undertake to carry out my research in such a way that:**

- there is no apparent legal objection to the nature or the method of research; and
- the research will not compromise staff or students or the other responsibilities of the University;
- the stated objective will be achieved, and the findings will have a high degree of validity;
- limitations and alternative interpretations will be considered;
- the findings could be subject to peer review and publicly available; and
- I will comply with the conventions of copyright and avoid any practice that would constitute plagiarism.

| **APPLICATION BY** | Full name | Signature | Date |
|---|---|---|---|
| **Principal Researcher/ Student/External applicant** | Daniel de Oliveira | | 12/02/2020 |
| **SUPPORTED BY** | **Full name** | **Signature** | **Date** |
| **Supervisor (where applicable)** | Dyllon Randall | | 17.02.2020 |

| **APPROVED BY** | Full name | Signature | Date |
|---|---|---|---|
| **HOD (or delegated nominee)** Final authority for all applicants who have answered NO to all questions in Section 1; and for all Undergraduate research (Including Honours). | | | |
| **Chair: Faculty EIR Committee** For applicants other than undergraduate students who have answered YES to any of the questions in Section 1. | R Behrens | | 25 Feb 2020 |

FF